US Army Corps of Engineers

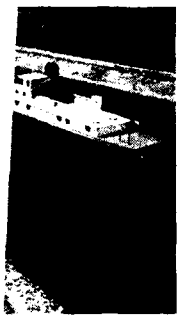

HYDRAULICS LABORATORY

TECHNICAL REPORT HL-90-15

VELOCITIES INDUCED BY COMMERCIAL NAVIGATION

by

Stephen T. Maynord

Hydraulics Laboratory

DEPARTMENT OF THE ARMY
Waterways Experiment Station, Corps of Engineers
3909 Halls Ferry Road, Vicksburg, Mississippi 39180-6199

September 1990
Final Report

Prepared for US Army Engineer District, Louisville
Louisville, Kentucky 40201-0059

Destroy this report when no longer needed. Do not return it to the originator.

The findings in this report are not to be construed as an official Department of the Army position unless so designated by other authorized documents.

The contents of this report are not to be used for advertising, publication, or promotional purposes. Citation of trade names does not constitute an official endorsement or approval of the use of such commercial products.

Unclassified

SECURITY CLASSIFICATION OF THIS PAGE

REPORT DOCUMENTATION PAGE

Form Approved
OMB No. 0704-0188

1a. REPORT SECURITY CLASSIFICATION Unclassified	1b RESTRICTIVE MARKINGS
2a. SECURITY CLASSIFICATION AUTHORITY	3 DISTRIBUTION/AVAILABILITY OF REPORT Approved for public release; distribution unlimited.
2b. DECLASSIFICATION/DOWNGRADING SCHEDULE	
4. PERFORMING ORGANIZATION REPORT NUMBER(S) Technical Report HL-90-15	5 MONITORING ORGANIZATION REPORT NUMBER(S)
6a. NAME OF PERFORMING ORGANIZATION USAEWES Hydraulics Laboratory 6b. OFFICE SYMBOL (If applicable) CEWES-HS-S	7a. NAME OF MONITORING ORGANIZATION
6c. ADDRESS (City, State, and ZIP Code) 3909 Halls Ferry Road Vicksburg, MS 39180-6199	7b. ADDRESS (City, State, and ZIP Code)
8a. NAME OF FUNDING/SPONSORING ORGANIZATION USAED, Louisville 8b. OFFICE SYMBOL (If applicable)	9 PROCUREMENT INSTRUMENT IDENTIFICATION NUMBER
8c. ADDRESS (City, State, and ZIP Code) PO Box 59 Louisville, KY 40201-0059	10 SOURCE OF FUNDING NUMBERS PROGRAM ELEMENT NO. / PROJECT NO. / TASK NO. / WORK UNIT ACCESSION NO.
11. TITLE (Include Security Classification) Velocities Induced by Commercial Navigation	
12. PERSONAL AUTHOR(S) Maynard, Stephen T.	
13a. TYPE OF REPORT Final report 13b. TIME COVERED FROM _____ TO _____	14. DATE OF REPORT (Year, Month, Day) September 1990 15. PAGE COUNT 137
16. SUPPLEMENTARY NOTATION Available from National Technical Information Service, 5285 Port Royal Road, Springfield, VA 22161.	
17 COSATI CODES FIELD / GROUP / SUB-GROUP	18 SUBJECT TERMS (Continue on reverse if necessary and identify by block number) Navigation effects, Propeller jets Navigation models, Return velocity

19. ABSTRACT (Continue on reverse if necessary and identify by block number)

Studies were conducted to determine the velocities induced by commercial navigation on large inland waterways. The velocity-inducing mechanisms addressed in this study include the propeller jet and the displacement effects of the vessel. Using flow visualization and model and prototype measurements, a better understanding of flow patterns near a moving vessel was obtained. Results show that the propeller jet is not the only mechanism producing significant velocities at the channel bottom. The displacement effects of the vessel also create significant bottom velocities. While return velocities have long been recognized as an effect of the vessel displacement, this study shows that the displacement effects induce a velocity beneath the tow that is generally larger than the return velocity and is not influenced by channel size except for relatively low blockage ratios. Predictive relations were developed for return velocities, propeller jet velocities, and displacement velocities.

20 DISTRIBUTION/AVAILABILITY OF ABSTRACT ☒ UNCLASSIFIED/UNLIMITED ☐ SAME AS RPT ☐ DTIC USERS	21 ABSTRACT SECURITY CLASSIFICATION Unclassified
22a. NAME OF RESPONSIBLE INDIVIDUAL	22b TELEPHONE (Include Area Code) / 22c OFFICE SYMBOL

DD Form 1473, JUN 86 *Previous editions are obsolete.*

SECURITY CLASSIFICATION OF THIS PAGE

Unclassified

PREFACE

The model study of the velocities induced by commercial navigation was authorized by the US Army Engineer Division, Ohio River (ORD), at the request of the US Army Engineer District, Louisville (ORL).

The study was conducted during the period July 1987 to September 1988 in the Hydraulics Laboratory of the US Army Engineer Waterways Experiment Station (WES) under the direction of Messrs. F. A. Herrmann, Jr., Chief, Hydraulics Laboratory; R. A. Sager, Assistant Chief, Hydraulics Laboratory; and G. A. Pickering, Chief, Hydraulic Structures Division (HSD), Hydraulics Laboratory. The tests were conducted by Dr. S. T. Maynord, Project Engineer, Spillways and Channels Branch (SCB), HSD, and Messrs. D. White and J. Hilbun, SCB, under the direct supervision of Mr. N. R. Oswalt, Chief, SCB. The report was written by Dr. Maynord and edited by Mrs. M. C. Gay, Information Technology Laboratory, WES.

During the course of the investigation, Messrs. L. Richardson, ORD, and D. Beatty, T. Siemsen, J. Kleckner, J. Baker, and B. Vessels of ORL visited WES to observe tests and discuss test results.

Commander and Director of WES during preparation of this report was COL Larry B. Fulton, EN. Technical Director was Dr. Robert W. Whalin.

CONTENT

CONVERSION FACTORS, NON-SI TO SI (METRIC)
UNITS OF MEASUREMENT

Non-SI units of measurement used in this report can be converted to SI (metric) units as follows:

Multiply	By	To Obtain
degrees (angle)	0.01745329	radians
feet	0.3048	metres
horsepower (550 foot-pounds (force) per second)	745.6999	watts
inches	2.54	centimetres
miles (US statute)	1.609347	kilometres
square feet	0.09290304	square metres

PART I: INTRODUCTION

Background

1. As a vessel moves through a body of water, it creates disturbances in the form of altered water levels such as waves or drawdown and altered velocity patterns such as increased velocities and turbulence intensity. These disturbances vary in intensity with such factors as vessel type, speed, size, and location; and channel size, shape, and ambient conditions. The intensity varies significantly with distance from the vessel. In large waterways this disturbance may be greatly diminished by the time it reaches the boundaries of the bed and bank. The ability to predict the intensity of these disturbances, both near and far removed from the vessel, is needed to better assess the physical impacts of navigation on environmental, channel stability, and other concerns within a waterway. At present, tools to predict the intensity of these disturbances are quite limited. The extensive body of European literature, some of which will be referenced herein, is primarily applicable to channels having a relatively small blockage ratio defined as

$$N = \frac{\text{waterway cross-sectional area*}}{\text{submerged cross-section area of vessel}} \quad (1)$$

Navigation in many US waterways exists on large rivers that have large blockage ratios. Information is needed on navigation effects in waterways having a wide range of blockage ratios.

Purpose of Study and Outline

2. The purpose of this study was to improve the understanding of flow patterns induced by moving tows and to develop tools for predicting the intensity of disturbance for navigation and waterway sizes typical of those

---

* For convenience, symbols and unusual abbreviations are listed and defined in the Notation (Appendix B).

found in the United States, particularly in the Ohio River basin. This study focused on the velocities induced by commercial shallow-draft navigation. Velocities resulting from both the propeller jet and from the displacement effects of the vessel were evaluated in this study.

3. The study will be documented in the following manner:

   a. Literature search.

   b. Flow visualization with a 1:20-scale model.

   c. Flow visualization and surface current patterns with the Olmsted Locks and Dam model.

   d. 1:20-scale physical model study of bottom velocities near the path of a moving tow.

   e. Prototype data collected by the US Army Engineer District (USAED), Louisville.

   f. Development of predictive relations.

Unless stated otherwise, all quantities are given in prototype values.

PART II: LITERATURE SEARCH

4. The literature search will be broken down into the following areas:

   a. Propeller jet studies.

   b. Displacement and return velocity studies.

   c. Field measurements of vessel-induced velocity.

Propeller Jet Velocity Studies

5. For the case of maneuvering navigation (vessel speed $V = 0$), the distribution of velocities has been studied by several investigators including Fuehrer and Romisch (1977), Blaauw and van de Kaa (1978), Bergh (1981), Louis Berger and Associates (1981), and Prosser (1986). The assumption of maneuvering navigation greatly simplifies the problem because wake effects are eliminated. Many of these studies involved prediction of bottom velocities for use in determining riprap size or scour depth. For vessels underway ($V \neq 0$), Fuehrer, Romisch, and Engelke (1981) stated, "Consequently a marked reduction of bottom velocity occurs. Furthermore the maximum bottom velocity takes place in an ever-increasing distance behind the ship." Gucinski (1982) conducted laboratory and field tests and determined that the moving vessel resuspends less sediment than the stationary vessel having the same propeller speed. Velocity measurements demonstrated that the propeller jet extends to a greater depth with the stationary vessel. Gucinski's results also showed that turbulence intensity at the bed was decreased with the higher tow speeds. Schale (1977) found that "the propeller jet of moving freight motorships, even with a high propeller loading, never comes in contact with the canal bottom but always rises along the shortest path to the surface of the water." Schale states that the propeller jet strikes the channel bottom under only the following conditions:

   a. Startup from a stationary condition.

   b. Whenever the water depth/draft ratio is less than 1.2.

   c. Maneuvering with hard rudder.

Schale's observation of the jet rising to the surface is consistent with the findings of Maxwell and Pazwash (1973) for shallow, submerged, axisymmetric jets. Schale (1977) also states that "the propeller jet itself is undetectable in the measurement plane lying 0.5 m above the bottom while in fact there

even prevails there a counterflow in the propeller direction. Thus the attacks upon the bottom material are attributable only to forces arising from displacement flow and from the therewith-integrated energy field of the ship's drive." This "energy field of the ship's drive" is believed to be the flow entering the propellers. Prosser (1986) presents a plot of bottom velocity due to propeller inflow versus blade tip clearance above bed.

6. Before discussing the applicable propeller jet studies, the basic relations used in many propeller jet studies will be developed. Propeller jets are often considered to be similar to submerged jets such that the same equations can be used. Albertson et al. (1950) defined the velocity distribution for a submerged jet discharging into an infinite fluid. The following assumptions apply:

a. Pressure is hydrostatic throughout flow.

b. Diffusion is dynamically similar under all conditions.

c. Longitudinal component of velocity varies according to normal or Gaussian probability function.

Unless otherwise stated, equations are presented in a form applicable to any set of units. The equations for flow through an orifice are as follows:

a. For the zone of flow establishment:

$$\frac{V_x}{V_o} = \exp\left[-\frac{\left(r + Cx - \frac{D_o}{2}\right)^2}{2(Cx)^2}\right] \tag{2}$$

where

V_x = velocity in x-direction at coordinates x,r

V_o = orifice velocity at outlet

r = radial distance from center of outlet

C = coefficient

x = distance from outlet measured along jet axis

D_o = orifice diameter

b. For the zone of established flow:

$$\frac{V(x)_{max}}{V_o} = \frac{1}{2C}\,\frac{D_c}{x} \tag{3}$$

where $V(x)_{max}$ is the velocity in x-direction at $x,r = 0$ and

$$\frac{V_x}{V(x)_{max}} = \exp\left[-\frac{1}{2C^2}\frac{r^2}{x^2}\right] \tag{4}$$

Based on the experimental results of Albertson et al. (1950), the flow becomes established at $x/D_o = 6.2$ and $C = 0.081$ for the orifice discharging into an infinite fluid. Equation 3 becomes

$$\frac{V(x)_{max}}{V_o}\frac{x}{D_o} = 6.2 \tag{5}$$

It is important to note that propeller jets behind moving vessels differ from the conditions addressed by Albertson et al. (1950) in the following ways:

a. The channel bottom and water surface inhibit jet spreading.

b. A moving jet is discharging into a moving flow field.

c. The propeller jet has a radial component of velocity.

d. The rudder splits the jet into two jets.

e. The Kort nozzle and open wheel are different from an orifice.

The following paragraphs summarize the five methods found in the literature for propeller jet velocities behind moving vessels.

Method 1: Fuehrer, Romisch, and Engelke

7. Equations are presented by Fuehrer, Romisch, and Engelke (1981) for estimating the maximum bottom velocity for moving vessels. Power functions are used instead of the exponential forms and are given as

$$\frac{V_b(x)}{V_o} = A\left[\frac{x}{D_p}\right]^{-a} \tag{6}$$

where

$V_b(x)$ = bottom velocity in x-direction at coordinate x

V_o = propeller jet velocity at $x = 0$

A = function of propeller height above bottom and if rudder is present behind propeller

D_p = propeller diameter

a = 0.6 if spreading is limited by bottom and water surface
= 0.3 if spreading is also limited by adjacent wall

The propeller jet velocity can be computed from

$$V_o = 1.6nD_p(K_{to})^{0.5} \tag{7}$$

where

n = propeller speed, revolutions per second

K_{to} = thrust coefficient at zero speed of advance

Often K_{to} is unknown and Fuehrer and Romisch (1977) proposed the relation

$$V_o = 0.95nD_p \tag{8}$$

to obtain V_o to within ±20 percent. Blaauw and van de Kaa (1978) proposed the following relation, which is not dimensionless

$$V_o = C'\left(\frac{P}{D_p^2}\right)^{1/3} \tag{9}$$

where

V_o = propeller jet velocity, m/sec

C' = 1.17 for ducted propellers
= 1.48 for nonducted propellers

P = engine power, kW

D_p = propeller diameter, m

Fuehrer, Romisch, and Engelke (1981) introduce a modified advance coefficient J defined as

$$J = \frac{V}{nD_p} \tag{10}$$

Using the modified advance coefficient, the relation for maximum bottom velocity for maneuvering versus moving navigation was found to be

$$V_{b,max} = V_{b,max,J=0}(1 - J) \tag{11}$$

where

$V_{b,max}$ = maximum bottom velocity for moving navigation

$V_{b,max,J=0}$ = maximum bottom velocity for maneuvering navigation (vessel speed = 0)

The maximum bottom velocity for maneuvering navigation is

$$V_{b,max,J=0} = EV_o \left(\frac{h_p}{D_p}\right)^{-1.0} \tag{12}$$

where

E = 0.25 for inland vessel, tunnel stern, twin rudder gear

h_p = distance from center line of propeller to bottom

Combining Equations 11 and 12 leads to

$$V_{b,max} = E \left(\frac{h_p}{D_p}\right)^{-1.0} V_o(1 - J) \tag{13}$$

Note that this technique addresses only the maximum bottom velocity, not the velocity field, which is of interest in this study. This technique does demonstrate the reduction in velocity that occurs with increasing vessel speed.

Method 2: Verhey

8. Verhey (1983) developed a method for determining the propeller velocities behind a moving vessel. The induced jet velocity for a moving vessel is

$$V_o = \left(V_a^2 + K_t \frac{8n^2D_p^2}{\pi}\right)^{0.5} \tag{14}$$

where

K_t = thrust coefficient (depends on ship speed)

π = 3.1416

V_a = entrance velocity defined as

$$V_a = (V + V_r)(1 - W) \tag{15}$$

where

V_r = return velocity as determined from Schijf (1949), Bouwmeester et al. (1977), or other methods

W = wake fraction (0.3–0.5 for push tows)

The contraction diameter D_o is

$$D_o^2 = D_p^2 \frac{K_t 4n^2 \frac{D_p^2}{\pi}}{V_o(V_o - V_a)} \tag{16}$$

9. The next step is determining the wake velocity, which is the velocity of the water set in motion behind the vessel acting in the same direction as the vessel is traveling. The wake velocity is assumed constant below a horizontal plane at $Z/D_o = 0.5$, where Z is the vertical coordinate measured from the center line of the propeller. Determination of the wake flow is based on the diffusion theory for jets given by Albertson et al. (1950). The wake flow equations are as follows:

a. The zone of flow establishment ($x/D_o \leq 6.2$):

$$V_w = V - (V - V_a) \exp\left[-76.2 \frac{\left(\frac{r}{D_o} + 0.081 \frac{x}{D_o} - 0.5\right)^2}{\left(\frac{x}{D_o}\right)^2}\right] \tag{17}$$

where V_w is the velocity of wake below $Z/D_o = 0.5$.

b. The zone of established flow ($x/D_o > 6.2$):

$$V_w = V - (V - V_a)_{max} \exp\left[-76.2 \frac{\left(\frac{r}{D_o}\right)^2}{\left(\frac{x}{D_o}\right)^2}\right] \tag{18}$$

with

$$\frac{(V - V_a)_{max}}{(V - V_a)} = 6.2 \left(\frac{x}{D_o}\right)^{-1.0} \tag{19}$$

10. The next step is to determine the propeller jet velocity at the desired x and r :

a. The zone of flow establishment:

Let the velocity increment U_2 be defined as

$$U_2 = V_o - V_a \tag{20}$$

Jet velocity is

$$\frac{V_x}{U_2} = \exp\left[-\frac{\left(\frac{r}{D_o} + \frac{Cx}{D_o} - 0.5\right)^2}{2\left(\frac{C(V_o - V)}{V_o}\right)^2 \left(\frac{x}{D_o}\right)^2}\right] \tag{21}$$

where

$$r = \left(y^2 + Z^2\right)^{0.5}$$

y = horizontal distance from the center line of the propeller

C = 0.18

b. The zone of established flow:

$$\frac{V_x}{V(x)_{max}} = \exp\left[-\frac{\left(\frac{r}{D_o}\right)^2}{2\left(\frac{C(V_o - V)}{V_o}\right)^2 \left(\frac{x}{D_o}\right)^2}\right] \tag{22}$$

where $V(x)_{max}$ is the maximum velocity at specified x, $r = 0$ defined as

$$\frac{V(x)_{max}}{U_2} = \left(\frac{2Cx}{D_o}\right)^{-b'} \tag{23}$$

where

$b' = 1 + J_a$

J_a = advance coefficient defined as

$$J_a = \frac{V_a}{nD_p} \tag{24}$$

The resulting bottom velocity in the propeller wash region V_e is

$$V_e = V_x + V_w - V \tag{25}$$

According to Verhey (1983)

> It must be stated that the method presented for calculation of the velocities in the propeller jet behind a sailing vessel is rather rough, compared to the method used to calculate the velocities behind maneuvering vessels. The uncertainties in the wake fraction W, the impossibility of measuring the velocities induced by the propeller alone and the schematizing of the flow field are some of the problems to be solved. Hence, the method presented can only give an indication of the velocities to be expected. It will be obvious that the velocities behind a maneuvering ship will be greater in all cases.

Method 3: Oebius

11. Oebius (1984) presents a method for determining the velocity field behind a moving vessel. The basic equations are as follows:

a. The diameter D_o defined as:

$$D_o = 2(0.67R_f + R_n) \tag{26}$$

where

R_f = blade radius (from outside of hub to blade tip)

R_n = hub radius

b. The zone of flow establishment ($x < x_o$):

$$V_x = V_o \exp\left[-0.5\left(\frac{r - DX}{\frac{D_o'}{2} - DX}\right)^2\right] \tag{27}$$

with the limit of the flow establishment zone x_o given by

$$x_o = 2D_o' \exp\left(1.265\frac{V_i}{V_o}\right) \tag{28}$$

where

D_o' = modified propeller diameter

V_i = velocity at infinity assumed equal to vessel speed

DX = distance from propeller center line to maximum velocity given by

$$DX = 0.32\, D_o'\left(\frac{x}{D_o'}\right)^{-0.1} \tag{29}$$

and the following equation which is not dimensionally correct

$$D_o' = 1.15 D_o V_i^{0.055} \tag{30}$$

c. The zone of established flow ($x > x_o$):

$$V_x = V(x)_{max} \exp\left[-0.5\left(\frac{r - DX}{\Sigma}\right)^2\right] \tag{31}$$

with

$$V(x)_{max} = 1.5V_o\left(\frac{x}{D_o'}\right)^{-\beta} \tag{32}$$

with

$$\beta = 0.6 \exp\left(-1.2\ \frac{V_i}{V_o}\right) \tag{33}$$

and

$$\Sigma = \frac{D_o'}{2} - DX + 0.0875(x - x_o) \tag{34}$$

and x_o according to Equation 28.

Method 4: Balanin and Bykov

12. Balanin and Bykov (1965) presented a method based on a free turbulent jet. However, one of the terms was not defined and this method was not pursued in this study.

Method 5: Hochstein

13. Hochstein and Adams (1986) present an equation for propeller jet velocities derived from equations presented by Blaauw and van de Kaa (1978). The Blaauw and van de Kaa (1978) equations were developed for vessel speed close to zero but Hochstein and others have used the equation in a wide variety of studies for vessels fully underway. The basic equation is

$$V(r) = \frac{CN_p\left(\frac{D_p P}{N_\nu}\right)^{1/3}}{r} \tag{35}$$

where

V(r) = maximum propeller jet velocity at radial distance r from propeller axis, fps

C = coefficient = 1.285

N_p = number of propellers

P = total engine power, hp

The difficulty in using this equation for tows underway is that the coefficient C must be determined for moving vessels. USAED, Huntington (1980b), references measurements on the Ohio River by the Huntington District in the determination of $C = 1.285$. However, most of the measurements were far from the towboat and probably were not the result of the propeller jet. Hochstein and Adams (1986) reference measurements on the Kanawha River that verify $C = 1.285$. Tow speed is implied in the coefficient C . The advantage of this method lies in its simplicity and ease of application.

Displacement and Return Velocity Studies

14. In addition to velocities induced by the propeller jet, the displacement of water by the moving vessel can also create significant vessel-induced velocities whose magnitude is primarily dependent on vessel speed, average channel depth, and the blockage ratio. The primary displacement-induced velocity acts opposite to the direction of travel and is referred to as "return velocity." The displacement-induced return velocity is also accompanied by a lowering of the water level between vessel and bank, which is referred to as "drawdown." This drawdown is greatest near the vessel and is responsible for vessel squat, which causes a vessel to have a reduced under-keel clearance when it is underway. Numerous techniques are available for determining the average return velocity and average water-level drawdown. Three of these will be presented in the following paragraphs. As given in USAED, Huntington (1980a), the approaches are one-dimensional and it is necessary that certain assumptions be made:

a. Constant ship speed, in a channel of uniform trapezoidal or rectangular cross section.

b. Straight channel of infinite length.

c. Uniform cross section of ship, disregarding shape.

d. Uniform return-current velocity around ship in channel cross section.

e. Uniform water-level depression alongside ship in channel cross section.

f. Squat over ship's length equal to water-level depression.

g. Friction losses disregarded.

The Permanent International Association of Navigation Congresses (PIANC) (1987) states that most methods are limited to waterway width/beam width ratios of 2–12 and recommended Schijf for loaded pushtows and Bouwmeester for other ship types.

Method 1: Schijf

15. Schijf (1949) used a conservation of energy approach and developed the equation for average water-level drawdown as

$$1 - \frac{1}{N} - \frac{z}{h} - \left[1 + 2\left(\frac{\frac{z}{h}}{\frac{V^2}{gh}}\right)\right]^{-1/2} = 0 \tag{36}$$

where

z = average water-level drawdown

h = average channel depth = area/top width

g = acceleration due to gravity

and the equation for average return velocity V_r as

$$1 - \frac{1}{N} - \frac{V^2}{2gh}\left[\left(1 + \frac{V_r}{V}\right)^2 - 1\right] - \left(1 + \frac{V_r}{V}\right)^{-1} = 0 \tag{37}$$

The equations have been graphically solved and are presented in Jansen and Schijf (1953). PIANC (1987) presents an alpha factor used to correct the Schijf method to improve the comparison between observed and computed values of drawdown and return velocity. At high enough vessel speeds, return velocities become large enough to reach critical conditions and a self-propelled vessel reaches its so-called limiting velocity, which cannot be exceeded. The Jansen and Schijf (1953) equation for limiting velocity is

$$1 - \frac{1}{N} + \frac{1}{2}\frac{V_{cr}^2}{gh} - \frac{3}{2}\left(\frac{V_{cr}^2}{gh}\right)^{1/3} = 0 \tag{38}$$

where V_{cr} is the limiting velocity for self-propelled ships. This relation has been verified in canals having relatively small values of N (<10) .

Method 2: Bouwmeester

16. Blaauw and van der Knaap (1983) provide a comprehensive evaluation of the various methods and conclude that the Bouwmeester et al. (1977) relation provides the best estimates for average return velocity and average water-level drawdown. The Bouwmeester relation is based on a conservation of momentum and water-level drawdown as shown:

$$\frac{(V + U_o)}{(gh)^{0.5}} = \left\{ \frac{\frac{2z}{h}\left(1 - \frac{1}{N}\right) - \left(\frac{z}{h}\right)^2\left(1 - \frac{b}{B_o}\right) + \frac{2}{3}\left(\frac{z}{h}\right)^3\left(\frac{sh}{B_o}\right)}{\left(\frac{d}{h}\right)^2\left(\frac{1}{N} + \frac{z}{h}\,\frac{b}{B_o}\right) + 2\left[\frac{1}{1 - \frac{z}{h} + \frac{sh}{B_o}\left(\frac{z}{h}\right)^2 - \frac{1}{N}} - 1\right]} \right\}^{0.5} \tag{39}$$

and for return velocity

$$\frac{V_r - U_o}{(gh)^{0.5}} = \frac{\frac{z}{h} - \left(\frac{sh}{B_o}\right)\left(\frac{z}{h}\right)^2 + \frac{1}{N}}{1 - \frac{z}{h} + \left(\frac{sh}{B_o}\right)\left(\frac{z}{h}\right)^2 - \frac{1}{N}} \left[\frac{V + U_o}{(gh)^{0.5}}\right] \tag{40}$$

where

U_o = ambient velocity in undisturbed channel

b = beam of vessel

B_o = surface width of waterway

s = cotangent of side slope angle

d = draft of vessel

The ambient velocity U_o is positive for upbound vessels and negative for downbound vessels.

Method 3: Hochstein

17. Hochstein (1967) developed the equation for return velocity

$$V_r = V[(aB - B + 1)^{0.5} - 1] \tag{41}$$

where

$$a = [N/(N-1)]^{2.5}$$

$B = 0.3\ e^{[1.8(V/V_{cr})]}$ if $V/V_{cr} \leq 0.65$

$e = 2.7183$

$B = 1$ if $0.65 < V/V_{cr} \leq 1$

For Ohio River studies, $B = 1$ was used by Louis Berger and Associates (USAED, Huntington, 1980b), and the basic equation becomes

$$V_r = V\left(\sqrt{a} - 1\right) \tag{42}$$

The limiting speed V_{cr} is determined by Hochstein as

$$V_{cr} = K\left[\frac{gA_o}{B_o}\right]^{0.5} \tag{43}$$

where

K = constrainment factor given in Hochstein and Cohen (1980)

A_o = cross-section area of the waterway

18. The same method for determining the limiting velocity V_{cr} is given in Fuehrer and Romisch (1977). A graph is provided giving the constrainment factor K as a function of $(h/d)(L/b)$ and (L/B_o), where L is the vessel length. The Jansen and Schijf (1953) and Fuehrer and Romisch (1977) relations for limiting velocity are compared in the following tabulation for conditions similar to those on the Ohio River:

L ft*	b ft	h ft	d ft	B_o ft	N	V_{cr} fps
1,000	105	20	9	1,800	38.1	21**
						20†

* A table of factors for converting non-SI units of measurement to SI (metric) units is found on page 3.

** Jansen and Schijf (1953)

† Fuehrer and Romisch (1977)

For a loaded tow sailing on the channel center line, both methods give similar results. The Fuehrer and Romisch (1977) study also describes tests to determine V_{cr} for vessels sailing off the center line in a uniform channel:

$$V_{cr}(\text{off axis}) = V_{cr}(1 - 0.15a') \tag{44}$$

where

a' = eccentricity factor for vessel sailing off channel center line, $z1/(0.5B_o)$

$z1$ = distance from canal axis to vessel

Fuehrer and Romisch also developed equations for the displacement velocity beneath the vessel

$$\alpha_Q = \left(\frac{h - d}{h}\right)\left[1.11 + 5.25\left(\frac{1}{N}\right)^{2.2}\right] \tag{45}$$

where

$$\alpha_Q = \frac{\text{actual discharge under vessel bottom}}{Vhb}$$

$$= \frac{(V + V_{bd})[h - (d + z)]b}{Vhb}$$

where V_{bd} is the displacement velocity beneath the vessel. Note that in Equation 45 the influence of channel size is small except for very low blockage ratios.

19. The variation of the return velocity from vessel to bank is also of importance in this study. Fuehrer and Romisch (1977) present an equation for determining the maximum return velocity

$$\frac{V_{r,max}}{V_r} = \alpha \tag{46}$$

with

$$\alpha = \max\left(1, 0.114\frac{B_o}{b} + 0.715\right) \tag{47}$$

where $V_{r,max}$ is the maximum return velocity at the vessel. α is an empirical shape factor used to increase the average return velocity obtained from either the Bouwmeester, Schijf, Hochstein, or other return velocity relations. For $\alpha < 1.5$, the shape of the return velocity distribution should be represented by a linear function (USAED, Huntington 1980b). Louis Berger and Associates (USAED, Huntington, 1980b) uses the following equation to determine the distribution of return velocity from vessel to bank for $\alpha > 1.5$

$$V_r(y) = V_{r,max} \exp(-y/K2) \tag{48}$$

where

$V_r(y)$ = return velocity as a function of distance from vessel

$K2 = B_{side} / (\alpha \{ 1 - \exp[-F(\alpha)\alpha]\})$

B_{side} = distance from vessel to bank (must be $\geq B_o/6$ according to USAED, Huntington (1980b))

$F(\alpha) = 0.42 + 0.52 \ln \alpha$

20. McNown (1976) states that as the ratio N of waterway cross-section area/vessel cross-section area becomes large (not quantified), the distribution of return velocity becomes nonuniform. Delft Hydraulics Laboratory (1979) presents the distribution of return velocities for a vessel moving both on the channel center line and close to one bank. Results showed a maximum velocity beneath and close beside the vessel. The maximum return velocity was located near the bow for the vessel on the center line and near the rear one-third point for the vessel near the bank. These results agree with the results of McNown (1976) regarding uniformity of the velocity distribution for vessels near the bank and nonuniformity of velocity distribution for vessels far away from the bank.

21. Most of the equations for return velocity assume that the vessel is sailing on the channel center line. Of importance to this study are also conditions where vessels sail off the channel center line. Marchal and Spronck (1977) determine the return velocities for this condition by treating each side of the vessel as being independent of the other side. To determine return velocities, the waterway area used in the predictive equations is equal to two times the area between the vessel center line and the bank on the side

for which the return velocities are being determined. For the side where the vessel is close to the bank, the waterway area used in the return velocity equations will be less than the actual waterway area. For the side with the greater distance from vessel to bank, the waterway area used in the equations will be larger than the actual waterway area. PIANC (1987) presents an equation for determining the effective area for vessels sailing off the channel center line in a prismatic channel. Blaauw et al. (1984) present a plot showing the variation of maximum return velocity with eccentricity.

22. The variation of the return velocities with distance from the vessel may be accompanied by a variation in the vertical velocity distribution. However, Fuehrer and Romisch (1977) observed a nearly uniform velocity distribution from bottom to water surface in the return velocity. They also observed a transition region next to the vessel that had transverse velocities. Blaauw et al. (1984) used the Schlichting (1968) formula for flow over rough plates to define the relationship between return velocity and shear stress.

Tow-Induced Velocities Measured in Field Studies

23. USAED, Huntington (1980a), conducted measurements of about 200 tows on the Ohio River as part of a study concerning the replacement lock at Gallipolis. Two-dimensional electromagnetic meters were used in shallow-water areas near the bank, and a three-dimensional electromagnetic meter was used on the river bottom near the path of the vessels. (One tow came within 16 ft of the meter. All other tows were 52 ft or greater from the three-dimensional meter.) The Huntington study recommends either Hochstein's or Bouwmeester's equation for return velocity. The supplement to the USAED, Huntington (1980a), report by Louis Berger and Associates (USAED, Huntington, 1980b) states that similar results are obtained from Hochstein and Schijf equations for return velocity. The Hochstein relation for return velocity was multiplied by a factor of 1.1 to obtain better agreement with measured values. The USAED, Huntington (1980a), report recommends the Blaauw and van de Kaa (1978) equation for propeller jet velocity. This report states that the area of impact from propeller jet velocities is 60-65 ft wide. Open-wheel propulsion systems were found to increase turbidity more than Kort nozzle systems.

24. Environmental Science and Engineering (ESE) (1981) conducted field

measurement of velocities for 30 tows on the upper Mississippi River and 29 tows on the Illinois River. Two-dimensional electromagnetic meters were installed 1 ft above the bottom at two positions adjacent to the navigation channel, one near the shore and the other near the sailing line. ESE reported that the effects of a tow were generally measurable more than 4 min before the tow reached the instruments. ESE reported that the Hochstein relation for return velocities underestimated the measured bottom velocities by a factor of 2 for nearshore velocities and by an average of 30 percent for offshore velocities. A correction factor was developed to improve the measured versus computed results. ESE pointed out that all comparisons were based on bottom velocities and that depth-averaged velocities would also be underestimated. ESE reported on a comparison of velocities at two depths (total depth 14.5 ft) that showed that the surface return velocity (6 ft below surface) due to tow passage was 1.5 times the bottom velocity (1 ft above bottom) due to tow passage.

25. Bhowmik (1981) conducted field measurements of velocity for 19 tows on the upper Mississippi and 22 tows on the Illinois Rivers. One-dimensional Price current meters were used to obtain velocities at depths of 0.95, 0.8, 0.6, and 0.2 of the depth measured from the surface.

26. Hochstein and Adams (1986) reported on velocity measurements taken on the Kanawha River to check the Hochstein relations for return and propeller jet velocities. Results showed good agreement between the observed data and the Hochstein relations.

Recommendations for Study

27. Based on analysis of the existing literature, the following list recommends areas in which additional study is needed:

a. Relations for propeller jet velocity for moving tows should consider speed in the analysis. Verhey (1983) is the most comprehensive relation but also requires the most input. The width of the propeller jet attack on the bottom for a moving tow needs to be defined.

b. Existing return velocity relations do not provide satisfactory comparisons with field data gathered in large rivers. Return velocity distribution equations need to be developed for tows moving in asymmetric cross sections at various positions across the section. The influence of ambient currents and tow direction needs to be evaluated.

c. The use of velocity in studies of navigation effects needs to be standardized. Consideration should be given to how the velocities are going to be used in the navigation effects studies. For example, in studies of sediment movement induced by navigation, most existing sediment transport relations are based on either shear stress or depth-averaged velocity. Depth-averaged velocity is valid for return velocities in the area between the vessel and the bank. However, depth-averaged velocity is meaningless in areas such as the propeller jet because bottom and surface velocities may be in different directions. In this case, techniques are needed to transfer bottom velocity to either shear stress or an equivalent depth-averaged velocity.

PART III: FLOW VISUALIZATION STUDIES WITH 1:20-SCALE MODEL

28. Flow visualization studies were conducted to gain a better understanding of the flow patterns near a moving vessel. The flume used in these studies represented slack-water conditions having zero ambient flow. Results from this study were primarily in the form of video tapes taken both underwater and from above the moving tow. Velocity vector plots for two of the test conditions and movement tests with lightweight plastic beads were also determined.

29. The physical model used in this study was constructed to a scale ratio of 1:20. The model layout is shown in Plate 1. A winch was located at one end of the model for use in the bead tests only. An array of nails was installed on the floor of the model and yarn strings approximately 0.25 ft (model) in length were attached to the nails 2 ft above the bottom (all dimensions are in prototoype unless stated otherwise). The yarn strings had a fairly significant resistance to movement, and other flow visualization techniques were tried. The best techniques found were dye and lightweight plastic beads. The dye was injected through 1/4-in.-diam (model) copper tubing placed on the channel bottom with 1/64-in.-diam (model) holes drilled in the top of the copper tubing. The plastic beads were used in qualitative movement tests that will be discussed in a later paragraph. The bottom of the model was painted white, and underwater lighting was used to improve light conditions beneath the tow. A cable was placed the full length of the model flume along the sailing line of the tow, and guides on the bow of the lead barge and the stern of the towboat were used to ensure a consistent sailing line. Depth of water ranged from 15 to 30 ft.

30. The 1:20-scale towboat represented a 5,600-hp towboat with twin 9-ft-diam propellers, Kort nozzles, and main and flanking rudders in line with each propeller shaft. The towboat dimensions were 45.6 ft wide by 209 ft long, and the towboat draft was 9 ft for all tests. All tests were conducted with a 0-deg rudder setting, and both propellers were turning the same speed. Looking at the stern of the towboat, the starboard propeller was turning counterclockwise and the port propeller was turning clockwise. Propeller speeds could be varied from 130 to 190 rpm. The 35-ft-wide by 195-ft-long barges drafted 9 ft when loaded and 1.5-2.0 ft when unloaded. The individual barges were lashed together to form a tow up to three wide by three long. The bows

of the lead barges were raked on a radius of 25 ft. The 25-ft radius was extended from the bottom of the barge for a vertical distance of 10 ft. The stern of the rear barges had boxed ends. The model is shown in Figure 1.

31. To ensure the similarity of flow patterns between model and prototype, the model was operated with an equal Froude number in model and prototype. The following relations were used to transfer quantities from model to prototype:

Characteristic	Dimension*	Scale Relations Model:Prototype
Length	$L_R = L_P/L_M$	1:20.0
Weight or volume	L_R^3	1:8,000.0
Time	$L_R^{1/2}$	1:4.4721
Velocity	$L_R^{1/2}$	1:4.4721
rpm	$1/L_R^{1/2}$	1:0.224

* Dimensions are in terms of length ratio.

Reduced scale navigation models have proportionally greater frictional forces than in the prototype. This results in slower tow speeds in the model than in the prototype. For these flow visualization studies, the speed difference was not considered to affect results. Several tests were conducted with a towing mechanism providing all the propulsion.

32. The following observations were made during the flow visualization tests:

a. In front of the tow, water was set in motion in the same direction as the tow. Just in front of the bow of the tow, velocities at the water surface were approximately equal to the tow speed. At the channel bottom, these velocities were reduced and depended on the depth of flow. Velocities 2 ft above the bottom at the bow of the towboat will be referred to as V_{bb} .

b. Just downstream of the bow (beneath the tow), there was a rapid reversal in flow that resulted in flow opposite to the direction of the tow. This flow is related to the displacement effects of the tow, and velocities will be referred to as V_{bd} . The maximum V_{bd} occurred approximately 40 ft behind the bow of the lead barge.

c. V_{bd} decreased toward the stern of the rear barge for the 15-ft depth and stayed about the same for the 30-ft depth. V_{bd} may be influenced by the suction effects of the propellers. The

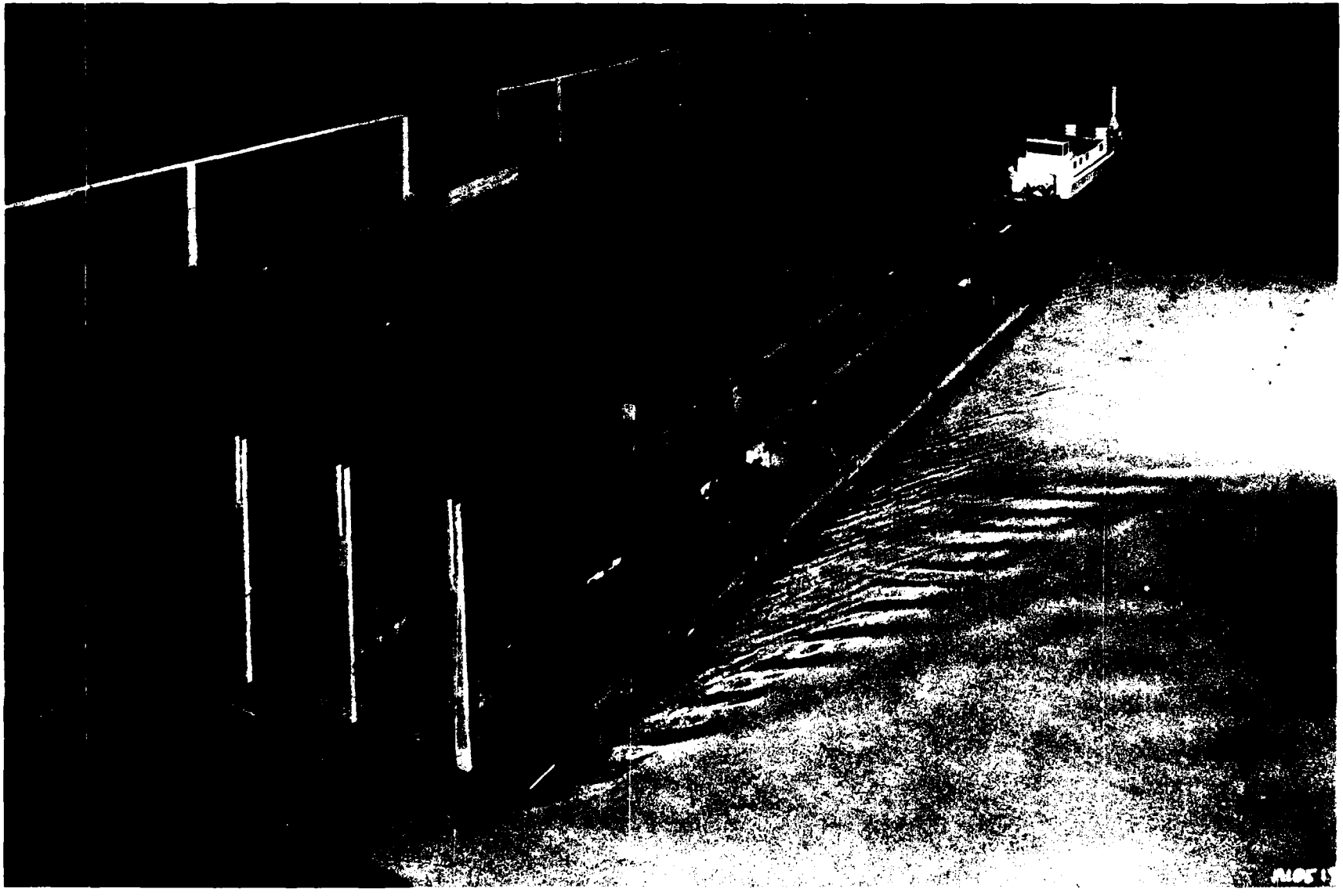

Figure 1. 1:20-scale barges, towboat, and flow visualization flume

magnitude of the suction effect will depend on several factors including the length of the towboat. The model towboat simulates a relatively long towboat (209 ft) and suction effects will be less than for the typical 5,600-hp towboat, which is about 150 ft in length.

d. From the bow to the stern of the towboat, there existed a highly complex flow field, based on observation of the dye movement beneath the towboat. Velocities in this region are influenced by the wake from the upstream barges, suction effects of the propeller, tow speed, depth, and other factors. At the 15-ft depth, flow patterns did not indicate significant velocities in a horizontal plane from the towboat bow to the propellers. However, the dye pointed up as the propellers passed over the dye location. Any velocity measurements taken in this region must be three-dimensional to be valid.

e. Behind the propellers, the dye pointed in the direction of the tow prior to the arrival of the propeller jet. This flow, which is in the same direction as the tow, results from infilling behind the towboat and is referred to as a wake flow.

f. In the propeller wash region, the velocity field is also complex and is generally opposite the direction of tow travel. Velocities are influenced by the wake of the barges and towboat, propeller jet, tow speed, depth, and other factors. Bottom velocities in this zone will be referred to as V_e . The width of the propeller jet attacking the bottom was observed to be about 50 ft, which compares well with the 60-65 ft reported in the Gallipolis study (USAED, Huntington, 1980a). Outside this region, the wake flow behind the barges of the tow creates a velocity field in the same direction as the tow.

g. Several tests were conducted with the propellers not spinning and the towing mechanism providing all the propulsion. These tests demonstrate that the tow sets a large volume of water into motion behind the tow and in the same direction as the tow. This water motion is opposite to the direction of the propeller jet and becomes significant for three-wide loaded tows in shallow water. These effects are accounted for by the term V_w in the Verhey (1983) method.

33. Velocity vector plots were prepared for tow configurations of three wide by three long loaded (Plate 2) and three wide by three long unloaded (Plate 3). The observations described in paragraphs 32a-g are shown in Plate 2. These represent approximate bottom velocity directions and magnitudes adjacent to the moving tow based on observation of the dye patterns. Propeller speed for both vector plots was 185 rpm.

34. Lightweight plastic beads having a specific gravity of 1.03 were used to conduct qualitative estimates of the movement of sediment. The plastic beads had a fall velocity in the 1:20-scale model equivalent to about a 3- to 4-mm quartz sand particle in the prototype. One hundred beads were placed

in a grouping about 2 in. (model) in diameter at various locations with respect to the channel center line. The location of the beads was recorded after each passage of the tow. The following conditions were tested with all tows being loaded:

Configuration Width (W) by Length (L)	Tow Speed mph	Propeller Speed, rpm	Initial Bead Location, ft Off Channel Center Line	Plate
3W × 3L	6.9	185	12.5	4
3W × 3L	6.9	0 (towing test)	12.5	5
3W × 3L	6.9	185	37.5	6
3W × 3L	6.9	185	90.0	7
3W × 1L	8.3	185	12.5	8

Most of the plots are relatively straightforward except for the beads placed at 37.5 ft off the channel (Plate 6). The plot indicates that the beads did not move significantly. However, the underwater camera showed that the beads moved approximately 25 ft opposite to the tow direction due to the displacement flows beneath the barges. The beads were then redeposited in about the original location by the wake flow behind the tow. The beads at 37.5 ft were not moved by the propeller jet.

PART IV: FLOW VISUALIZATION TESTS OF SURFACE CURRENT PATTERNS WITH OLMSTED MODEL

35. Flow visualization tests were conducted in the upper pool of the existing 1:120-scale navigation model of the Olmsted Locks and Dam on the Ohio River. These tests were conducted to determine the effectiveness of conventional flow pattern visualization techniques as applied to visualization of flows generated by moving vessels. These tests used still photography with a 4-sec (model) shutter speed to document the movement of confetti during passage of the tows at various positions in the channel. The overhead camera was positioned 16 ft above the water surface of the model. The 3/4- by 3/4-in. (model) confetti was placed in the slack-water pool, and the test was conducted only after all movement of the confetti ceased. Tests of two channel sizes were conducted: a standard 15-barge tow (105 ft wide by 9-ft draft by 1,150 ft long) operating in a 3,600-ft-wide channel and a standard 15-barge tow operating in a 2,200-ft-wide channel. The scale ratios were 1:120 and 1:70 for the 3,600-ft-wide and 2,200-ft-wide channels, respectively. Tests were conducted under slack-water conditions.

36. Model quantities were transferred to the prototype by means of the following relations:

Characteristic	Dimension*	Scale Relations Model:Prototype	
		1:120-Scale Model	1:70-Scale Model
Length	$L = L_R = \frac{\text{Prototype Length}}{\text{Model Length}}$	1:120	1:70
Velocity	$V = L_R^{1/2}$	1:10.95	1:8.37
Time	$T = L_R^{1/2}$	1:10.95	1:8.37

* Dimensions are in terms of length.

37. A cross section and tow locations for the 1:120-scale channel are shown in Plate 9. Also shown are the limits of the photographic coverage, which was approximately the right half of the channel, and the blockage ratio N . The following tests were conducted:

Test	Scale Ratio	Tow Location	Tow Speed, mph	Distance Moved, ft	Photo
1	1:70	A	7.6	375	1
2	1:70	B	7.5	368	2
3	1:70	C	7.0	345	3
4	1:120	A	10.0	643	4
5	1:120	B	8.7	559	5
6	1:120	C	7.6	488	6

The white lines perpendicular to the tow center line in Photos 1-6 are 480 ft apart in the 1:120 scale and 280 ft apart in the 1:70 scale and can be used to scale distance in both directions. The "distance moved" value in the tabulation refers to the distance the tow moved during the 4 sec (model) that the shutter of the camera was open. For example, in Photo 1a, the *O* shows the position of the bow of the tow when the shutter was opened. The *C* in Photo 1b shows the position of the bow when the shutter was closed. Points *O* and *C* were 375 ft apart, as given in the tabulation. The tow traveled a significant portion of the total photograph, which is important to remember when evaluating the flow patterns.

38. Analysis of the photographs shows that the 1:70-scale tow produced surface movement from tow to bank even for position A, which was farthest from the bank. Significant movement parallel to the tow resulting from return velocities was observed as expected. The 1:120-scale tow produced surface movement only in a width of about 300-400 ft on each side of the tow. Surface movement for the 1:120-scale tow was predominantly away from the tow, and no significant movement parallel to the tow was observed. Quantitatively, the photographs for the 1:70-scale tow can be used to define the distribution of return velocities at the surface. Photos 1, 2, and 3 were used to define the maximum velocity parallel to the tow, and results are shown in Plates 10, 11, and 12, respectively. To determine velocity, the length of the confetti streak was scaled off the photograph. This length was divided by the prototype time that the camera shutter was open or $4(\sqrt{70}) = 33.5$ sec. The surface velocities are roughly equal to the depth-averaged velocities and can be compared to the computed average return velocities using the Bouwmeester relation (average for entire cross section).

PART V: 1:20-SCALE PHYSICAL MODEL INVESTIGATION OF BOTTOM VELOCITIES NEAR THE PATH OF A MOVING TOW

Description

39. The 1:20-scale physical model tow was used to measure velocities near the path of a moving tow. A sketch showing model limits is shown in Plate 13. Also shown in Plate 13 are the locations of the velocity meters used in the study. Three channel types were used in this study representing navigation in an unconfined channel, navigation near one bank, and navigation on the center line of a confined channel. A channel cross section at the velocity meter location shown in Plate 13 is shown in Plate 14.

40. Details of the 1:20-scale tow are given in paragraph 30. The thrust coefficient for the propellers at zero speed of advance equals 0.51. The Kort nozzles on the model towboat were removed to conduct several open- wheel runs. Results from the open-wheel tests were qualitative because the propellers were designed for Kort nozzles. The unconfined channel tests were conducted with the port propeller turning counterclockwise (as viewed from the rear of the towboat) and the starboard propeller turning clockwise. At this point in the study it was determined that the propellers of most towboats rotate in the opposite direction to that used in the unconfined channel tests. The propellers were switched for the near-bank and confined channel tests.

41. The scale relations are the same as those given in paragraph 31. Because excess frictional forces are present in scaled navigation models, an added force is required in the model to obtain equivalent speeds in model and prototype. In this investigation, a towing mechanism was used to provide the added force and, because of the limited model length, ensure a constant vessel speed while the model tow was in the test section.

42. Two-dimensional electromagnetic velocity meters were initially placed in the model, but the measured velocities fluctuated rapidly when the tow was in the vicinity of the meters. This occurred even when the tow was not moving. Further investigation of the velocity meters revealed that the frequency response was not fast enough to monitor the rapid changes that were taking place in both velocity magnitude and direction. A Nixon series 400 propeller meter having a rotor diameter of 0.038 ft (model) was tested in the model. A strip-chart recorder was used to record output from the Nixon

meter. Exhaustive tests to determine the frequency response of the system were not conducted, but measured velocities were compared with flow patterns observed beneath the vessel. At the bow of the loaded tow traveling in 15 ft of water, a rapid flow reversal occurred when velocities changed from positive to negative in about 0.5 sec. The velocity metering system captured this flow reversal, showing that the response was adequate for this study. The propeller meter could not measure direction and had a threshold velocity of about 0.5 fps (0.1 fps in model).

Test Results

43. Tests conducted for the three cross-section types are summarized in Tables 1-3. The limited model length prevented testing tows longer than two barges long plus the towboat. In many tests the limited model length required that the tow be stopped and the test ended before the observed velocites approached zero. The observed velocity plots shown in Appendix A are explained by a master legend, and the relationship between velocity meter reading and prototype velocity is given in Table A1. Multiple tests were conducted for each combination shown in Tables 1-3, and a representative test was selected for each combination. The observed velocities for selected tests for the three cross-section shapes are shown in Appendix A. Tests 1-40 are for the unconfined channel. Tests 114-231 are for the near-bank tests. Tests 300-330 are for the confined channel tests.

44. A series of tests were conducted with the near-bank channel configuration to determine the distance from the tow at which the velocity 6 in. above the channel bottom was equal to 0.5 fps. These tests were conducted on the side of the tow opposite the near bank. Because the velocity meter could not measure velocities this low, dye was injected 6 in. above the channel bottom and the time required for the dye to traverse a fixed distance was used to determine these velocities. Results were as follows:

Test No.	Depth, ft	Tow Speed fps	Distance from Cable or Tow Center Line, ft	Velocity 6 in. Above Channel Bottom, fps
200	15	6.7	300	0.5
201	15	11.2	850	0.5
208	30	6.8	130	0.5
209	30	11.4	190	0.5

45. The following observations were made about the model velocities near the path of the vessel:

a. For equal vessel and propeller speeds, the unloaded tow produced higher propeller jet bottom velocities than did the loaded tow. This is very likely the result of the wake flow (which acts opposite to the propeller jet) being stronger behind the loaded tow. In reality, for equal propeller speeds, the unloaded tow would be going faster than the loaded tow and propeller jet velocity at the bottom for the unloaded tow would be reduced. This reduction would be the result of two factors. (1) the speed of the propeller jet relative to the bottom would be reduced; and (2) the higher speed would produce a larger wake flow, also counteracting the propeller jet velocity at the bottom.

b. For loaded tows, the maximum center-line displacement velocities were only slightly less than the maximum center-line propeller jet velocities (both 2 ft above bottom). However, the higher turbulence intensity of the propeller jet will cause the propeller jet to have a greater transport capacity.

c. At equal channel depths, bottom center-line displacement velocities were relatively unaffected by the change in channel cross-section, which means that return velocity was not contributing to the total velocity for the blockage ratios used in this study.

d. Velocities outside the vessel (measured 27.5 ft from the edge of the barge) were significiantly influenced by blockage ratio, which means that return velocity was contributing to the total velocity.

e. The towing tests (propeller speed of 0) demonstrated that a large wake flow develops behind a vessel. The wake flow moved in the same direction as the vessel and persisted for relatively long periods of time.

f. The effects of tow length could not be defined because of the limited range of this parameter. The tests of open-wheel versus Kort nozzle were also inconclusive since only Kort nozzle type propellers were available.

g. The direction of velocities behind the towboat measured 26 ft from the center line was not well defined. The dye injections demonstrated that this is a borderline area for the influence of the propeller jet, which means that the observed velocity could have been a wake flow.

h. Bow velocities were always less than the displacement velocity, but for loaded tows traveling in shallow water, the bow velocities were as high as 2.5 fps.

PART VI: PROTOTYPE DATA COLLECTED BY USAED, LOUISVILLE

46. Prototype tests were conducted by USAED, Louisville, in 1987 at Ohio River mile 581. The tests were conducted with leased towboats to obtain data regarding velocities near the river bottom at a limited number of depths. The details of the prototype tests conducted by USAED, Louisville, are shown in Tables 4-6. Three different tow configurations are represented by the prototype tests: (a) towboat behind one unloaded barge (*Steve Kuhr* (all tests), *John Matthews* (all tests), *Harold Turner* (tests 01-04)), (b) towboat behind one loaded barge which is smaller than the towboat (*Harold Turner* (tests 05-08)), and (c) towboat operating in wake region of three-wide loaded barges (*Harold Turner* (tests 09-13)). A cross section showing the tow locations, cross-sectional areas, and widths is shown in Plate 15. As in the physical model, measurement of velocities beneath a moving tow in the prototype is a difficult task. Directions and magnitudes change rapidly and the two-dimensional electromagnetic velocity meters used in the prototype may not have been fast enough in their frequency response to capture the changes occurring under the vessels. The meters were positioned to measure velocities in the horizontal plane only.

47. A summary listing of the observed prototype velocities is given in Table 7. This listing presents the velocity magnitude and direction for five points along the tow. These five points are shown in Plate 2. Each entry represents the maximum observed for that location. The entries with a *??* could not be described by a single value. The following presents observations about each of the five locations:

a. Bow velocities. Bow velocities are those ahead of a tow. For loaded tows, these velocities can extend a considerable distance in front of the tow. For the four tests (*Harold Turner* tests 05-08) having a one-wide loaded barge (35 ft wide) in 22 ft of water, the average distance ahead of the tow in which the bow affected the measured bottom velocity was about 300 ft. For the five tests (*Harold Turner* tests 09-13) having three-wide loaded barges (105 ft wide) in 22 ft of water, the average distance was about 550 ft. This shows that for the tests with one unloaded barge, the bow velocity caused by the towboat can extend upstream of the bow of the unloaded barge.

b. Displacement velocity near bow of barge(s). This location was selected because this was the location of the maximum displacement velocity in the physical model. Similar to the bow velocities, the displacement velocities for the tests with one unloaded barge were affected by the bow effect from the towboat.

Most of the upbound tows caused an increase in the bottom velocity above the ambient velocity in a direction opposite the tow. This was consistent with the observation of displacement velocity in the physical model. Displacement velocity for the downbound tows was far less consistent. Some of the tows created an upstream velocity (*Steve Kuhr* test 06) or a reduction in the ambient velocity (*Steve Kuhr* test 08). Both of these results were anticipated, based on observation of the physical model. But in some of the downbound tests, the displacement velocities were in the downbound direction (*John Matthews* tests 04 and 10), which is opposite to observations in the physical model. This may have been the result of the bow effect from the towboat. In the *Harold Turner* three-wide downbound tests (tests 9, 11, and 13), the displacement velocities approached zero, which was radically different from the upbound tests and from observations in the physical model.

c. Displacement velocity near stern of barge(s). This location was selected to define the combined effect of displacement velocity, suction effects of the propellers, and the bow wave at the front of the towboat for tests with one unloaded barge.

d. Velocities entering the propellers. These velocities are the result of the suction effects in the propellers, the displacement effects of the towboat, and the wake effects of the barges. Only suction and displacement effects occur for the tests having one barge ahead of the towboat, and both effects are in a direction opposite the tow direction based on observation of the physical model. In the upbound tests, the velocities are downstream for most of the tests as expected. In the downbound tests, many of the tests have velocities in an upbound direction. But in several of the downbound tests (*Steve Kuhr* test 08; *John Matthews* tests 02 and 04; *Harold Turner* tests 02, 04, 06, 08, 11, 13), velocities are in the same direction as the towboat, which is opposite to the expected direction or the direction observed in the upbound tests. It should be noted that the velocities beneath the towboat were the maximum observed at any of the five locations in the prototype tests. It was also noted that dye injection in the flow visualization tests showed strong vertical components near the propellers, and two-dimensional velocity measurements were suspect in this region.

e. Velocities in propeller wash. These velocities are the result of two opposing velocities. The propeller jet acts in a direction opposite to the tow direction. The wake flow velocities act in the same direction as the tow. Most of the downbound tests had bottom velocities in a downstream direction, which is opposite that observed in the physical model. Only *John Matthews* tests 02 and 04 had propeller wash velocities opposite the tow direction. For the upbound tows, about half of the tows had downstream propeller wash, but magnitudes were less than 0.3 fps. For the other upbound tows, the propeller wash was skewed in a generally upstream direction.

48. Based on data from this set of prototype tests, the variations between flow direction in model and prototype suggest three possibilities:

a. The flow direction indicated by the prototype meters is incorrect.

b. The understanding of velocities around moving tows is incorrect.

c. The tow was not centered over the meter and the wake flow was measured, not the propeller wash.

PART VII: DEVELOPMENT OF PREDICTIVE RELATIONS

49. Using model and prototype data, predictive relations were developed for the following three areas:

a. Return velocity for vessels sailing off the channel center line in nonprismatic channels.

b. Propeller jet velocities for moving tows.

c. Velocities immediately beside and beneath the vessel due to displacement effects.

In these relations the following sign convention will be used: (a) downstream flows are positive, (b) upstream flows are negative, and (c) for slack-water conditions, flows opposite tow direction are positive. All velocities are assumed to act parallel to the axis of the channel, which is the same as the tow, and tow-induced and ambient velocities are added or subtracted, depending on direction.

Return Velocities

Method 1: Effective Area Method

50. Two methods of computing return velocity were developed in this study.

51. Return velocities were determined in this analysis using the Bouwmeester et al. (1977) method. Modifications were required to determine the effective area for vessels sailing at any distance off the channel center line and/or in a natural channel cross section. Marchal and Spronck (1977) treated each side of the vessel as being independent of the other for the vessel sailing off the channel center line. Using this assumption, the waterway area used in the Bouwmeester equation would be twice the area of the side for which return velocity is being computed. This assumption was tested using the Olmsted model data shown in Plates 10-12. The average return velocities were computed using the Bouwmeester method for the left and right sides of the vessel using effective area $2 \times A_{side}$ and effective width $2 \times B_{side}$ and are shown in the following tabulation:

Tow Location	Computed $V_{r,\ Left}$ fps	$N_{Left} = \frac{2A_{Left}}{A_m}$	Computed $V_{r,\ Right}$ fps	$N_{Right} = \frac{2A_{Right}}{A_m}$
A	0.35	45	0.40	37
B	0.31	51	0.45	31
C	0.19	69	1.1	13

Note: A_{Left} = waterway area on left side of vessel.
A_m = submerged cross-sectional area of midship section.

The comparison with the model data is good with the exception of $V_{r,\ Right}$ at tow location C. The measured return velocities are less than the computed, indicating that a portion of the return flow on the right side is either going under the vessel or passing to the left (in front) of the vessel. One way to handle this is to define an effective area A_{eff} and effective width B_{eff} that should be used when the vessel sails close to a bank line. PIANC (1987) presents a method for determining an effective area for vessels sailing off the center line, but this method is applicable only to prismatic channels. A method is needed that can define an effective area and width for any shape of channel when the vessel sails near the bank. The empirical relation used herein is

$$A_{eff} = A_{factor}\ (2A_{side}) \tag{49}$$

where

A_{eff} = effective area for determining return velocity for vessels sailing near a bank line

A_{side} = area of side for which return velocity is being computed

$A_{factor} = [A_o/(2A_{side})]^P$

P = empirical coefficient

The effective width is determined by

$$B_{eff} = B_{factor}\ (2B_{side}) \tag{50}$$

where

B_{eff} = effective width for determining return velocity for vessels sailing near a bank line

$B_{factor} = [B_o/(2B_{side})]^P$

B_{side} = surface width of side for which return velocities are being computed

Note that the A_{factor} and B_{factor} equal 1 for a vessel sailing on the center line of a prismatic channel. The average depth is computed from

$$h = \frac{A_{eff}}{B_{eff}} \tag{51}$$

Blockage ratio and then return velocity are computed for each side of the vessel. To determine P, it is known that $P = 0$ for all $N_{side} \geq 31$, where N_{side} is the blockage ratio for each side of the vessel, based on the results in the tabulation. For $V_{R,\ right}$ at location C of the Olmsted data, various P values were tested and $P = 0.475$ resulted in good agreement between observed and calculated values. Plotting these data in Plate 16 with P versus N_{side} defines a tentative relationship for determination of A_{eff} and B_{eff} for vessels sailing in channels having low N_{side}. More data are needed to refine this relationship, but good correlation was found using this effective area to compute Schijf's limiting velocity and the method developed by Fuehrer and Romisch (1977) given by Equation 44.

Method 2: total area method

52. One of the problems associated with the effective area method is that in some cases the return velocity equations show that the ship is traveling at speeds greater than the critical speed when the tow is close to one bank. When this happens, no solution is obtained. In the total area method, the average return velocity is computed for the entire cross-section and then this value is proportioned on the port and starboard sides of the vessel (V_{rs}) depending on the position of the tow in the cross section. This technique eliminates almost all of the critical speed problems associated with method 1. Another problem with method 1 involves the use of the Bouwmeester equation in an asymmetric channels. One of the required inputs for Bouwmeester is the bank slope, which can be difficult to define in an asymmetric channel. For that reason, method 2 used the original Schijf (1949) equation (without correction) since it requires only h, N, and V. Using data shown in Table 8 from the Delft Hydraulics Laboratory (1979) and from

1:35- and 1:70-scale models reported in Maynord* the following equation was obtained

$$\frac{V_{rs}}{V_r} = 0.42 \text{ skew} + 0.58 \tag{52}$$

where skew = $A_o/(2A_{side})$. Method 2 was used to compute the Olmsted model conditions given in Plates 10-12 as follows:

Tow Location	Computed V_r	
	Left	Right
A	0.35	0.38
B	0.32	0.40
C	0.26	0.61

Agreement with the observed data is good but additional data are needed.

53. Once the average return velocity for each side of the vessel is determined, the distribution from vessel to bank is needed. Using data from the Delft Hydraulics Laboratory (1979) and the 1:35- and 1:70-scale models (Table 8), the ratio of maximum return velocity near the vessel V_{rsm} to the average return velocity for the side of the vessel was found to have the following relationship:

$$\alpha = \frac{V_{rsm}}{V_{rs}} = 0.024(N_{side}) + 0.75 \tag{53}$$

where $N_{side} = \frac{2A_{side}}{A_m}$

This relationship is similar to Fuehrer and Romisch (1977) except that an area ratio (N_{side}) is used rather than a width ratio. The ratio α was found to be a good parameter for defining the type of velocity distribution as follows:

---

* S. T. Maynord. 1989 (May). "Return Velocity Distribution and Flow Visualization for Commercial Navigation," letter report, US Army Engineer Waterways Experiment Station, Vicksburg, MS.

α Value	Distribution	Equation
$\alpha \leq 1.0$	Uniform	$V_r(y) = V_{rs}$
$\alpha > 1.0$	Exponential	$\frac{V_r(y)}{V_{rs}} = \alpha \exp\left[-C\left(\frac{y - b}{B_{side} - b}\right)\right]$

where $C = 2(\alpha - 1)$. Additional data are needed to better define the relationship of C and α .

Propeller Jet Velocities

54. Both the Verhey (1983) and Oebius (1984) methods for propeller jet velocities were evaluated using some of the physical model results. The Verhey method, which includes the wake effects found to be significant in this study, gave the most realistic results. For these reasons the Verhey method was chosen for further testing and development using the physical model data. The following presents several modifications and how input parameters were defined in the Verhey method:

a. The following propeller thrust coefficients at zero speed of advance from Prosser (1986) are used in the Verhey method:

Pitch/propeller diameter	0.8	0.9	1.0
K_{to} (Kort nozzle)	0.37	0.44	0.51

b. The Verhey method was calibrated to velocities 2 ft above bottom only.

c. The wake coefficient was defined as

$$W = \text{Maximum of} \begin{cases} 0.4\left(\frac{d}{Dep}\right) + 0.04\left(\frac{b}{Dep}\right) \\ \text{or} \\ 0.3 \end{cases} \quad (54)$$

where Dep is the local depth of flow. Draft and beam are for either the barges or the towboat, whichever has the maximum cross-sectional area. This results in values of W ranging from 0.3 to 0.52 for typical drafts $\leq$ 9 ft, depth $\geq$ 15 ft, and beam $\leq$ 105 ft.

d. Advance coefficient J_a is specified ≤ 1 and is used to modify the thrust coefficient at zero speed of advance according to

$$K_t = K_{to}(1 - J_a) \tag{55}$$

e. The Verhey method is modified to account for two propellers and uses distance from each propeller to determine velocity from each propeller and then adds the two velocities together as shown in Plate 17. The combined velocities are limited to the maximum velocity in the jet.

f. Verhey uses the contraction diameter D_o to define the strength of the wake flow at the channel bottom. A better representative size would depend on the vessel cross section and the water depth. Conceptually the strength of the wake at the bottom behind the vessel will increase for increasing vessel cross section and will decrease for increasing clearance beneath the vessel. Several relations were tried and the following empirical relation was found to give satisfactory characteristic dimension of the wake flow strength:

$$DW = 0.1 \left(\frac{bd}{Dep - d} \right) \tag{56}$$

Beam and draft are for either the barges or towboat, whichever has the maximum cross-sectional area.

g. The coefficients C and b' are used in the Verhey method to compute the propeller jet contribution to the total velocity. The coefficient C varies the location where the maximum jet velocity occurs, and the coefficient b varies the magnitude and rate of decay downstream of the propellers. Verhey used the relation $(V_o - V)/V_o$ to reduce C for the moving tow. Results from the physical model demonstrated a better correlation with a parameter frequently used in propeller jet studies, distance from propeller axis to channel bottom/propeller diameter. The empirical relation developed for C is

$$\text{Maximum of} \quad C = 0.17 - 0.39 \frac{h_p}{D_p} \quad \text{or} \quad C = 0.04 \tag{57}$$

This C was used in Equations 21-23. The coefficient b' was found to vary with advance coefficient J_a and h_p/D_p according to

$$b' = 0.52 + J_a + 0.24 \left(\frac{h_p}{D_p}\right) \tag{58}$$

Variation of C and b' with h_p/D_p accounts for the limited jet spreading that occurs because of the channel bottom.

55. A comparison of velocities calculated with the Verhey method with physical model velocities is shown in Plates 18-25. The Verhey method was not compared to the prototype data due to the uncertainty of the prototype tow location.

Displacement Velocity Near Vessel

56. Velocities generated at the bow of the vessel V_{bb} in the same direction as the vessel were used in the analysis of the following equation

$$V_{bb} = f(V, Dep, d, b) \tag{59}$$

When grouped into dimensionless parameters

$$\frac{V_{bb}}{V} = f\left(\frac{d}{Dep}, \frac{b}{Dep}\right) \tag{60}$$

Channel size and return velocity effects were found to be small when data from the three physical model channel sizes were compared and were not used in the analysis. The resulting best-fit equation based on the physical model data for bow velocity is

$$\frac{V_{bb}}{V} = 0.18 \left(\frac{b}{Dep}\right)^{0.6} \left(\frac{d}{Dep}\right)^{1.64} \tag{61}$$

Observed and predicted prototype and model bow velocities are listed in Tables 9 and 10, respectively. Because of the bow effects of the towboat for the tests with one unloaded barge, the only prototype tests that can be compared to the model derived regression equations are *Harold Turner* tests 05-13. The observed prototype values (Table 9) compare reasonably well with computed values from the model derived equation.

57. Even in extremely wide waterways having essentially zero average return velocity, tow movement can create significant displacement velocities immediately beside and beneath the barges and towboat. The magnitude of these velocities will be dependent primarily on the water depth, tow draft, beam, and vessel speed. The analysis of Fuehrer and Romisch (1977) in Equation 45 was tested, but results showed that the beam width is also an important parameter, even in wide waterways. A comparison of bottom velocities from similar vessels in the unconfined, one near-bank, and confined channels is shown in Table 11. The velocity immediately beneath the vessel V_{bd} at the axis of the vessel is relatively independent of channel size and return velocity. The Fuehrer and Romisch equation also shows this due to the limited influence of $1/N$ in Equation 45. A regression analysis of the physical model data was conducted using the following dimensionless ratios

$$\frac{V_{bd}}{V} = f\left(\frac{b}{Dep}, \frac{d}{Dep}\right) \tag{62}$$

and resulted in the following equation

$$\frac{V_{bd}}{V} = 0.16 \left(\frac{b}{Dep}\right)^{0.54} \left(\frac{d}{Dep}\right)^{0.68} \tag{63}$$

Observed and predicted prototype and model velocities are shown in Tables 12 and 13, respectively. Similar to the bow velocities, the prototype displacement velocities observed for the one unloaded tow cannot be compared to the model relations because of the towboat influence. Again only the *Harold Turner* tests 05-13 can be compared to the model-derived relations for displacement velocity. In every case, the model relations overestimated the center-line displacement velocities observed in the prototype. These

differences between model and prototype velocities are likely caused by a combination of the following factors:

a. The velocity meter was 15 in. above bottom in the prototype and 24 in. above the bottom in the model.

b. The effects of ambient flows are unknown. All model tests were conducted in slack water. Prototype upbound and downbound tests exhibited significant differences. In this analysis the ambient flows were added or subtracted from the observed velocity depending on tow direction.

c. The model velocity meter had a threshold velocity of 0.5 fps, which means that model regression analysis did not have data below this value while much of the prototype data were below this value.

d. The bottom roughness was greater in the prototype. This will move the higher velocities away from the channel bottom.

e. Most importantly, the prototype meter did not have a very fast frequency response and was not capturing the peak velocity that occurs near the bow of the barges. For this reason the model-derived relation is retained for estimating velocities in the prototype.

58. Velocities immediately adjacent to the moving vessel will also be significant even in waterways having negligible average return velocity. Comparison of the velocities measured 27.5 ft from the edge of the barges (V_{out} in Table 11) shows that the channel size is a significant parameter, or stated otherwise, that the return velocity is contributing to the total V_{out} . V_{out} is similar to $V_{r,max}$ used by Fuehrer and Romisch (1977) with one important difference. V_{out} is a bottom velocity whereas $V_{r,max}$ is a depth-averaged velocity. It is likely that the depth-averaged velocity and the bottom velocity at 2 ft are relatively close because the boundary layer has not grown. Determination of V_{out} will require the following type of analysis:

$$V_{out} = f(\text{displacement velocity}) + f\begin{pmatrix}\text{return velocity or}\\ \text{blockage ratio}\end{pmatrix} \qquad (64)$$

which is similar to the approach given by Fuehrer and Romisch (1977) for velocities beneath the vessel. The problem with this approach is that model and prototype data are not available to evaluate this approach fully Initially, this approach was discarded and the following relation used by Fuehrer and Romisch (1977) was evaluated:

$$\frac{V_{out}}{V_r} = f\left(\frac{B_o}{b}\right) \tag{65}$$

The correlation between these two parameters was very poor. An approximation was used that allowed evaluation of Equation 64. The same factors driving V_{bd} in Equation 63 were assumed to drive the f(displacement velocity) term in Equation 64. Data were needed that had a negligible contribution from the term f(blockage ratio) in Equation 64. The only data meeting this requirement were the *Steve Kuhr* and *John Matthews* prototype data that were discussed in Part VI. From this prototype data the coefficient in the f(displacement velocity) term was derived

$$\frac{V_{out}}{V} = 0.06\left(\frac{b}{Dep}\right)^{0.54}\left(\frac{d}{Dep}\right)^{0.68} + f(\text{blockage ratio}) \tag{66}$$

Note that $(b/Dep)^{0.54}(d/Dep)^{0.68}$ was taken from the equation for V_{bd}. The next step in the analysis was to subtract the first term of the right side of Equation 66 from the observed V_{out}/V for all of the physical model data and the *Harold Turner* prototype data. This left the term f(blockage ratio), which was evaluated as a function of the blockage ratio N. The resulting equation is

$$\frac{V_{out}}{V} = 0.06\left(\frac{b}{Dep}\right)^{0.54}\left(\frac{d}{Dep}\right)^{0.68} + 1.24\left(\frac{1}{N}\right) \tag{67}$$

Observed and predicted model and prototype velocities are compared in Table 14. Computed prototype values were generally larger than observed and may have been a result of uncertainty in the location of the tow relative to the meter as well as other factors mentioned in paragraph 57.

Relationship Between Velocity and Shear Stress

59. The force/unit area or shear stress is often a more descriptive parameter than bottom or depth-averaged velocity. For a given shear stress,

bottom velocity varies widely depending on distance from the bottom. Most sediment transport relations are based on shear stress. Only a few are based on velocity, and most of these use depth-averaged velocity. Shear stress has rarely been easily or accurately estimated from a single point velocity or depth-averaged velocity. Relations (to be discussed subsequently) exist to do this, but the problem lies in their application. With most open-channel flow problems, the boundary layer is fully developed and extends from the bottom to the water surface. For vessel-induced flows, the boundary layer has not become fully developed, which makes the determination of shear stress more difficult and the use of velocity less reliable. The following paragraphs present methods for determining the relationship between shear stress and the velocities induced by the vessel:

a. Return velocities from vessel to bank. This method (Blaauw et al. 1984) uses the equation

$$\tau = \frac{1}{2} C_{fr} \rho V_r^2 \tag{68}$$

where

τ = shear stress

C_{fr} = local skin friction coefficient

ρ = water density

The local skin friction coefficient is defined by Schlicting (1968) as

$$C_{fr} = \left(2.87 + 1.58 \log \frac{X}{k_s}\right)^{-2.5} \tag{69}$$

where

X = distance from beginning of boundary layer development to maximum velocity

k_s = equivalent sand roughness

= 3 to 4 d_{50}

Blaauw et al. (1984) define X as

$$X = \frac{V_r}{V_r + V} L \tag{70}$$

where L is the ship length. Equations 68–70 provide a method of transferring return velocity into shear stress acting on the channel bottom.

b. Propeller jet velocity. In the same method as in subparagraph a, Blaauw and van de Kaa (1978) define $C_{fr} = 0.06 - 0.11$ for propeller jet flow. In a later study Verhey (1983) says that C_{fr} can vary from 0.06 to 0.36. The higher values of C_{fr} in the propeller jet versus the return flow are due to the higher turbulence levels. Bottom velocity from the propeller jet equations is used in Equation 68. The distance from the beginning of the propeller jet velocity to the maximum propeller jet velocity is approximately four times the clearance from the bottom of the propeller to the channel bottom. A local skin friction coefficient of two to three times the value obtained from Equation 69 is recommended for propeller jet flows.

c. Displacement velocities beneath vessel. The distance from the flow reversal at the bow of the lead barge to the point of maximum velocity due to the displacement current is three to four times the clearance beneath the bottom of the barge. This distance is used for X , and Equations 68 and 69 are proposed for determining the shear stress caused by the displacement flow beneath the vessel.

PART VIII: SUMMARY AND CONCLUSIONS

60. Analysis of the existing literature demonstrated the following needs relative to navigation effects in large waterways found in many parts of the United States:

a. Propeller jet (wash) velocity is strongly affected by tow speed, and any predictive relation should consider speed explicitly. The width (if any) of propeller jet attack on the channel bottom needs to be defined.

b. Return velocity relations need to be applicable to vessels moving in asymmetric channels at various positions in the cross section with various ambient velocities.

c. The use of velocity in navigation effects studies needs to be standardized, and methods are needed for converting velocity to bed shear stress.

61. Using flow visualization and model and prototype measurements, this investigation has demonstrated the following flow patterns near the path of a moving tow:

a. Bow velocities. Bow velocities are dependent primarily on the water depth, draft, beam width, and vessel speed. Bow velocities act in the same direction as the vessel and have been recorded as far as 550 ft in front of the vessel for three-barge-wide loaded tows in 21 ft of water. Maximum bow bottom velocities occurred just beneath the bow of the vessel and were up to 2.9 fps for a three-barge-wide loaded tow traveling in 15 ft of water.

b. Center-line displacement velocites. Center-line displacement velocity V_{bd} under the barges or the towboat is also primarily dependent on water depth, draft, beam width, and vessel speed. V_{bd} acts opposite the direction of the tow and reached a maximum at a location three to four times the clearance beneath the vessel downstream from the bow. Maximum V_{bd} exceeded 4 fps for a three-barge-wide loaded tow traveling in 15 ft of water.

c. Velocities beneath towboat. Velocities in this region are affected by many factors including wake flow from barges, flow entering propellers, and displacement velocity from the towboat. Flow near the propellers is highly three-dimensional, and neither the model or prototype velocity measurements can be considered reliable in this zone. Flow visualization demonstrated that the yarn strings and dye used as indicators pointed straight up as the propellers passed over the indicator position.

d. Propeller jet velocities. Velocities in the propeller wash region are affected by many factors including wake flow from barges and towboat, propeller type, size and speed, open wheel or Kort nozzle, water depth, and tow speed. For the moving tow,

these factors combine to produce a relatively narrow propeller jet path (60 ft wide) moving opposite to the tow and, on each side of the propeller jet, a wake flow moving in the same direction as the tow. The 60-ft width of propeller jet needs better definition regarding the effects of such factors as tow speed, towboat size, and propeller speed and size.

e. Velocities outside path of vessel. Unlike the velocities beneath the vessel, velocity outside the path of the vessel was significantly affected by channel size, meaning that the return velocity was contributing to the total velocity.

62. Predictive relations were developed for return velocities, propeller jet velocities, and displacement velocities. For vessels sailing off the channel center line and/or in nonprismatic channels, two methods were developed so that average return velocity could be computed for each side of the vessel. A method was proposed for estimating the distribution of return currents from vessel to shore. Additional studies are needed to define the influence of ambient currents. Photographic techniques were demonstrated as being an effective tool for determining the distribution of return velocity.

63. The Verhey (1983) method for propeller jet velocities was applied using the physical model data. Several empirical coefficients required in the Verhey method were determined from the physical model data. The primary advantages of this method are the incorporation of vessel speed and the wake flow effects in determining propeller jet velocity.

64. After the appropriate physical parameters were selected, empirical relations were developed for bow velocity, displacement velocity beneath the vessel, and velocity outside the path of the vessel.

65. Relations were presented for determining the relation between velocity and shear stress that are based on accepted boundary layer theory.

REFERENCES

Albertson, M. L., Dai, Y. B., Jensen, R. A., and Rouse, H. 1950. "Diffusion of Submerged Jets," Transactions, American Society of Civil Engineers, Vol 115, Paper No. 2409, pp 639-697.

Balanin, V. V., and Bykov, L. S. 1965. "Selection of Leading Dimensions of Navigation Canal Sections and Modern Methods of Bank Protection," Twenty-first International Navigation Congress, Permanent International Association of Navigation Congresses, Stockholm, Section 1, Subject 4, pp 151-170.

Bergh, H. 1981. "The Influence on Harbors of the Action of the Jet Behind a Propeller," Bulletin No. TRITA-VBI-104, Hydraulics Laboratory, Royal Institute of Technolcgy, Stockholm, Sweden.

Bhowmik, N. G. 1981. "Resuspension and Lateral Movement of Sediment by Tow Traffic on the Upper Mississippi and Illinois Rivers," Contract Report 269, Illinois Institute of Natural Resources, submitted to Upper Mississippi River Basin Commission.

Blaauw, H. G., and van de Kaa, E. J. 1978. "Erosion of Bottom and Banks Caused by the Screw Race of Maneuvering Ships," Publication No. 202, Delft Hydraulics Laboratory, Delft, The Netherlands, presented at the Seventh International Harbour Congress, Antwerp, May 22-26.

Blaauw, H., and van der Knaap, F. 1983. "Prediction of Squat of Ships Sailing in Restricted Water," Eighth International Harbour Congress, Antwerp, Belgium, 13-17 June, pp 2.81-2.93.

Blaauw, H. G., van der Knaap, F. C. M., de Groot, M. T., and Pilarcyk, K. W. 1984. "Design of Bank Protection of Inland Navigation Fairways," Publication No. 320, Delft Hydraulics Laboratory, Delft, The Netherlands.

Bouwmeester, J., van de Kaa, E. J., Nuhoff, H. A., and Orden, R. G. J. 1977. Twenty-fourth International Navigation Congress, Permanent International Association of Navigation Congresses, Leningrad, Section 1, Subject 3, pp 139-158.

Delft Hydraulics Laboratory. 1979 (Nov). "Investigation Program Concerning Ship Induced Water Motions and Design of Bank Protections," Research Program M 1115, Delft, The Netherlands.

Environmental Science and Engineering. 1981. "Navigation Impact Study," prepared for Illinois Natural History Survey, Grafton, IL.

Fuehrer, M., and Romisch, K. 1977. "Effects of Modern Ship Traffic on Inland- and Ocean-Waters and Their Structures," Twenty-fourth International Navigation Congress, Permanent Internatinal Association of Navigation Congresses, Leningrad, Section 1, Subject 3, pp 79-94.

Fuehrer, M., Romisch, K., and Engelke, G. 1981. "Criteria for Dimensioning the Bottom and Slope Protection and for Applying the New Methods of Protecting Navigation Canals," Twenty-fifth International Navigation Congress, Permanent International Association of Navigation Congresses, Edinburgh, Section 1, Subject 1, pp 29-50.

Gucinski, H. 1982 (Sep). "Sediment Suspension and Resuspension From Small-Craft Induced Turbulence," Report No. EPA 60013-82-084, prepared for US Environmental Protection Agency, Annapolis, MD, by Anne Arundel Community College, Arnold, MD.

Hochstein, A. B. 1967. "Procedural Instructions for Establishing the Feasibility of Navigable Conditions on Canals for Composite Use" (Author's name appears on report as A. B. Gokhshteyn), translated from Russian for Headquarters, US Army Corps of Engineers, Washington, DC.

Hochstein, A. B., and Adams, C. E., Jr. 1986. "A Numerical Model of the Effects of Propeller Wash and Ship-Induced Waves from Commercial Navigation in an Extended Navigation Season on Erosion, Sedimentation, and Water Quality in the Great Lakes Connecting Channels and Harbors," prepared for US Army Engineer District, Detroit, Detroit, MI.

Hochstein, A. B. and Cohen, M. 1980. "Interaction Between Tow Traffic and Channel," Proceedings of Water Resources Forum, Houston, TX.

Jansen, P., and Schijf, J. B. 1953. Eighteenth International Navigation Congress, Permanent International Association of Navigation Congresses, Rome, Section 1, Communication 1, pp 175-197.

Louis Berger and Associates. 1981 (Oct). "Analysis of Impact of Navigation on the Tennessee-Tombigee Waterway," prepared for US Department of Justice, Washington, DC, by Louis Berger and Associates, East Orange, NJ, pp 2-1 to 2-7.

Marchal, J., and Spronck, R. 1977. "Behavior of Boats and Tows at the Time of Passage, Overtaking or During Crossing in a Rectilinear Canal" (Comportement des Bateaux et Convois Pousses, Lors du Passage, du Depassement (Trematage) ou du Croisement dans un Canal Rectiligne"), Twenty-fourth International Navigation Congress, Permanent International Association of Navigation Congresses, Leningrad, Section 1, Subject 3, pp 5-19.

Maxwell, W. H. C., and Pazwash, H. 1973 (Apr). "Axisymmetric Shallow Submerged Turbulent Jets," Journal of the Hydraulics Division, American Society of Civil Engineers, Vol 99, No. HY4, pp 637-652.

McNown, J. S. 1976 (Aug). "Sinkage and Resistance for Ships in Channels," Journal Waterways, Harbors and Coastal Engineering, American Society of Civil Engineers, Vol. 102, No. WW1, pp 287-300.

Oebius, H. U. 1984. "Loads on Beds and Banks Caused by Ship Propulsion Systems," International Conference on Flexible Armoured Revetments Incorporating Geotextiles, London, 29-30 March, pp 13-23.

Permanent International Association of Navigation Congresses. 1987. "Guidelines for the Design and Construction of Flexible Revetments Incorporating Geotextiles for Inland Waterways," Report of Working Group 4 of the Permanent Technical Committee 1, Supplement to Bulletin No. 57, Brussels, Belgium.

Prosser, M. J. 1986 (Feb). "Propeller Induced Scour," RR 2570, BHRA and British Ports Association, Cranfield, Bedford, Great Britain.

Schale, E. 1977. "Stress and Changes Produced in the Waterway Boundary by Navigation," Zeitschrift Fver Binnenschiffahrt Und Wasserstrassen, No. 7, pp 16-22.

Schijf, J. B. 1949. Seventeenth International Navigation Congress, Lisbon, Section 1, Subject 2, pp 61-78.

Schlichting, H. 1968. Boundary-Layer Theory, McGraw Hill, 6th Edition, New York.

Verhey, H. J. 1983. "The Stability of Bottom and Banks Subjected to the Velocities in the Propeller Jet Behind Ships," Publication No. 303, Delft Hydraulics Laboratory, Delft, The Netherlands, presented at 8th International Harbour Congress, Antwerp, Belgium, June 13-17, 1983.

US Army Engineer District, Huntington. 1980a. "Gallipolis Locks and Dam Replacement, Ohio River, Phase 1, Advanced Engineering and Design Study, General Design Memorandum; Appendix J, Volume 1, Environmental and Social Impact Analysis," Huntington, WV.

US Army Engineer District, Huntington. 1980b. "Gallipolis Locks and Dam Replacement, Ohio River, Phase 1, Advanced Engineering and Design Study, General Design Memorandum; Appendix J, Volume 1, Environmental and Social Impact Analysis, Exhibit 2, Analysis of the Effect of Tow Traffic on the Physical Components of the Environment," prepared by Louis Berger and Associates, Inc., East Orange, NJ, for US Army Engineer District, Huntington, Huntington, WV.

Table 1

Bottom Velocity Tests

Unconfined Channel

Test No.	Propeller Speed, rpm	Barge Configuration*	Draft ft	Depth ft	Speed fps	Velocity Meter Location**
15	185	3W × 2L	9	15	11.1	A
14	135	3W × 2L		15	6.8	A
22	185	3W × 2L		30	11.1	A
21	135	3W × 2L		30	6.7	A
13	185	1W × 1L		15	11.2	B
12	135	1W × 1L		15	6.6	B
29	185	1W × 1L		30	11.5	B
28	135	1W × 1L		30	6.7	B
9	185	3W × 2L	2	15	11.1	A
8	135	3W × 2L		15	6.5	A
25	185	3W × 2L		30	11.4	A
24	135	3W × 2L		30	6.8	A
11	185	1W × 1L		15	11.0	B
10	135	1W × 1L		15	6.7	B
27	185	1W × 1L		30	11.6	B
26	135	1W × 1L		30	6.8	B
16	TOW	3W × 2L	9	15	10.6	A
23	TOW	3W × 2L		30	11.1	
18	185	3W × 1L		15	11.3	
17	135	3W × 1L		15	6.8	
20	185	3W × 1L		30	11.3	
19	135	3W × 1L		30	6.5	
31	185	3W × 2L		30	11.5	C
30	135			30	6.8	C
39	185			15	11.1	C
38	135			15	6.5	C
40	TOW			15	11.1	C
42	185†			15	8.1	A
41	135†			15	5.9	A

Notes: All tests conducted with Kort nozzle.
Propeller rotation: When viewed from the stern, left propeller has counterclockwise rotation; right propeller has clockwise rotation.

* W = width: L = length.

** A = center line and 80 ft from center line, both 2 ft above bottom.
B = center line and 45 ft from center line, both 2 ft above bottom.
C = 26 and 45 ft from center line, both 2 ft above bottom.

† No towing assist.

Table 2

Bottom Velocity Tests

Near-Bank Channel

Test No.	Propeller Speed, rpm	Barge Configuration*	Draft ft	Depth ft	Speed fps	Velocity Meter Location**
201	185	3W × 2L	9	15	11.2	A
200	135	3W × 2L		15	6.7	A
209	185	3W × 2L		30	11.4	A
208	135	3W × 2L		30	6.8	A
203	185	1W × 1L		15	11.3	B
202	135	1W × 1L		15	6.7	B
211	185	1W × 1L		30	11.3	B
210	135	1W × 1L		30	6.8	B
228	185	3W × 2L	2	15	11.2	A
227	135	3W × 2L		15	6.5	A
220	185	3W × 2L		30	11.4	A
219	135	3W × 2L		30	6.7	A
207	185	1W × 1L		15	11.4	B
206	135	1W × 1L		15	6.8	B
213	185	1W × 1L		30	11.2	B
212	135	1W × 1L		30	6.5	B
205†	185	3W × 2L	9	15	11.2	A
204†	135			15	6.7	A
218†	185			30	11.2	A
217†	135			30	6.6	A
229	185			15	11.2	C
230	135			15	6.6	
231	TOW			15	12.2	
215	185			30	11.2	
214	135			30	6.7	
216	TOW			30	6.7	
114	TOW			15	10.5	A
117	TOW			30	11.4	A
222††	150	3W × 1L		21	12.1	A
221††	100	3W × 1L			8.5	A
226††	150	1W × 1L			18.1	B
225††	100	1W × 1L			8.8	B
224††	150	1W × 1L	2		18.1	B
223††	100	1W × 1L	2		13.3	B

Notes: Propeller rotation: When viewed from the stern, left propeller has clockwise rotation; right propeller has counterclockwise rotation.

* W = width; L = length.

** A = center line and 80 ft from center line, both 2 ft above bottom.
B = center line and 45 ft from center line, both 2 ft above bottom.
C = 26 and 45 ft from center line, both 2 ft above bottom.

† Open-wheel test.

†† Reproduces prototype tests of MV *Harold Turner*.

Table 3

Bottom Velocity Tests

Confined Channel

Test No.	Propeller Speed, rpm	Barge Configuration*	Draft ft	Depth ft	Speed fps	Velocity Meter Location**
301	185	3W × 2L	9	15	10.0	A
300	135	3W × 2L		15	6.6	A
321	185	3W × 2L		30	11.2	A
320	135	3W × 2L		30	6.6	A
310	185	1W × 1L		15	11.3	B
309	135	1W × 1L		15	6.6	B
333	185	1W × 1L		30	11.0	B
332	135	1W × 1L		30	6.3	B
304	185	3W × 2L	2	15	10.6	A
303	135	3W × 2L		15	6.6	A
327	185	3W × 2L		30	11.2	A
326	135	3W × 2L		30	6.6	A
307	185	1W × 1L		15	11.3	B
306	135	1W × 1L		15	6.5	B
330	185	1W × 1L		30	11.3	B
329	135	1W × 1L		30	6.5	B
316†	185	3W × 2L	9	15	11.5	A
315†	135			15	6.6	A
318†	185			30	11.2	A
317†	135			30	6.6	A
313	185			15	11.2	C
312	135			15	6.7	
314	TOW			15	12.0	
324	185			30	11.2	
323	135			30	6.6	
325	TOW			30	12.9	
302	TOW			15	9.7	A
319	TOW			30	12.6	A

Notes: Propeller rotation: When viewed from the stern, left propeller has clockwise rotation; right propeller has counterclockwise rotation.

* W = width; L = length.

** A = center line and 80 ft from center line, both 2 ft above bottom.
B = center line and 45 ft from center line, both 2 ft above bottom.
C = 26 and 45 ft from center line, both 2 ft above bottom.

† Open-wheel test.

Table 4

Steve Kuhr Prototype Tests

Data File for Towboat Study: summer 1987

Date: 29 July 1987

Towboat name: *Steve Kuhr* HP Rating: 1,500

Towboat dimensions (L × W × D), ft: 70 × 24 × 7

Number of screws: 3 Open versus Kort: Open

Barge Configuration: 1 wide × 1 long (Unloaded)

Barge Dimension (L × W × D): 195 × 35 × 1.25

Overall Tow Dimensions (L × W): 265 × 35

Propeller Diameter, in.: 60 Propeller Pitch, in.: 46

Red Gear Ratio: 5.17:1

Approximate River Velocity, fps: 0.46

Run	Up (U) or Down (D)	Propeller Speed, rpm	Speed, fps	Clock (EDT)
L1072901	U	155	6.6	1028
02	D	155	7.4	1051
03	U	230	9.5	1110
04	D	230	11.0	1124
05	U	310	13.9	1137
06	D	310	14.7	1149
07	U	155	7.4	1439
08	D	155	7.8	1500
09	U	230	9.8	1515
10	D	230	10.6	1533
11	U	310	13.9	1546
12	D	310	13.9	1556
13	U	310	14.7	1610

Results

Runs 01 to 06 in shallow water, about 16-17 ft deep. Vessel exhibited noticeable squat (about 9 in.) only at highest speed/rpm.

Runs 07 to 12 in deeper water, about 21-22 ft deep. Vessel exhibited minimal squat at all speeds/rpms.

Speed indicated is relative to land tracking station.

Table 5

John Matthews Prototype Tests

Data File for Towboat Study: summer 1987

Date: 31 July 1987

Towboat name: *John Matthews* HP Rating: 4,200

Towboat dimensions (L × W × D), ft: 148 × 35 × 8.5

Number of screws: 2 Open versus Kort: Kort

Barge Configuration: 1 wide × 1 long (Unloaded)

Barge Dimension (L × W × D): 195 × 35 × 1.25

Overall Tow Dimensions (L × W): 335 × 35

Propeller Diameter, in.: 96 Propeller Pitch, in.: 84

Red Gear Ratio: 3.958:1

Approximate River Velocity, fps: 0.29

Run	Up (U) or Down (D)	Propeller Speed, rpm	Speed, fps	Clock (EDT)
L1073101	U	100	8.4	1107
02	D	100	8.6	1123
03	U	160	13.3	1134
04	D	160	13.8	1145
05	U	225	15.7	1203
06	D	225	20.3 (18.8)*	1220
07	U	100	8.0	1531
08	D	100	8.4	1550
09	U	160	13.3	1605
10	D	160	13.3	1617
11	U	225	19.2	1633
12	D	225	19.2	1648

* (18.8) based on event marks.

Results

Runs 01 to 06 in shallow water, about 16-17 ft deep. Vessel exhibited noticeable squat (up to about 24 in.) only at highest speed/rpm.

Runs 07 to 12 in deeper water, about 21-22 ft deep. Vessel exhibited considerable squat (up to about 18 in.) at highest speeds/rpm.

Speed indicated is relative to land tracking station.

Table 6

Harold Turner Prototype Tests

Data File for Towboat Study: summer 1987

Date: 5 August 1987

Towboat name: *Harold Turner* HP Rating: 5,600

Towboat dimensions (L × W × D), ft: 140 × 42 × 9

Number of screws: 2 Open versus Kort: Kort

Propeller Diameter, in.: 110 Propeller Pitch, in.: 100

Red Gear Ratio: 4.345:1

Approximate River Velocity, fps: 0.50

Run	Up (U) or Down (D)	Propeller Speed, rpm	Speed, fps	Clock (EDT)	Loaded (L) or Unloaded (U)	Overall Dimensions, ft
L1080501	U	100	13.4	1120	1W × 1L U	335L × 42W
02	D	100	12.9	1130	1W × 1L U	335L × 42W
03	U	150	16.7	1154	1W × 1L U	335L × 42W
04	D	150	16.7	1208	1W × 1L U	335L × 42W
05	U	100	9.6	1323	1W × 1L L	335L × 42W
06	D	100	9.3	1339	1W × 1L L	335L × 42W
07	U	150	15.9	1400	1W × 1L L	335L × 42W
08	D	150	17.6	1413	1W × 1L L	335L × 42W
09	D	165	8.3	1520	3W × 5L L	1,115L × 105W
10	U	100	9.0	1545	3W × 1L L	335L × 105W
11	D	100	9.6	1607	3W × 1L L	335L × 105W
12	U	150	12.4	1627	3W × 1L L	335L × 105W
13	D	150	12.9	1645	3W × 1L L	335L × 105W

Results

Runs 01 to 13 all in deep water, about 22 ft deep, and farther from Kentucky bank than any other runs. Run 09 is *F. M. Baker*, an opportunistic tow that had an identical towboat to *Harold Turner*.

Speed indicated is relative to land tracking station.

Table 7

Observed Prototype Velocities

MV	Water Depth at Tow ft	Tow Configuration*	Test No.	Upbound (U) or Downbound (D)	Propeller Speed rpm	V fps	Ambient Bottom Velocity fps	Observed Velocity, fps**				
									Displacement			
								Bow of Barge	Bow of Barge	Stern of Barge	Entering Propeller	Propeller Wash
Steve Kuhr	16	11U	01	U	155	6.6	0.26	0.09(200)	0.53(187)	0.25(195)	1.6(180)	0.1(167)
			02	D		7.4		0.63(185)	0.30(188)	0.48(230)	0.70(?)	0.5(155)
			03	U	230	9.5		0.11(246)	0.67(191)	0.57(246)	1.5(177)	0.2(150)
			04	D		11.0		0.57(199)	0.11(218)	0.30(210)	0.44(330)	0.4(150)
			05	U	310	13.9		0.07(41)	0.85(178)	0.22(154)	2.6(188)	0.3(220)
			06	D		14.7		0.71(193)	0.22(358)	0.55(207)	1.97(10)	0.55(160)
	21	11U	07	U	155	7.4	0.18	0.04(200)	0.32(166)	0.16(172)	0.75(207)	0.1(240)
			08	D		7.8		0.3((182)	0.05(151)	0.19(126)	0.48(208)	0.26(190)
			09	U	230	9.8		NO DATA				
			10	D		10.6		0.34(160)	0.05(174)	0.42(21)	0.68(350)	0.24(182)
			11	U	310	13.9		NO DATA				
			12	D		13.9		0.47(195)	0.02(51)	0.55(182)	1.48(20)	0.3(200)
			13	U		14.7		0.11(136)	0.58(176)	0.3(154)	1.6(201)	0.3(240)
John Matthews	16	11U	01	U	100	8.4	0.15	0.09(220)	0.44(200)	0.28(122)	1.7(?)	0.2(?)
			02	D		8.0		0.42(185)	0.10(63)	0.57(193)	1.2(204)	0.35(315)
			03	U	160	13.3		0.04(105)	0.32(208)	0.21(107)	1.7(185)	0.3(312)
			04	D		13.8		0.54(189)	0.26(201)	0.48(186)	1.0(174)	0.5(325)
			05	U	225	15.7		0.32(360)	0.03(270)	0.22(16)	2.3(24)	1.9(67)
			06	D		20.3		0.35(183)	0.60(31)	0.56(42)	1.63(22)	0.5(?)
	21	11U	07	U	100	8.0	0.16	0.26(177)	0.47(177)	0.3(179)	1.1(177)	0.25(190)
			08	D		8.4	0.16	0.20(213)	0.07(245)	0.25(222)	0.5(31)	0.3(110)
			09	U	160	13.3		0.03(201)	0.31(198)	0.07(274)	1.1(194)	0.24(126)
			10	D		13.3		0.42(183)	0.22(174)	0.45(184)	0.44(26)	0.45(140)
			11	U	225	19.2		0.27(296)	0.19(243)	0.35(272)	1.3(176)	0.2(102)
			12	D		19.2		0.50(222)	0.19(185)	0.55(183)	1.0(8)	0.3(196)

(Continued)

* 11U = 1 wide × 1 long unloaded
11L = 1 wide × 1 long loaded
35L = 3 wide × 5 long loaded
31L = 3 wide × 1 long loaded

** Value in parentheses following velocity is azimuth, with a value of 180 deg being downstream.

Table 7 (Concluded)

MV	Water Depth at Tow ft	Tow Configuration	Test No.	Upbound (U) or Downbound (D)	Propeller Speed rpm	V fps	Ambient Bottom Velocity fps	Observed Velocity, fps				
									Displacement			
								Bow of Barge	Bow of Barge	Stern of Barge	Entering Propeller	Propeller Wash
Harold Turner	21	11U	01	U	100	13.4	0.15	0.4(251)	0.12(204)	0.08(278)	1.3(163)	0.2(?)
			02	D		12.9		0.32(168)	0.17(174)	0.58(168)	1.0(160)	0.46(161)
			03	U	150	16.7		0.06(330)	0.09(258)	0.38(320)	1.6(184)	0.4(95)
			04	D		16.7		0.52(162)	0.35(163)	0.66(164)	1.3(154)	0.56(153)
	21	11L	05	U	100	9.6		0.19(119)	0.71(209)	0.44(171)	1.1(124)	??
			06	D		9.3		0.76(168)	0.14(?)	??	0.8(163)	0 35(195)
			07	U	150	15.9		??	0.8(200)	0.85(188)	1.8(179)	0.3(80)
			08	D		17.6		1.0(142)	0.47(?)	0.4(198)	1.3(150)	0.5(190)
	21	35L	09	D	165	8.3		1.4(144)	0.09(101)	??	??	??
	21	31L	10	U	100	9.0		1.2(94)	1.4(120)	1.5(113)	1.3(114)	0.9(115)
			11	D		9.6		1.3(148)	0.09(135)	1.2(135)	1.0(138)	1.1(160)
			12	U	150	12.4		1.1(90)	1.4(129)	1.5(197)	1.4(216)	??
			13	D		12.9		2.0(119)	0.12(88)	2.5(120)	2.6(120)	1.5(134)

Table 8

Return Velocity Data

Identifier	V_{rs}/V_r	Side	Skew	N_{side}	V_{rsm}/V_{rs}
Delft Hydraulics Laboratory (1979)					
Figure 6	0.83	Port	0.57	63.5	2.34
	2.18	Starboard	3.96	9.2	1.00
Figure 7	0.79	Port	0.57	63.5	2.26
	2.49	Starboard	3.96	9.2	1.00
Figure 5	1.00	Port	1.00	36.3	1.71
	1.00	Starboard	1.00	36.3	1.71
1:35 scale*					
Test 22	1.32	Port	1.50	12.6	1.06
	0.84	Starboard	0.75	25.2	1.29
Test 23	1.60	Port	3.00	6.3	1.00
	0.87	Starboard	0.60	31.5	1.47
Test 24	0.94	Port	1.00	18.9	1.13
	1.05	Starboard	1.00	18.9	1.05
1:70 scale*					
Test 47, 47A	1.00	Port	1.00	12.5	1.05
	1.00	Starboard	1.00	12.6	1.07
Test 48, 48A	0.94	Port	0.66	19.0	1.03
	1.17	Starboard	2.03	6.2	1.00
Test 54, 54A	1.10	Port	1.43	8.8	1.00
	0.95	Starboard	0.77	16.3	1.15

* S. T. Maynord. 1989 (May). "Return Velocity Distribution and Flow Visualization for Commercial Navigation," letter report, US Army Engineer Waterways Experiment Station, Vicksburg, MS.

Table 9

Observed Versus Computed Prototype Bow Velocities

Test No.	Tow Config-uration*	Upstream (U) or Downstream (D)	Propeller Speed rpm	V fps	Ambient Bottom Velocity fps	V_{bb}, fps* Observed	V_{bb}, fps* Compared
05	11L	U	100	9.6	0.15	0.19(119)	0.47(360)
06	11L	D	100	9.3		0.76(168)	0.69(180)
07	11L	U	150	15.9		??	
08	11L	D	150	17.6		1.0(142)	1.2(180)
09	35L	D	165	8.3		1.4(144)	1.1(180)
10	31L	U	100	9.0		1.2(94)	0.96(360)
11	31L	D	100	9.6		1.3(148)	1.2(180)
12	31L	U	150	12.4		1.1(90)	1.4(360)
13	31L	D	150	12.9		2.0(119)	1.6(180)

Note: All data are from *Harold Turner* tow.

* 11U = 1 wide × 1 long unloaded
11L = 1 wide × 1 long loaded
35L = 3 wide × 5 long loaded
31L = 3 wide × 1 long loaded

** Value in parentheses following velocity is azimuth, with a value of 180 deg being downstream.

Table 10

Observed Versus Computed Model Bow Velocities

Test No.	V_{bb}, fps Observed	V_{bb}, fps Computed
15	2.90	2.77
14	1.90	1.70
22	0.50	0.58
21	0.00	0.35
13	1.55	1.44
12	1.00	0.85
29	0.00	0.31
11	0.00	0.12
10	0.00	0.07
27	0.00	0.02
16	2.50	2.65
23	0.00	0.58
18	4.10	2.82
17	1.55	1.70
20	0.57	0.59
19	0.00	0.34
42	1.55	2.02
41	1.40	1.47
201	3.45	2.80
200	1.80	1.67
209	0.57	0.60
208	0.00	0.36
203	1.40	1.46
202	0.80	0.86
211	0.00	0.30
210	0.00	0.18
220	0.00	0.05
207	0.00	0.12
206	0.00	0.07
205	3.20	2.80
204	1.80	1.67
218	0.57	0.59
217	0.00	0.35
114	2.30	2.62
117	0.50	0.60
222	2.35	1.42
221	1.23	1.00
226	1.60	1.10
225	0.00	0.53
224	0.00	0.09
223	0.00	0.06
301	2.15	2.50
300	1.60	1.65
321	0.00	0.59
320	0.00	0.35
310	1.30	1.46
309	0.57	0.85
333	0.00	0.30
304	0.00	0.22
315	1.55	1.65
318	0.00	0.59
317	0.00	0.35
302	1.55	2.42
319	0.00	0.66

Table 11

Comparison of Model Bottom Velocities for Three Channel Types (9-ft Draft)

Width	Depth	Vessel Speed, fps			Test No.			$V_{bd}CL$, fps			V_{out}, fps		
		Uncon	lNear	Conf	Uncon	lNear	Conf	Uncon	lNear	Conf	Uncon	lNear	Conf
3W	15	11.1	11.2	10.0	15	201	301	3.7	4.1	3.9	2.2	2.6	3.4
	15	6.8	6.7	6.6	14	200	300	2.7	2.9	2.4	1.3	1.5	2.0
	30	11.1	11.4	11.2	22	209	321	1.2	1.5	1.7	1.3	1.4	1.6
	30	6.7	6.8	6.6	21	208	320	0.7	0.8	0.8	0.0	0.0	1.5
1W	15	11.2	11.3	11.3	13	203	310	2.6	2.7	2.4	1.2	1.2	1.2
	15	6.6	6.7	6.6	12	202	309	1.4	1.2	1.2	0.6	0.0	1.4
	30	11.5	11.3	11.0	29	211	333	0.7	0.7	0.7	0.0	0.0	1.1
3W	15	10.6	10.5	9.7	16*	114	302	2.3	3.7	3.0	1.3	2.3	2.5
	30	11.1	11.4	12.6	23*	117	319	1.4	1.5	1.7	1.2	1.4	1.5
								$V_{bd}26$			$V_{bd}45$		
3W	15	11.1	11.2	11.2	39	229	313	3.2	3.5	3.4	2.4	2.8	2.4
	15	6.5	6.6	6.7	38	230	312	2.0	2.9	3.2	1.7	2.3	2.6
	30	11.5	11.2	11.2	31	215	324	1.8	1.5	1.5	1.6	1.5	1.2
	30	6.8	6.7	6.6	30	214	323	1.2	0.8	1.1	1.0	0.6	1.1
	15	11.1	12.2	12.0	40*	231	314	2.8	3.2	3.2	2.2	2.2	2.4

Note: Uncon = unconfined
lNear = near-bank
Conf = confined
$V_{bd}CL$ = bottom displacement velocity at tow center line.
$V_{bd}26$ = bottom displacement velocity at 26 ft from tow center line.
$V_{bd}45$ = bottom displacement velocity at 45 ft from tow center line.
V_{out} = bottom displacement velocity at 27.5 ft from edge of barge.
* Towing test.

Table 12

Observed Versus Computed Prototype Center-Line Displacement Velocities

Test No.	Tow Configuration*	Upstream (U) or Downstream (D)	Propeller Speed rpm	V fps	Ambient Bottom Velocity fps	V_{bb}, fps* Observed	V_{bb}, fps* Compared
05	11L	U	100	9.6	0.15	0.71(209)	1.3(180)
06	11L	D	100	9.3		0.14(?)	0.95(360)
07	11L	U	150	15.9		0.8(200)	2.0(180)
08	11L	D	150	17.6		0.47(?)	1.9(360)
09	35L	D	165	8.3		0.09(101)	1.6(360)
10	31L	U	100	9.0		1.4(120)	2.1(180)
11	31L	D	100	9.6		0.09(135)	1.9(360)
12	31L	U	150	12.4		1.4(129)	2.8(180)
13	31L	D	150	12.9		0.12(88)	2.6(360)

Note: All data are from *Harold Turner* tow.

* 11U = 1 wide × 1 long unloaded
11L = 1 wide × 1 long loaded
35L = 3 wide × 5 long loaded
31L = 3 wide × 1 long loaded

** Value in parentheses following velocity is azimuth, with a value of 180 deg being downstream.

Table 13

Observed Versus Computed Model Center-Line Displacement Velocities

Test No.	V_{bb}, fps Observed	V_{bb}, fps Computed	Test No.	V_{bb}, fps Observed	V_{bb}, fps Computed
15	3.70	3.58	207	1.15	0.73
14	2.70	2.19	206	0.65	0.43
22	1.20	1.54	205	4.20	3.62
21	0.70	0.93	204	2.80	2.16
13	2.60	1.99	218	1.80	1.55
12	1.40	1.17	217	1.10	0.91
29	0.70	0.87	114	3.70	3.39
11	0.60	0.70	117	1.50	1.58
10	0.50	0.42	222	4.00	2.59
27	0.50	0.32	221	2.20	1.82
16	2.30	3.42	226	2.30	2.14
23	1.40	1.54	225	0.90	1.04
18	5.80	3.65	224	0.65	0.77
17	2.70	2.19	223	0.65	0.56
20	1.70	1.56	301	3.90	3.23
19	0.80	0.90	300	2.40	2.13
42	3.10	2.61	321	1.70	1.55
41	1.55	1.90	320	0.75	0.91
201	4.10	3.62	310	2.40	2.01
200	2.90	2.16	309	1.20	1.17
209	1.50	1.58	333	0.74	0.84
208	0.80	0.94	304	1.00	1.23
203	2.70	2.01	315	0.78	2.13
202	1.15	1.19	318	1.55	1.55
211	0.70	0.86	317	1.06	0.91
210	0.50	0.52	302	3.00	3.13
220	0.50	0.57	319	1.70	1.74

Table 14

Observed Versus Computed V_{out}, Model and Prototype

Physical Model Data				Prototype Data			
Test No.	N	V_{out} Observed	V_{out} Computed	Test No.	N	V_{out} Observed	V_{out} Computed
15	15.00	2.22	2.26	1	67.9	0.30	0.42
14	15.00	1.32	1.38	2	67.9	0.15	0.40
22	27.60	1.35	1.07	3	67.9	0.30	0.59
21	27.60	0.00	0.65	4	67.9	0.16	0.62
13	38.10	1.23	1.11	5	67.9	0.71	0.85
12	38.10	0.62	0.65	6	67.9	0.52	0.84
29	76.20	0.00	0.51	7	134.5	0.22	0.30
11	171.40	0.97	0.34	8	134.5	0.17	0.28
10	171.40	0.00	0.20	10	134.5	0.22	0.39
27	342.90	0.00	0.16	12	134.5	0.29	0.52
16	15.00	1.26	2.16	13	134.5	0.37	0.59
23	27.60	1.23	1.07	1	45.0	0.08	0.73
18	15.00	2.50	2.30	3	45.0	0.78	1.15
17	15.00	1.75	1.38	4	45.0	0.75	1.14
20	27.60	0.85	1.09	5	45.0	1.77	1.30
19	27.60	0.00	0.63	7	67.9	0.50	0.49
42	15.00	1.47	1.65	8	67.9	0.30	0.48
41	15.00	0.00	1.20	9	67.9	0.50	0.81
201	11.10	2.57	2.60	10	67.9	0.40	0.77
200	11.10	1.49	1.56	11	67.9	0.69	1.16
209	21.80	1.43	1.24	12	67.9	0.84	1.13
208	21.80	0.00	0.74	1	112.7	0.73	0.81
203	25.00	1.25	1.31	1	112.7	0.59	0.72
202	25.00	0.00	0.78	3	112.7	0.99	1.00
211	38.10	0.00	0.69	4	112.7	0.78	0.95
210	38.10	0.00	0.41	5	112.7	0.55	0.59
220	57.10	0.00	0.46	6	112.7	0.86	0.51
207	85.70	1.00	0.43	7	112.7	1.19	0.96
206	85.70	0.00	0.26	8	45.1	1.53	1.80
205	11.10	2.83	2.60	9	45.1	1.22	0.82
204	11.10	1.47	1.56	10	45.1	0.90	1.0(
218	21.80	0.98	1.22	11	45.1	0.93	0.96
217	21.80	1.26	0.71	12	45.1	1.44	1.36
114	11.10	2.29	2.44	13	45.1	1.89	1.31
117	21.80	1.43	1.24	--	--	--	--
222	15.60	2.28	1.93	--	--	--	--
221	15.60	1.61	1.36	--	--	--	--
226	29.80	0.98	1.55	--	--	--	--
225	29.80	0.00	0.75	--	--	--	--
224	120.00	0.00	0.47	--	--	--	--

(Continued)

Table 14 (Concluded)

Physical Model Data				Prototype Data			
Test No.	N	V_{out} Observed	V_{out} Computed	Test No.	N	V_{out} Observed	V_{out} Computed
223	120.00	0.50	0.35	--	--	--	--
301	6.35	3.36	3.16	--	--	--	--
300	6.35	1.99	2.08	--	--	--	--
321	12.70	1.57	1.67	--	--	--	--
320	12.70	1.47	0.98	--	--	--	--
310	19.00	1.24	1.49	--	--	--	--
309	19.00	1.43	0.87	--	--	--	--
333	38.10	1.11	0.67	--	--	--	--
304	28.60	0.63	0.92	--	--	--	--
315	6.35	2.46	2.08	--	--	--	--
318	12.70	1.47	1.67	--	--	--	--
317	12.70	1.47	0.98	--	--	--	--
302	6.35	2.55	3.07	--	--	--	--
319	12.70	1.53	1.88	--	--	--	--

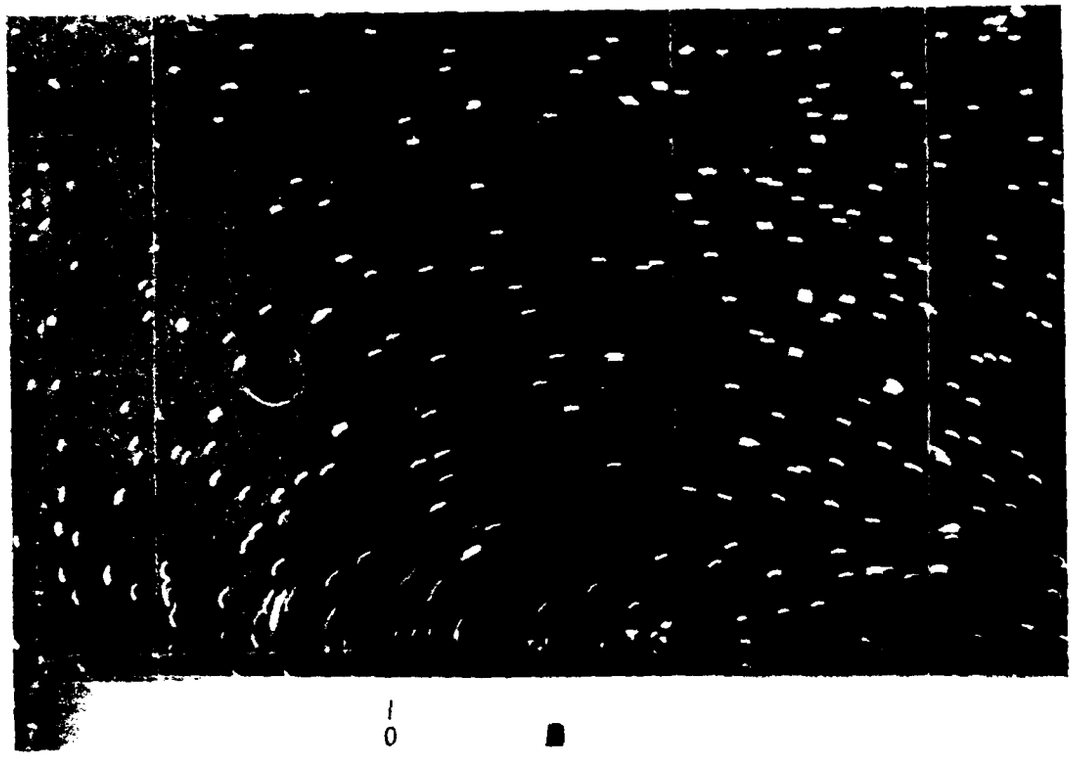

a. Bow of tow

b. Stern of tow

Photo 1. Surface current patterns, 1:70-scale tow, location A

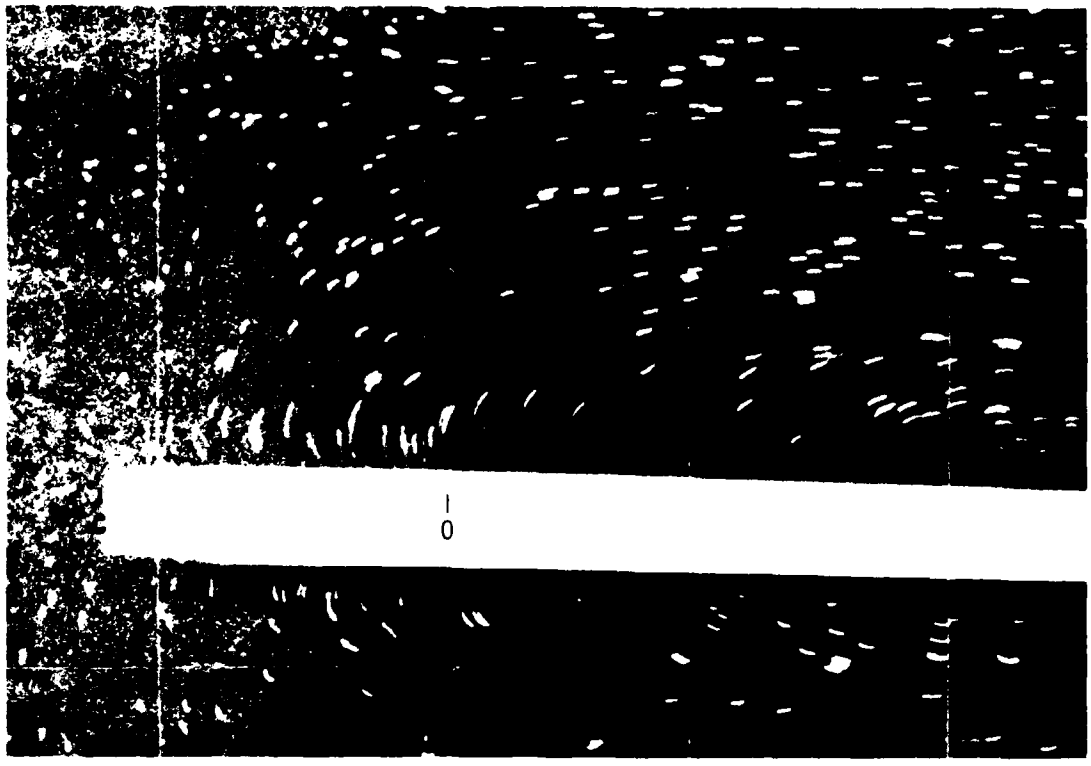

a. Bow of tow

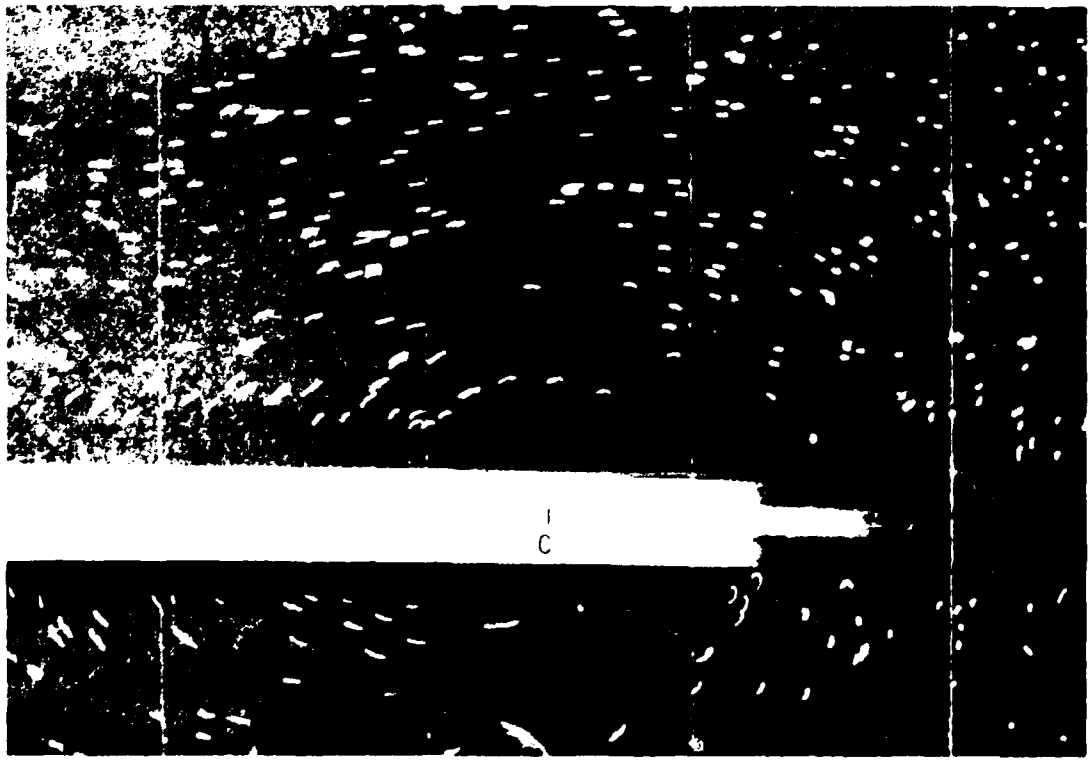

b. Stern of tow

Photo 2. Surface current patterns, 1:70-scale tow, location B

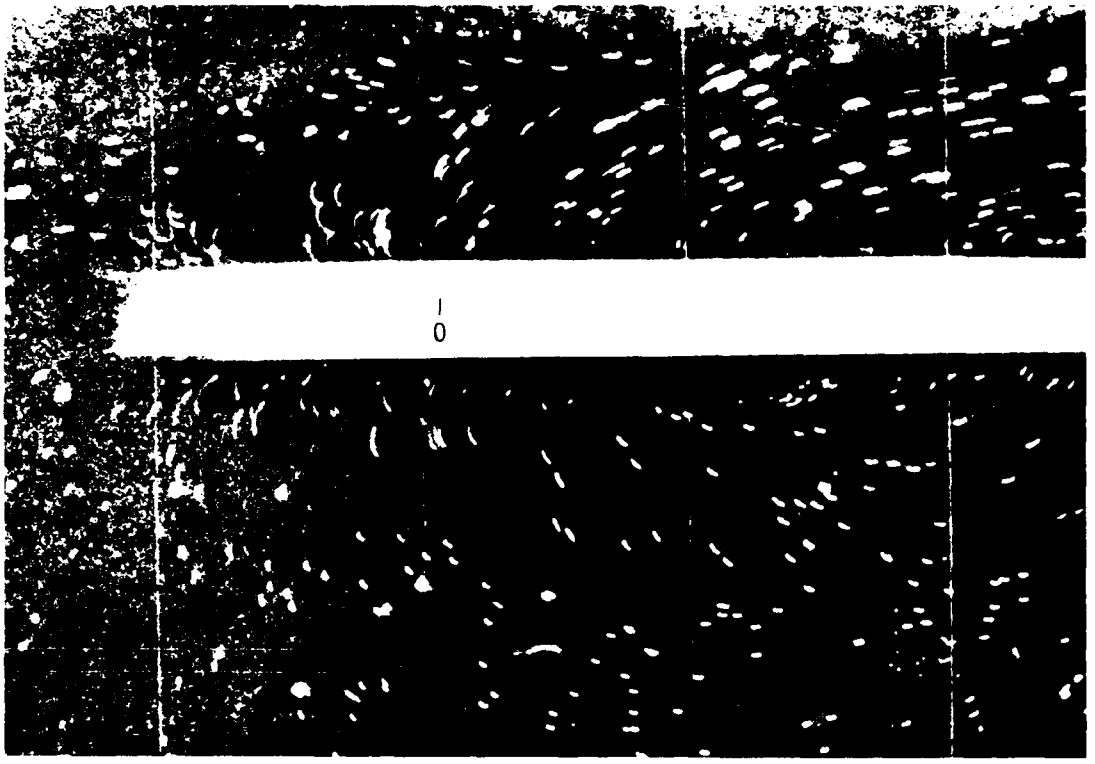

a. Bow of tow

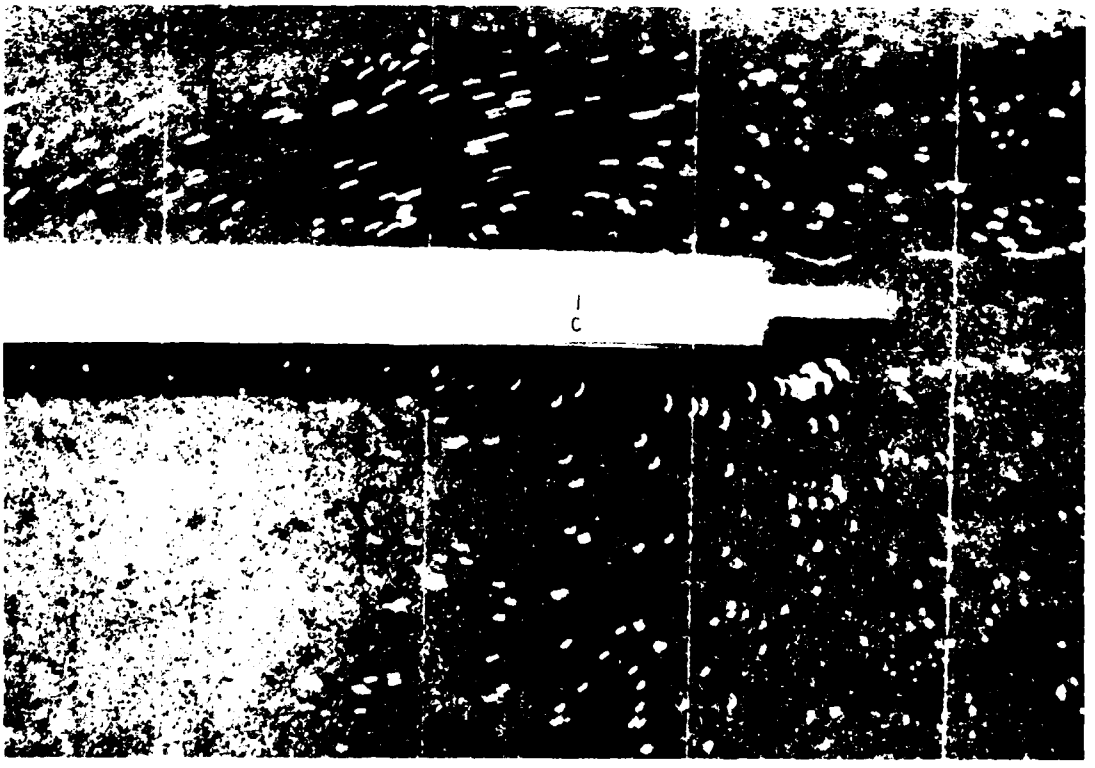

b. Stern of tow

Photo 3. Surface current patterns, 1:70-scale tow, location C

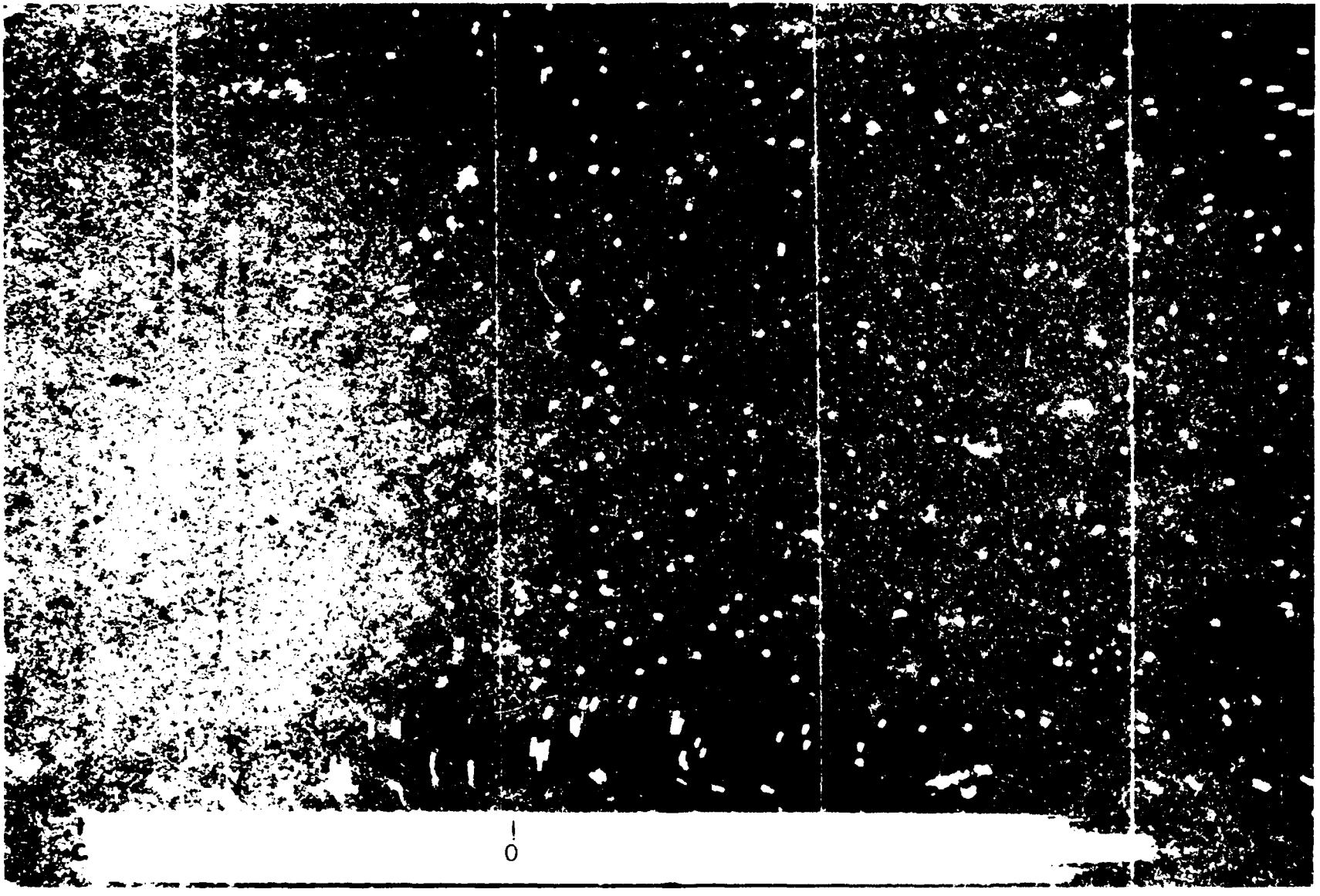

Photo 4. Surface current patterns, 1:120-scale tow, location A

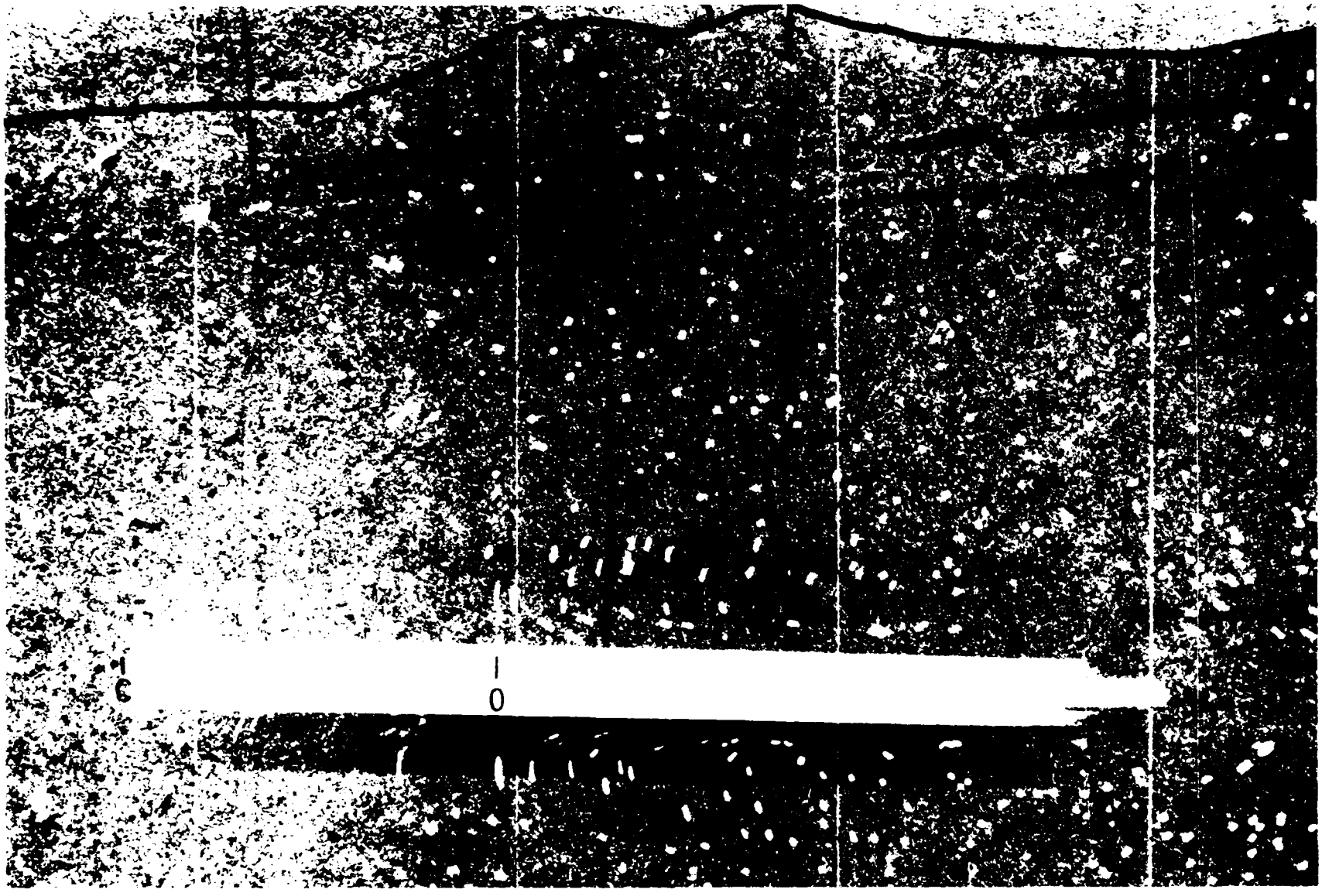

Photo 5. Surface current patterns, 1:120-scale tow, location B

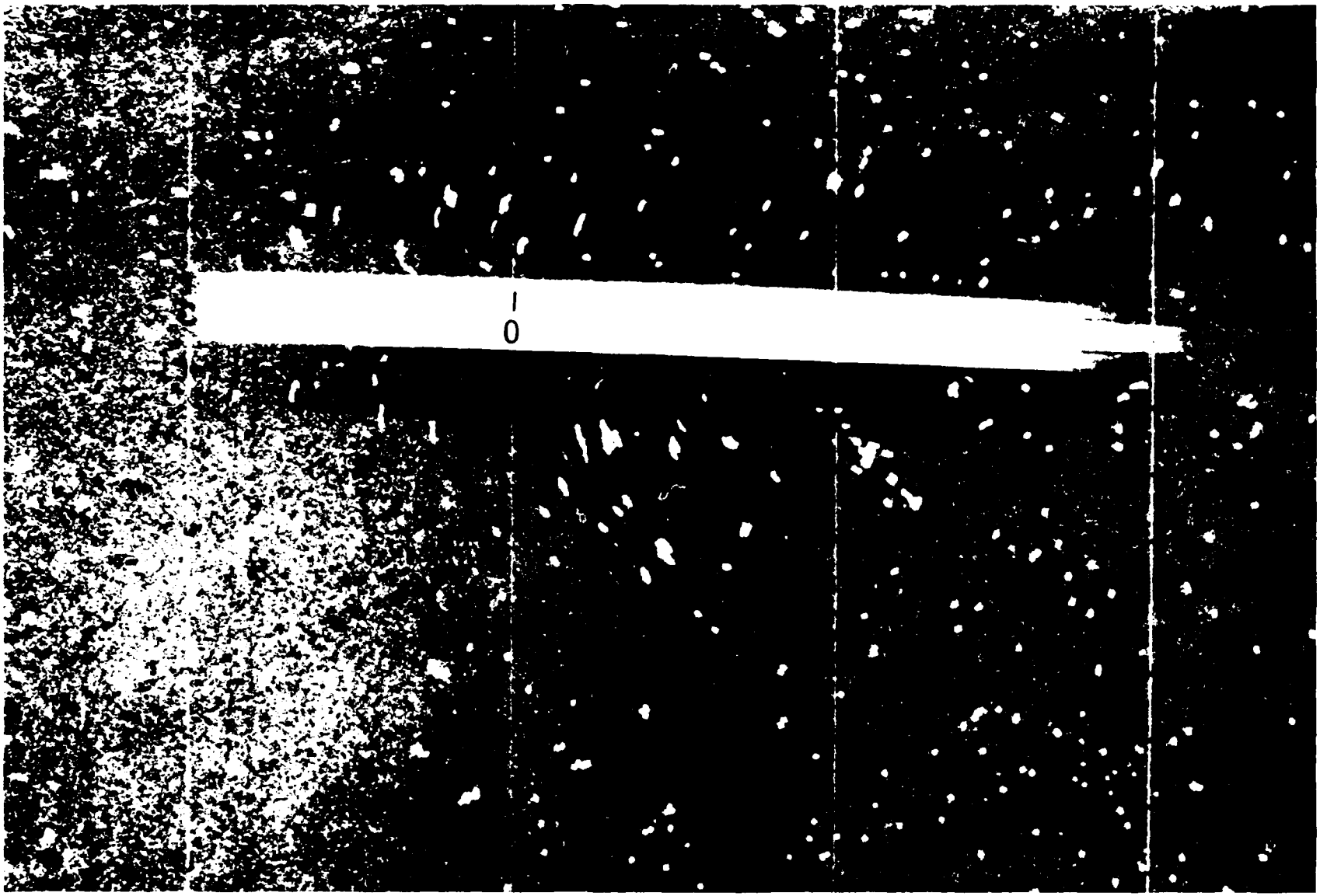

Photo 6. Surface current patterns, 1:120-scale tow, location C

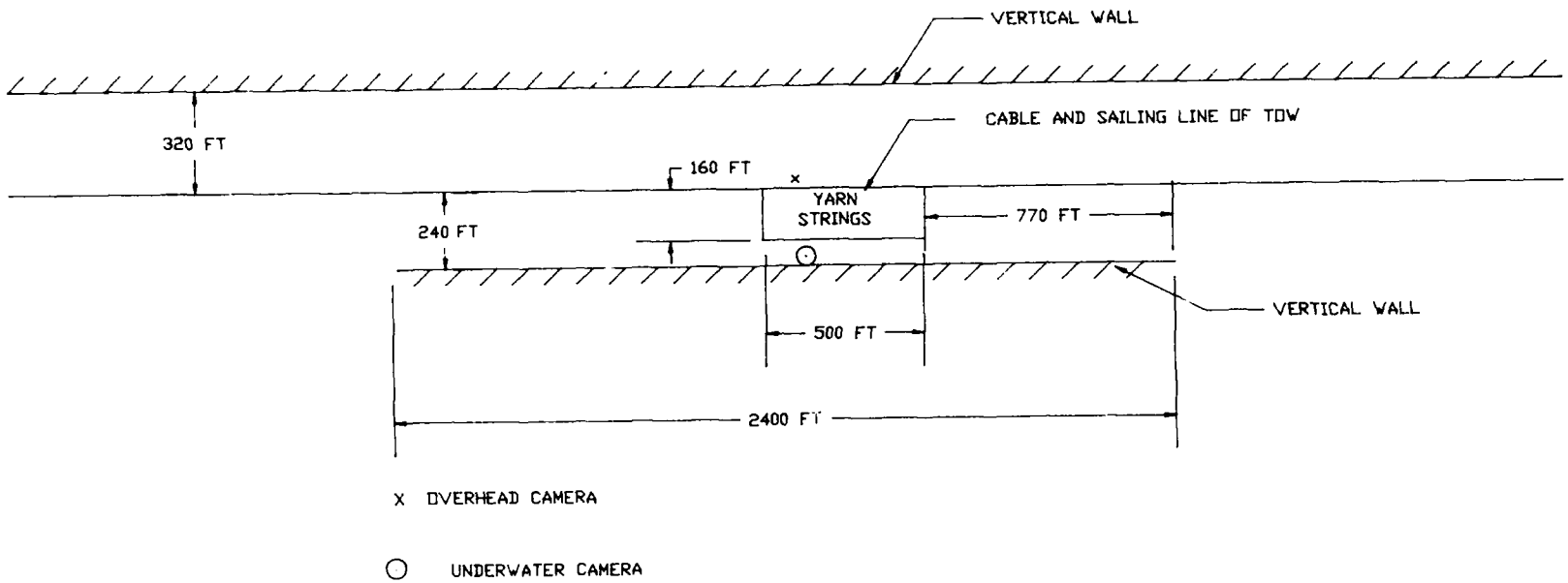

MODEL LAYOUT

1:20 - SCALE FLOW

VISUALIZATION STUDY

NOTE: ALL DIMENSIONS IN PROTOTYPE FEET

PLATE 1

PLATE 2

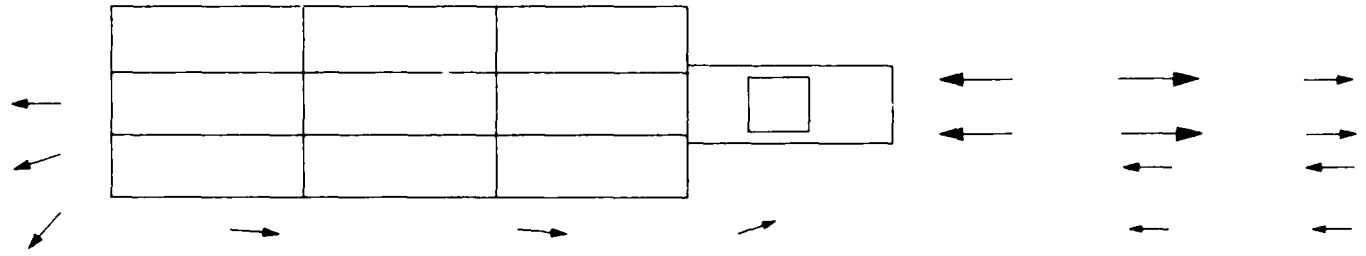

PLAN VIEW

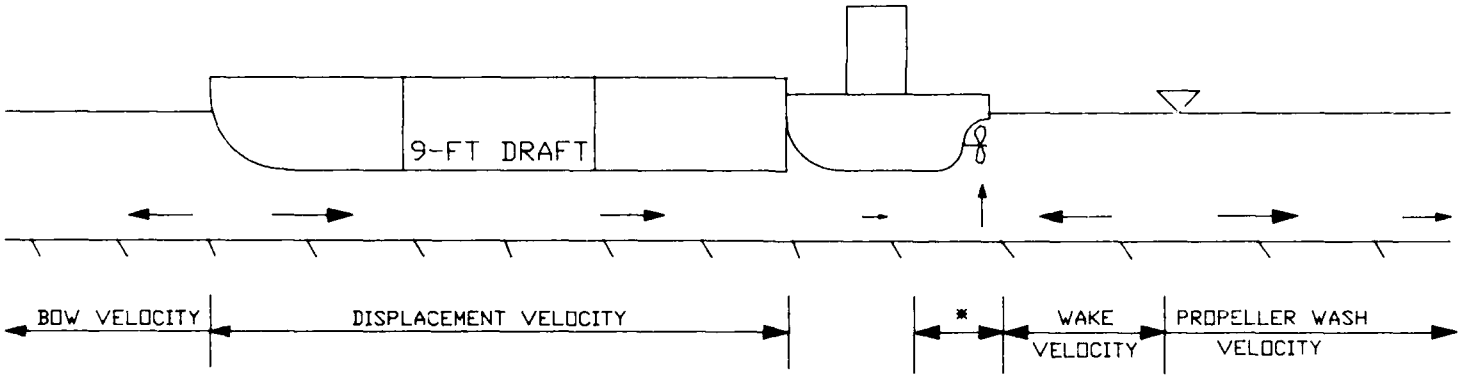

ELEVATION VIEW AT TOW AXIS

* VELOCITY ENTERING PROPELLER

NOTE: ARROW LENGTH IS ONLY A QUALITATIVE INDICATOR OF MAGNITUDE

VELOCITY VECTORS

DEPTH 21 FT, LOADED BARGES
TOW SPEED 6.9 MPH
PROPELLER SPEED 185 RPM

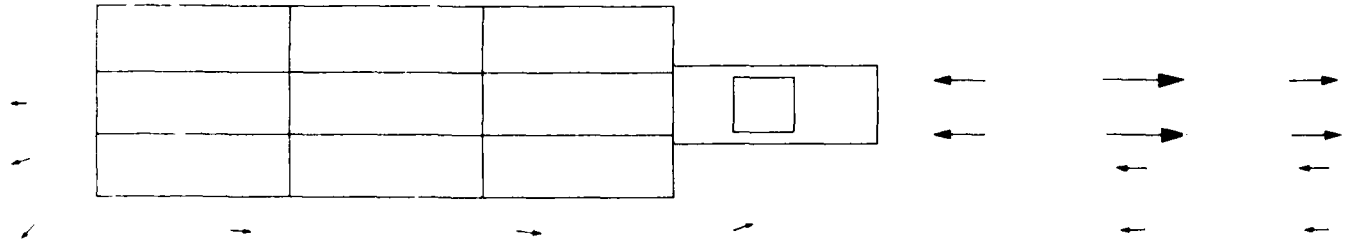

PLAN VIEW

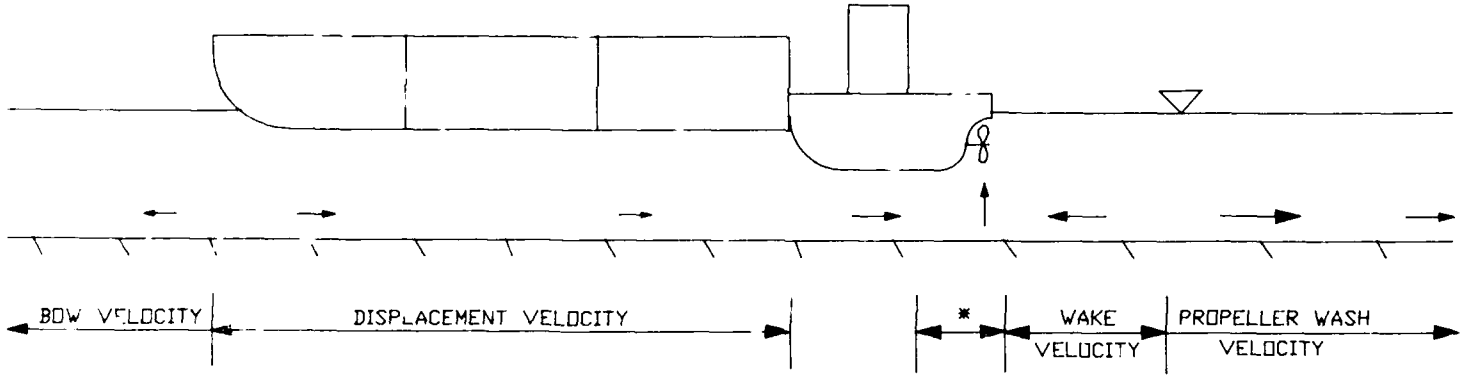

ELEVATION VIEW AT TOW AXIS

* VELOCITY ENTERING PROPELLER

NOTE: ARROW LENGTH IS ONLY A QUALITATIVE INDICATOR OF MAGNITUDE

VELOCITY VECTORS

DEPTH 21 FT, UNLOADED BARGES
TOW SPEED 9.5 MPH
PROPELLER SPEED 185 RPM

PLATE 3

PLATE 4

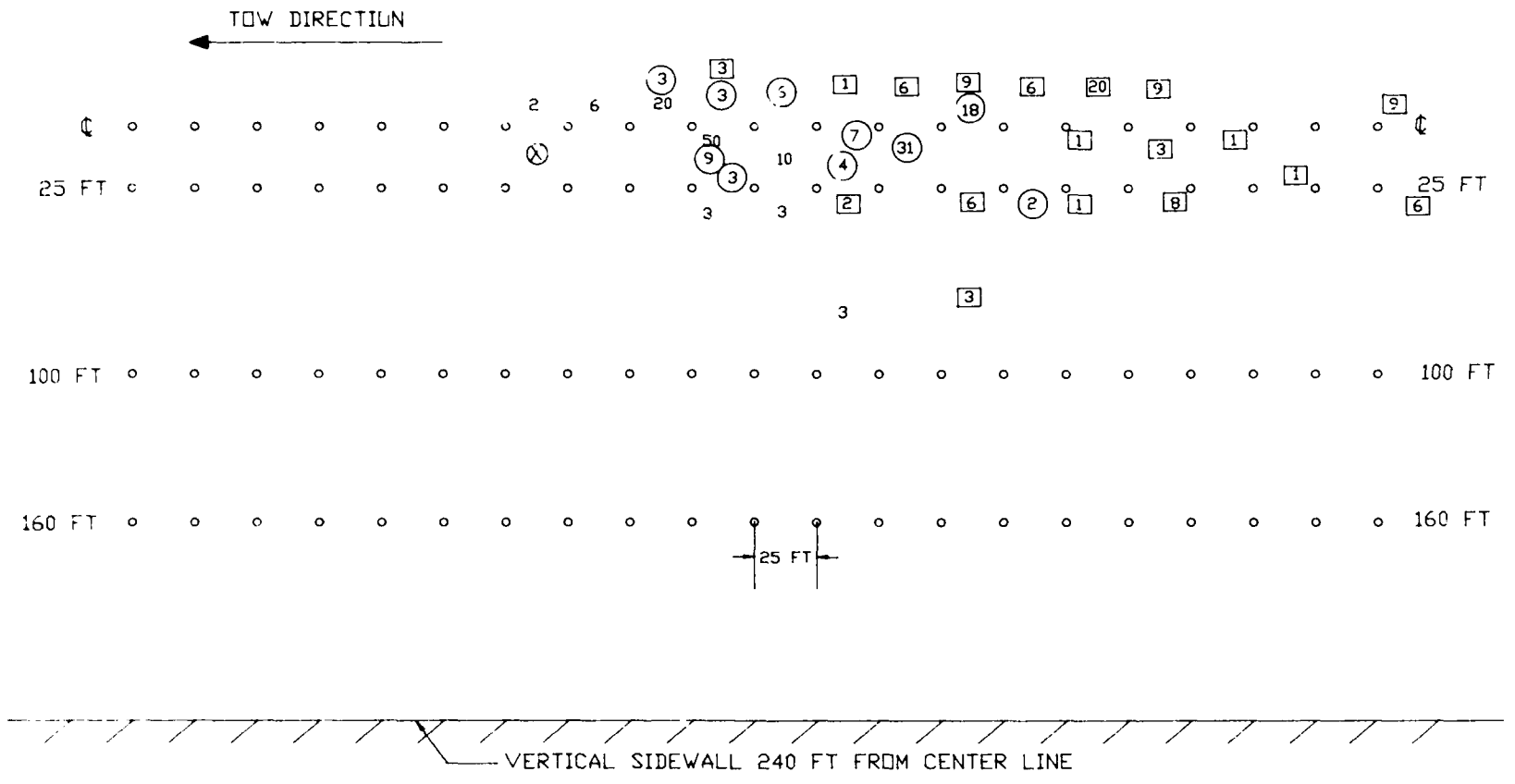

⊗ INITIAL LOCATION FOR 100 BEADS
10 NUMBER OF BEADS AND LOCATION AFTER 1ST RUN
(10) NUMBER OF BEADS AND LOCATION AFTER 2ND RUN
[10] NUMBER OF BEADS AND LOCATION AFTER 3RD RUN

PLASTIC BEAD TESTS

3W X 3L LOADED TOW
TOW SPEED 6.9 MPH
PROPELLER SPFED 185 RPM
BEADS 12.5 FT OFF CHANNEL CENTER LINE

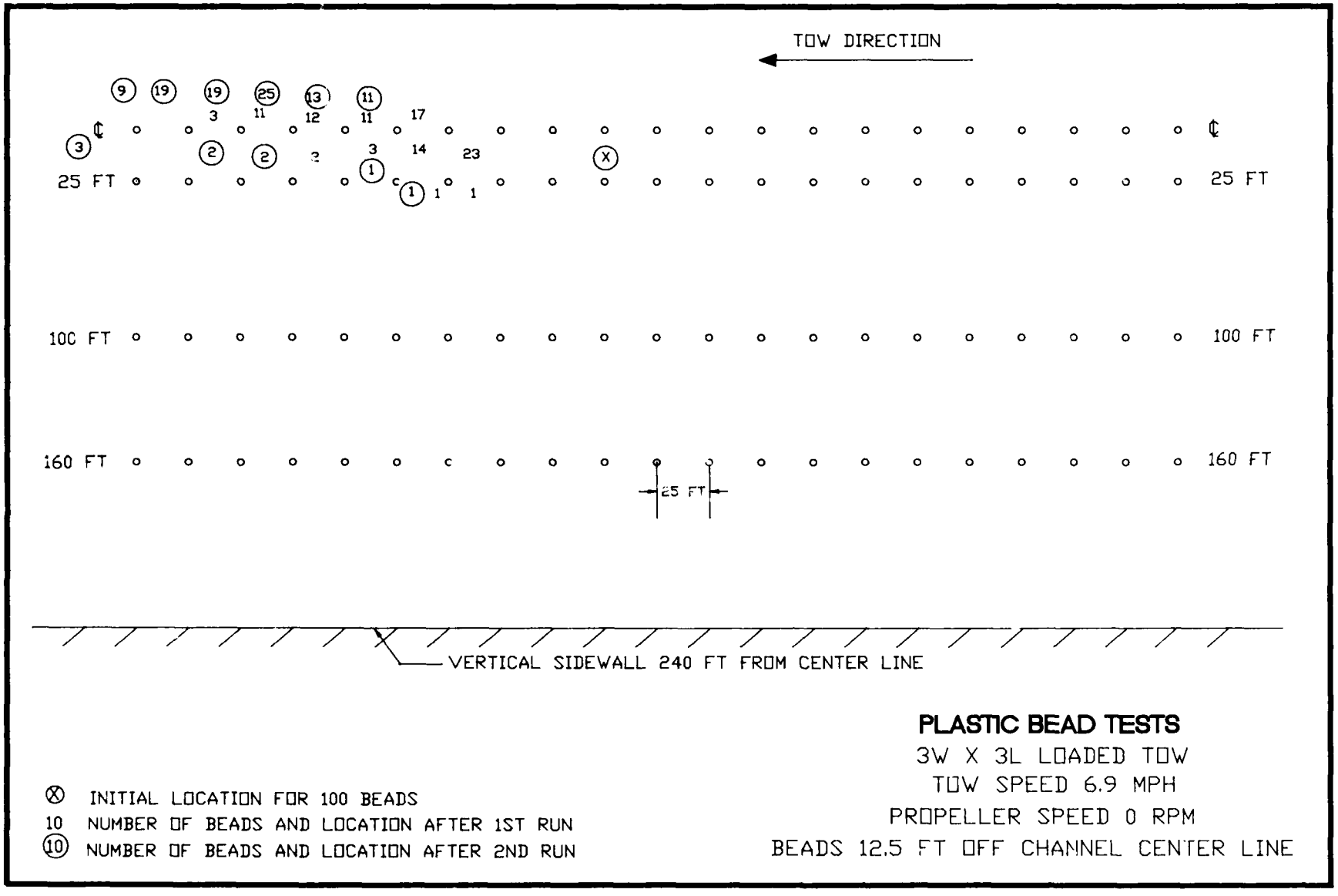

PLASTIC BEAD TESTS

3W X 3L LOADED TOW

TOW SPEED 6.9 MPH

PROPELLER SPEED 0 RPM

BEADS 12.5 FT OFF CHANNEL CENTER LINE

⊗ INITIAL LOCATION FOR 100 BEADS

10 NUMBER OF BEADS AND LOCATION AFTER 1ST RUN

⑩ NUMBER OF BEADS AND LOCATION AFTER 2ND RUN

PLATE 5

PLATE 6

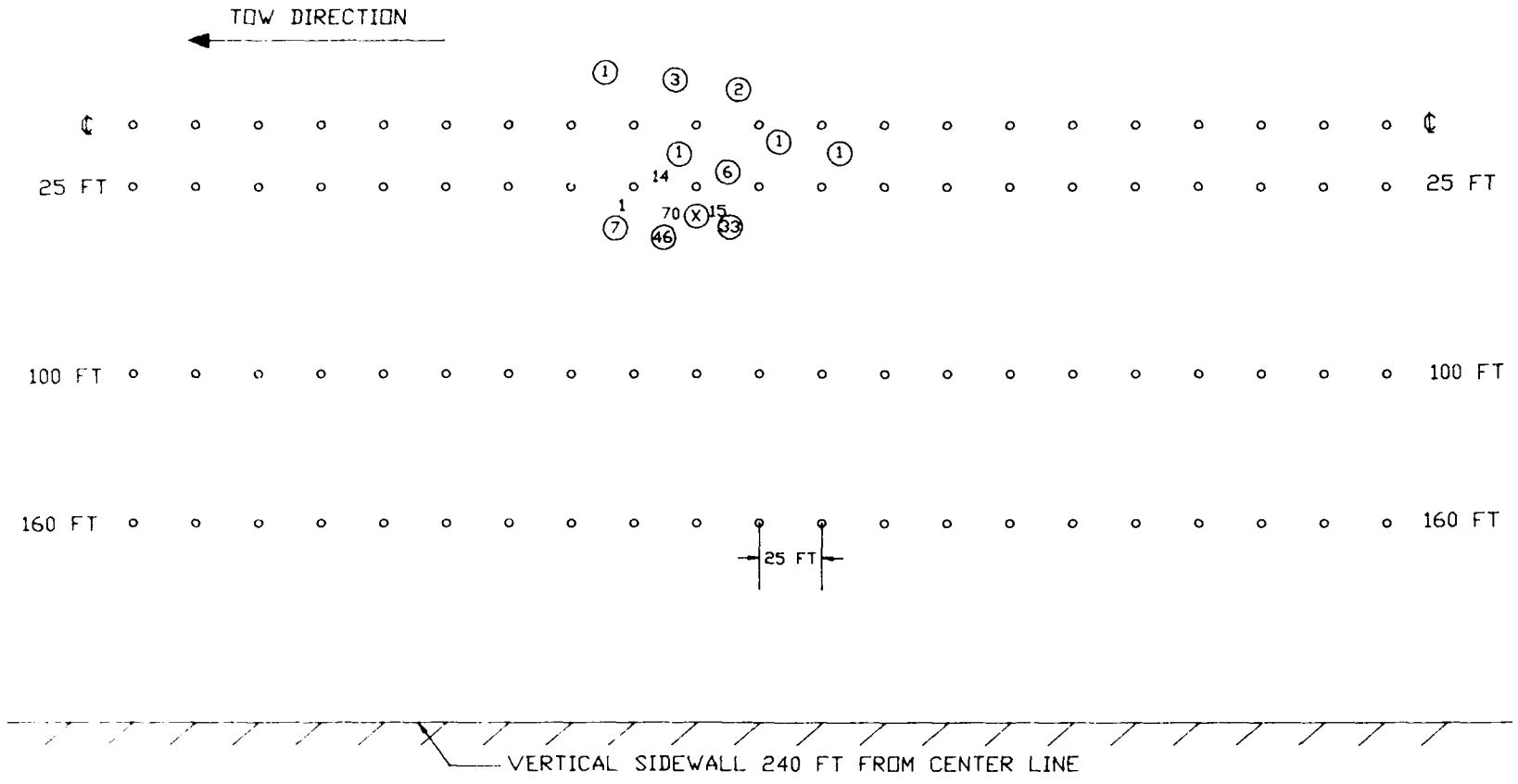

PLASTIC BEAD TESTS

3W X 3L LOADED TOW
TOW SPEED 6.9 MPH
PROPELLER SPEED 185 RPM
BEADS 37.5 FT OFF CHANNEL CENTER LINE

⊗ INITIAL LOCATION FOR 100 BEADS
10 NUMBER OF BEADS AND LOCATION AFTER 1ST RUN
⑩ NUMBER OF BEADS AND LOCATION AFTER 2ND RUN

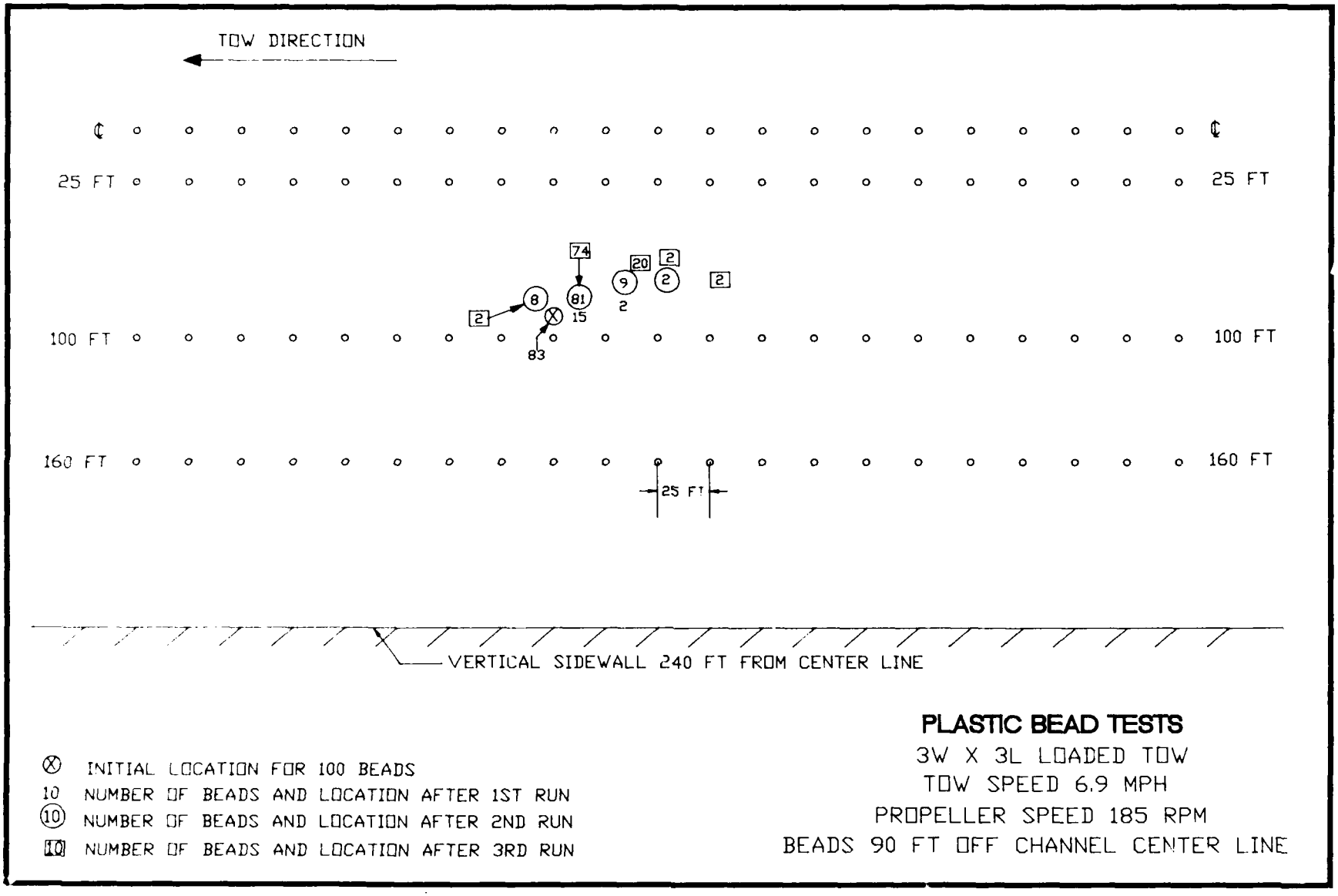

⊗ INITIAL LOCATION FOR 100 BEADS
10 NUMBER OF BEADS AND LOCATION AFTER 1ST RUN
(10) NUMBER OF BEADS AND LOCATION AFTER 2ND RUN
[10] NUMBER OF BEADS AND LOCATION AFTER 3RD RUN

PLASTIC BEAD TESTS
3W X 3L LOADED TOW
TOW SPEED 6.9 MPH
PROPELLER SPEED 185 RPM
BEADS 90 FT OFF CHANNEL CENTER LINE

PLATE 7

PLATE 8

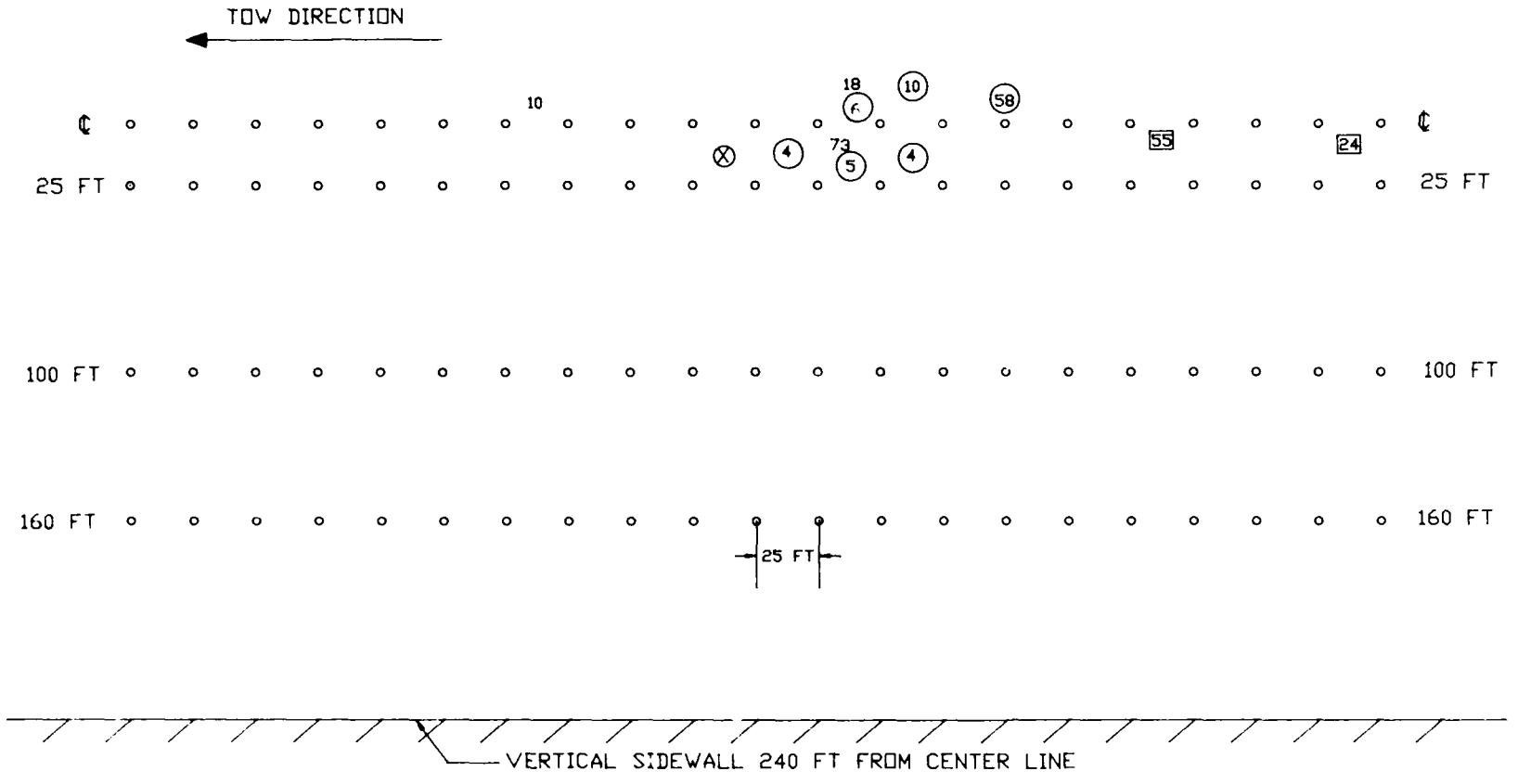

⊗ INITIAL LOCATION FOR 100 BEADS
10 NUMBER OF BEADS AND LOCATION AFTER 1ST RUN
(10) NUMBER OF BEADS AND LOCATION AFTEP 2ND RUN
[10] NUMBER OF BEADS AND LOCATION AFTER 3RD RUN

PLASTIC BEAD TESTS
3W X 1L LOADED TOW
TOW SPEED 8.3 MPH
PROPELLER SPEED 185 RPM
BEADS 12.5 FT OFF CHANNEL CENTER LINE

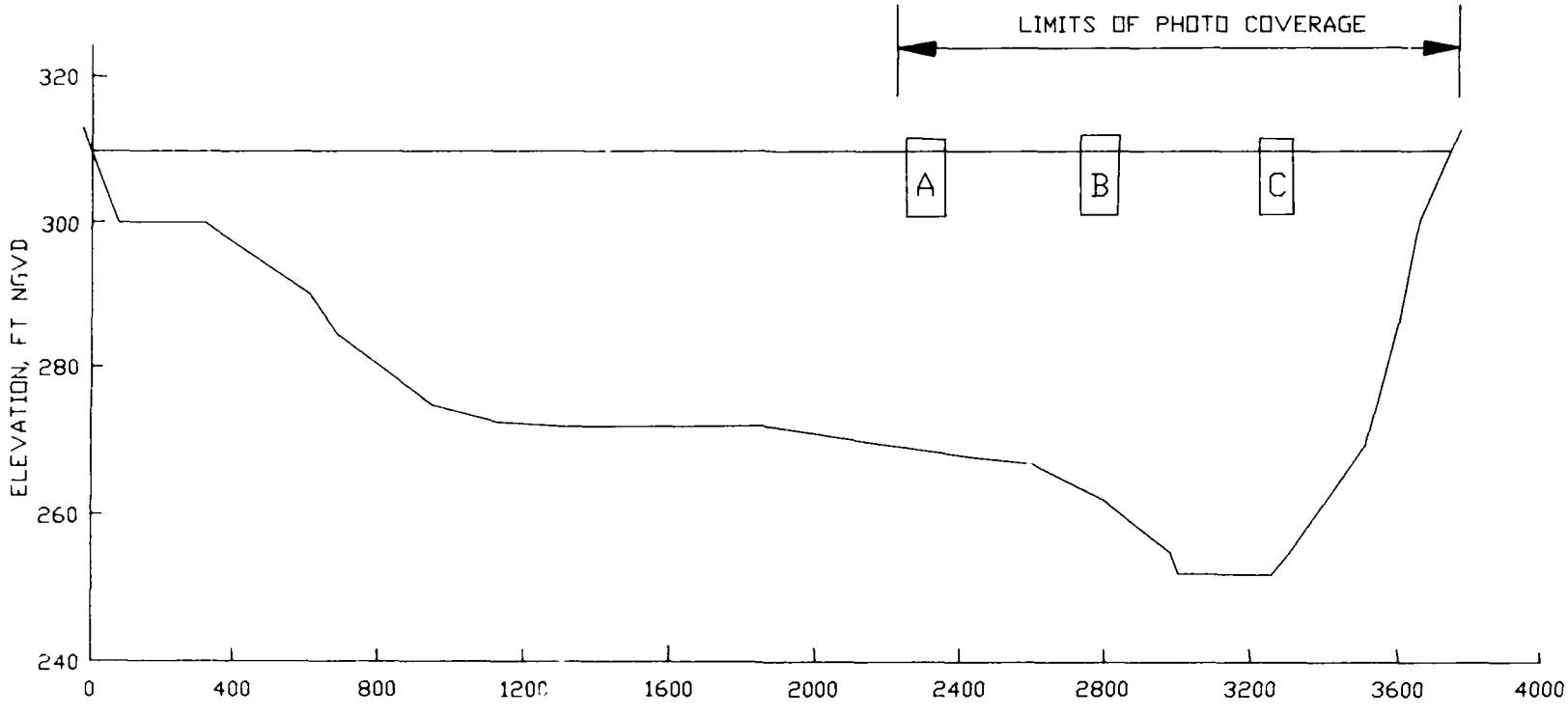

$$N = \frac{\text{WATERWAY AREA}}{\text{TOW AREA}} = \frac{132{,}000}{9(105)} = 140$$

TOW LOCATIONS FOR 1:120 SCALE MODEL

RANGE 9, OLMSTED MODEL

POOL ELEVATION 310

PLATE 9

PLATE 10

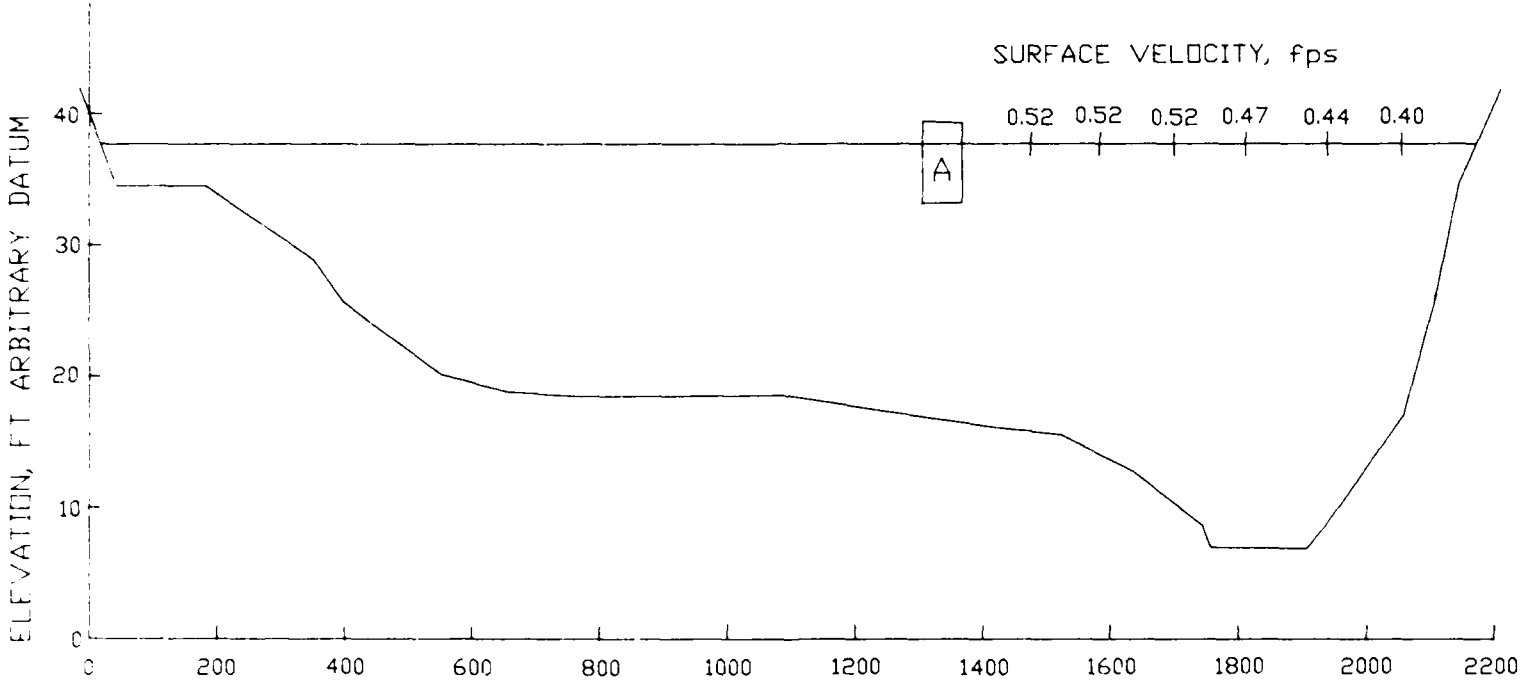

$$N = \frac{\text{WATERWAY AREA}}{\text{TOW AREA}} = \frac{38{,}800}{9(105)} = 41$$

BOUWMEESTER RETURN VELOCITY = 0.37 fps

VELOCITIES FOR 1:70 TOW

TOW POSITION A

TOW SPEED 7.6 MPH

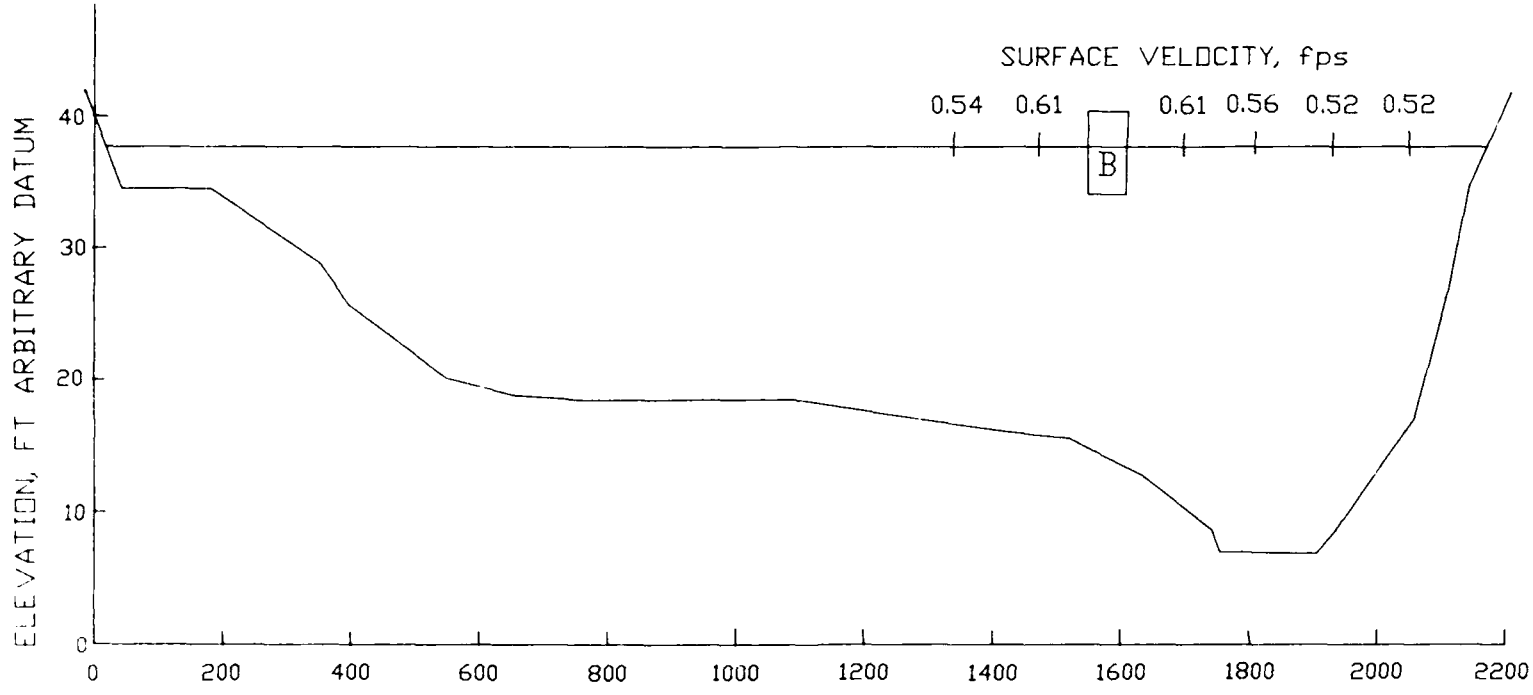

$$N = \frac{\text{WATERWAY AREA}}{\text{TOW AREA}} = \frac{38{,}800}{9(105)} = 41$$

BOUWMEESTER RETURN VELOCITY = 0.36 fps

VELOCITIES FOR 1:70 TOW

TOW POSITION B

TOW SPEED 7.5 MPH

PLATE 11

PLATE 12

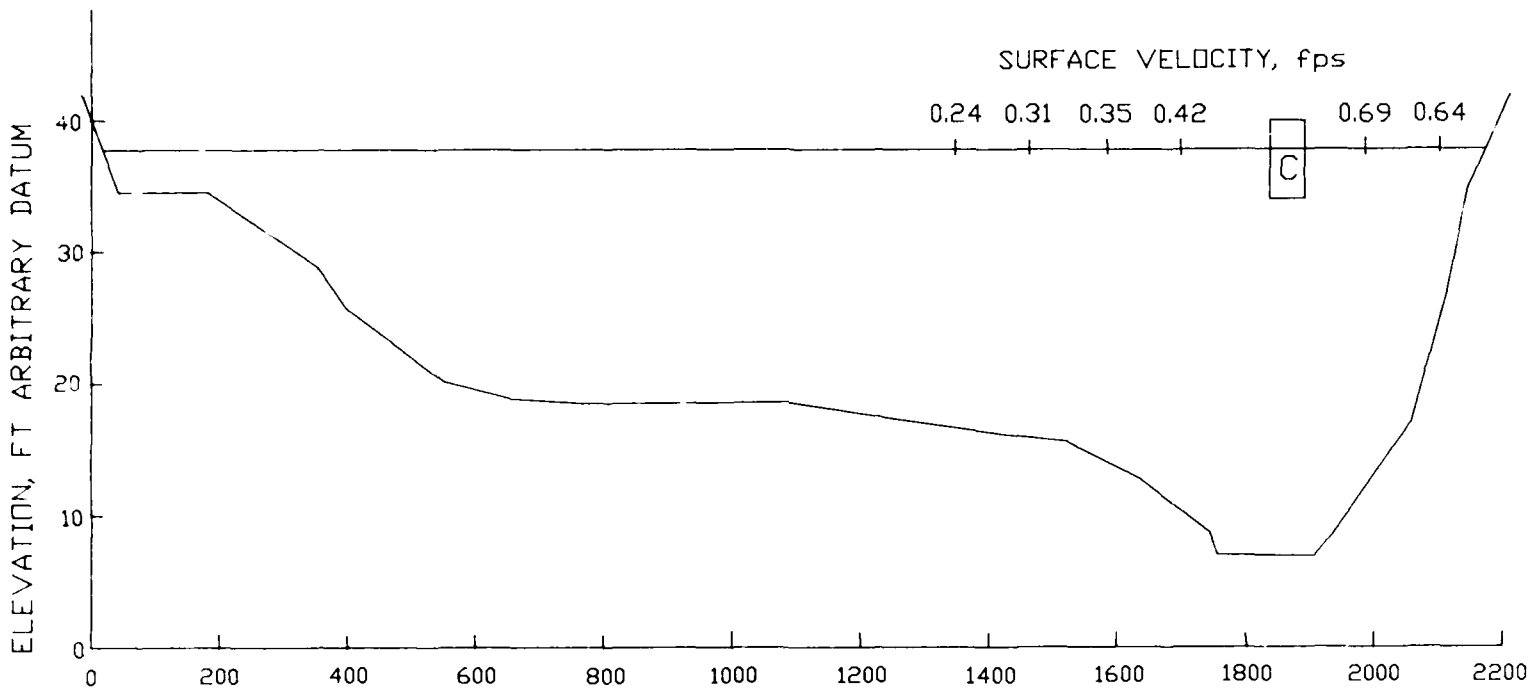

$$N = \frac{\text{WATERWAY AREA}}{\text{TOW AREA}} = \frac{38{,}800}{9(105)} = 41$$

BOUWMEESTER RETURN VELOCITY = 0.33 fps

VELOCITIES FOR 1:70 TOW

TOW POSITION C

TOW SPEED 7.0 MPH

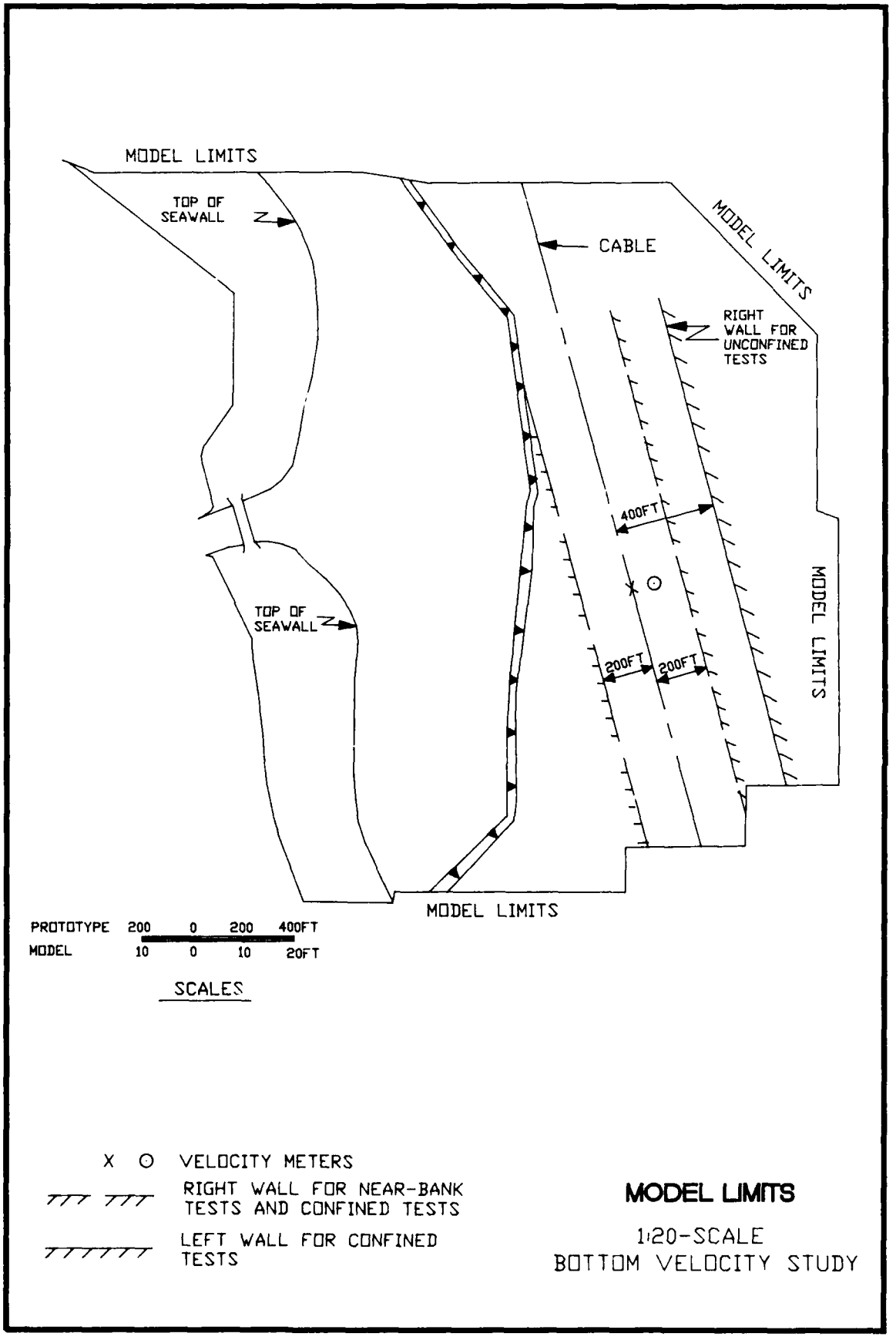
MODEL LIMITS
TOP OF SEAWALL
CABLE
MODEL LIMITS
RIGHT WALL FOR UNCONFINED TESTS
400FT
TOP OF SEAWALL
200FT
200FT
MODEL LIMITS
MODEL LIMITS
PROTOTYPE 200 0 200 400FT
MODEL 10 0 10 20FT
SCALES
X O VELOCITY METERS
RIGHT WALL FOR NEAR-BANK TESTS AND CONFINED TESTS
LEFT WALL FOR CONFINED TESTS
MODEL LIMITS
1:20-SCALE
BOTTOM VELOCITY STUDY

PLATE 13

PLATE 14

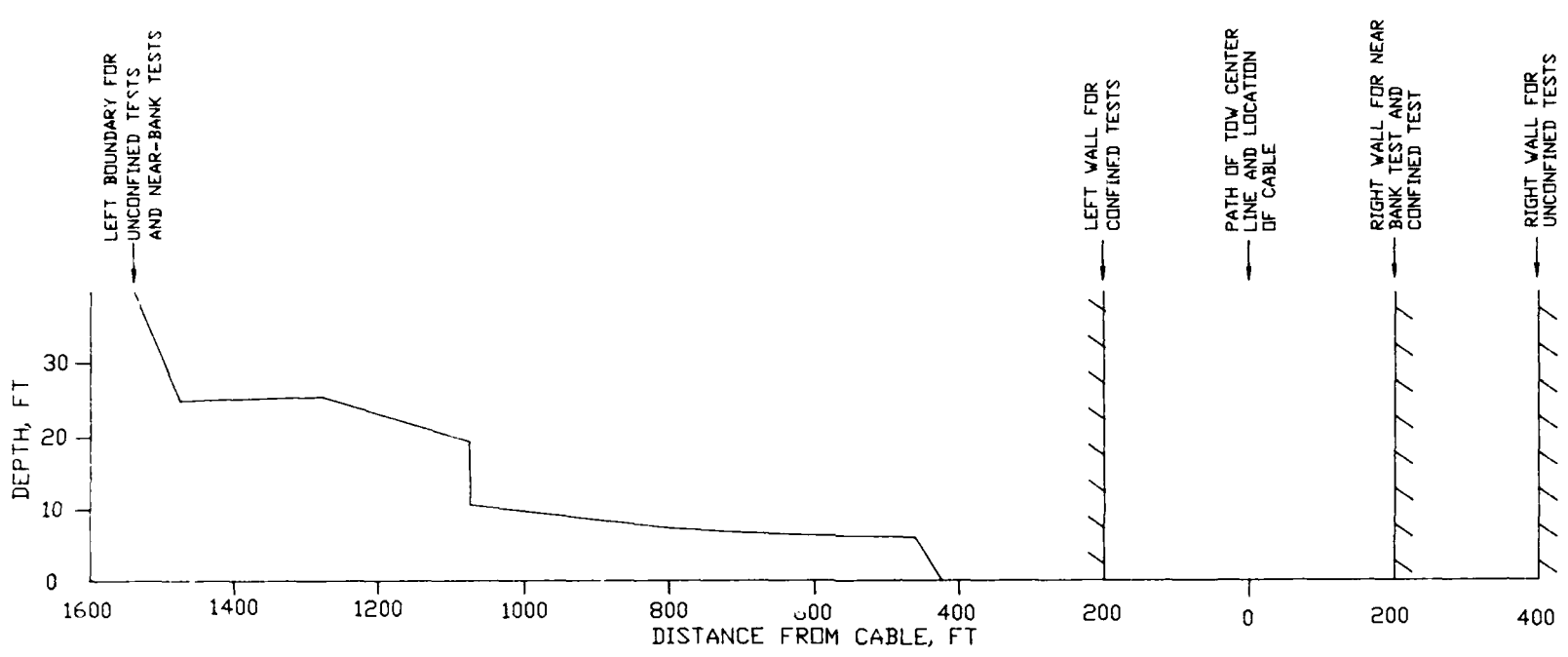

CONDITION	AREA, SQ FT TOTAL	AREA, SQ FT LEFT OF CABLE
15-FT DEPTH		
UNCONFINED	16,800	0
NEAR BANK	13,800	10,800
CONFINED	6,000	3,000
30-FT DEPTH		
UNCONFINED	41,500	29,500
NEAR BANK	35,500	29,500
CONFINED	12,000	6,000

CHANNEL CROSS SECTIONS

BOTTOM VELOCITY STUDY

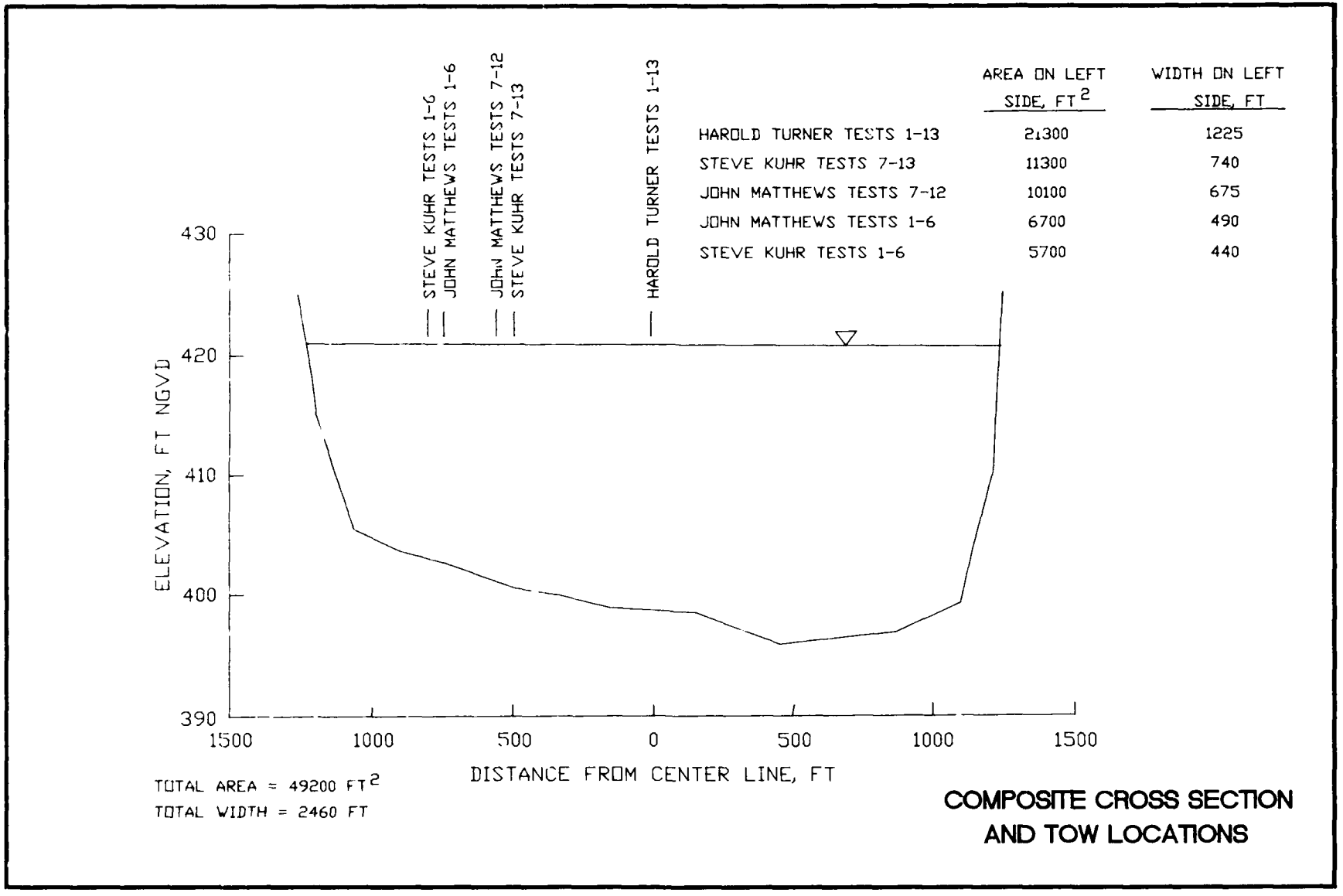
STEVE KUHR TESTS 1-6
JOHN MATTHEWS TESTS 1-6
JOHN MATTHEWS TESTS 7-12
STEVE KUHR TESTS 7-13
HAROLD TURNER TESTS 1-13
AREA ON LEFT SIDE, FT2
WIDTH ON LEFT SIDE, FT
HAROLD TURNER TESTS 1-13 21300 1225
STEVE KUHR TESTS 7-13 11300 740
JOHN MATTHEWS TESTS 7-12 10100 675
JOHN MATTHEWS TESTS 1-6 6700 490
STEVE KUHR TESTS 1-6 5700 440
ELEVATION, FT NGVD
430
420
410
400
390
1500
1000
500
0
500
1000
1500
DISTANCE FROM CENTER LINE, FT
TOTAL AREA = 49200 FT2
TOTAL WIDTH = 2460 FT
COMPOSITE CROSS SECTION AND TOW LOCATIONS

PLATE 15

PLATE 16

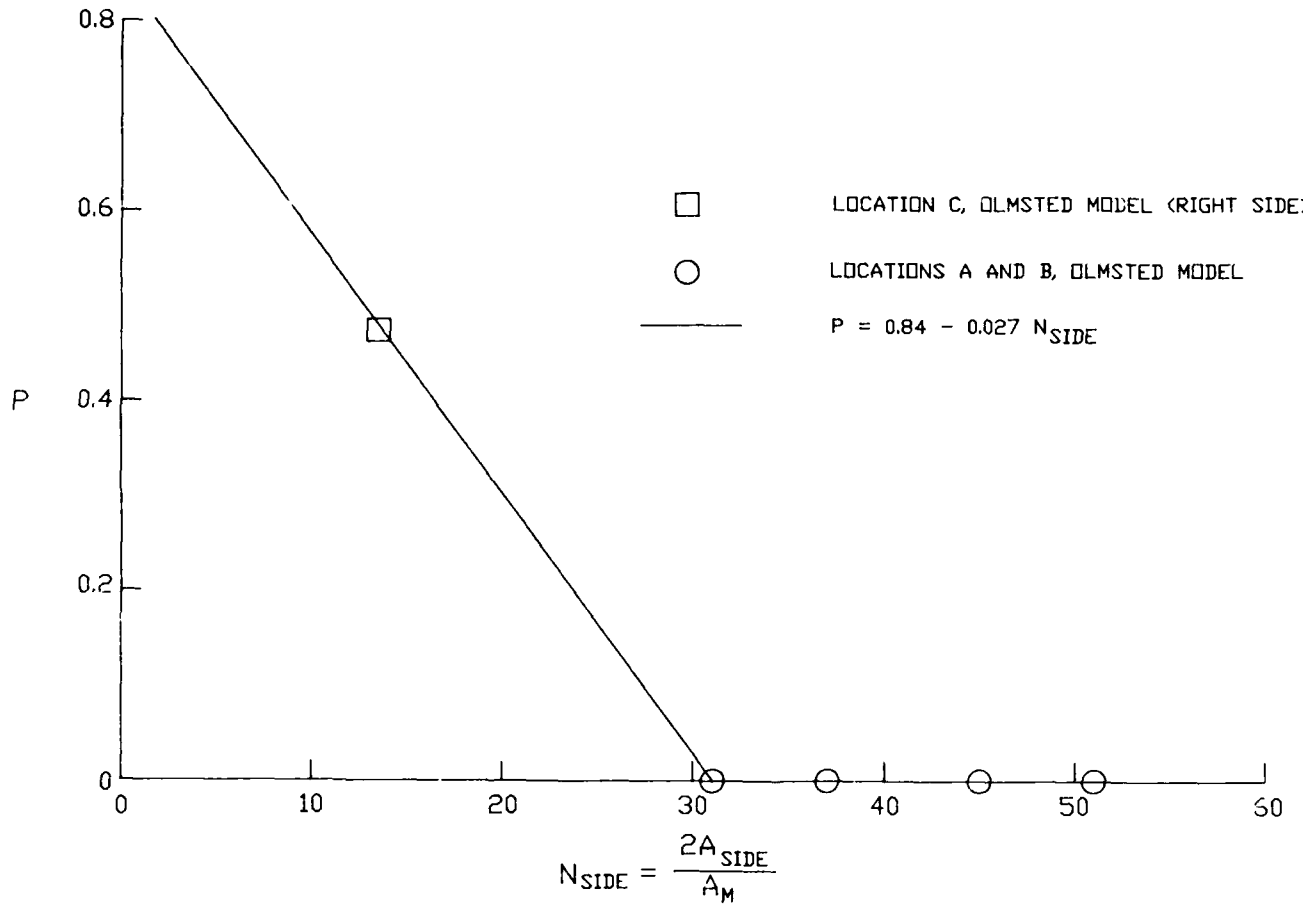

P VERSUS N_{SIDE}

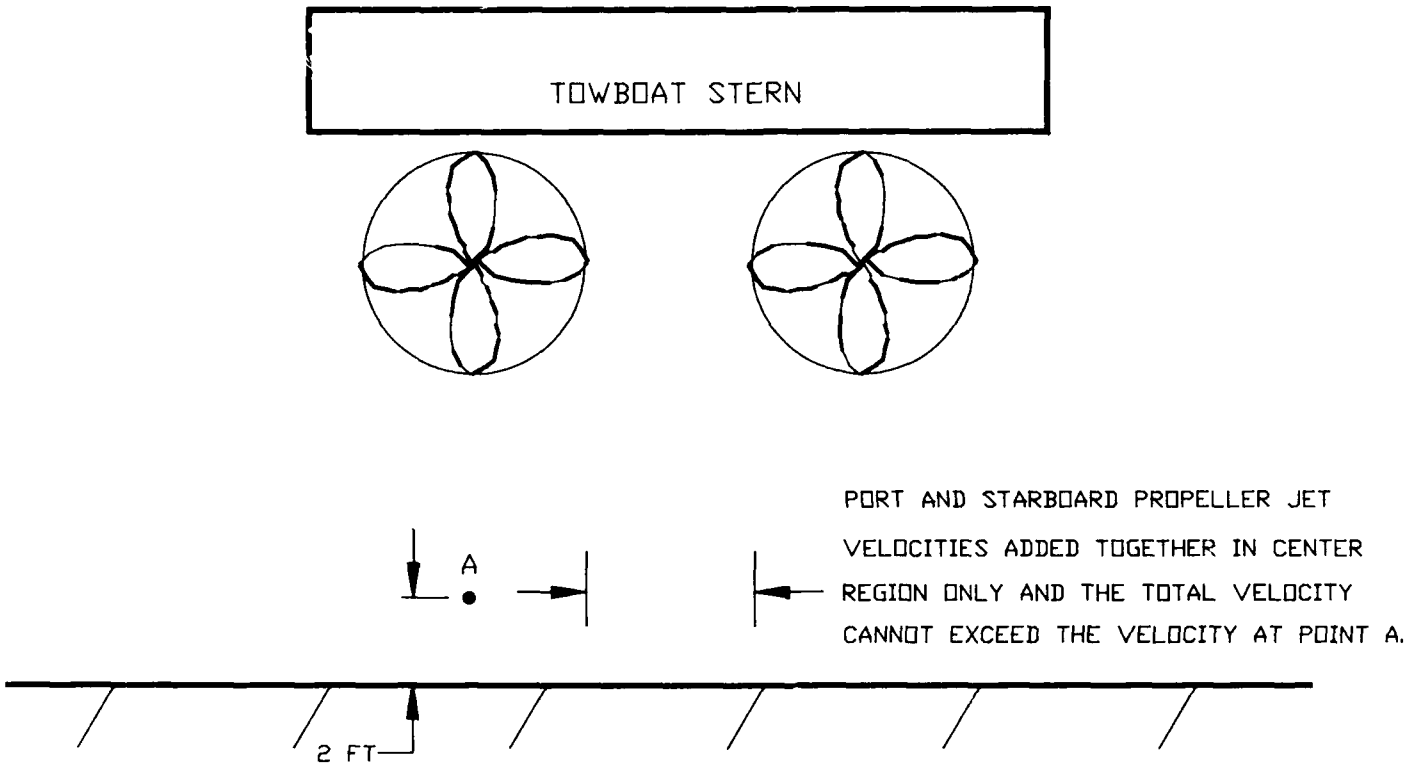

DETERMINATION OF PROPELLER JET VELOCITIES

PLATE 17

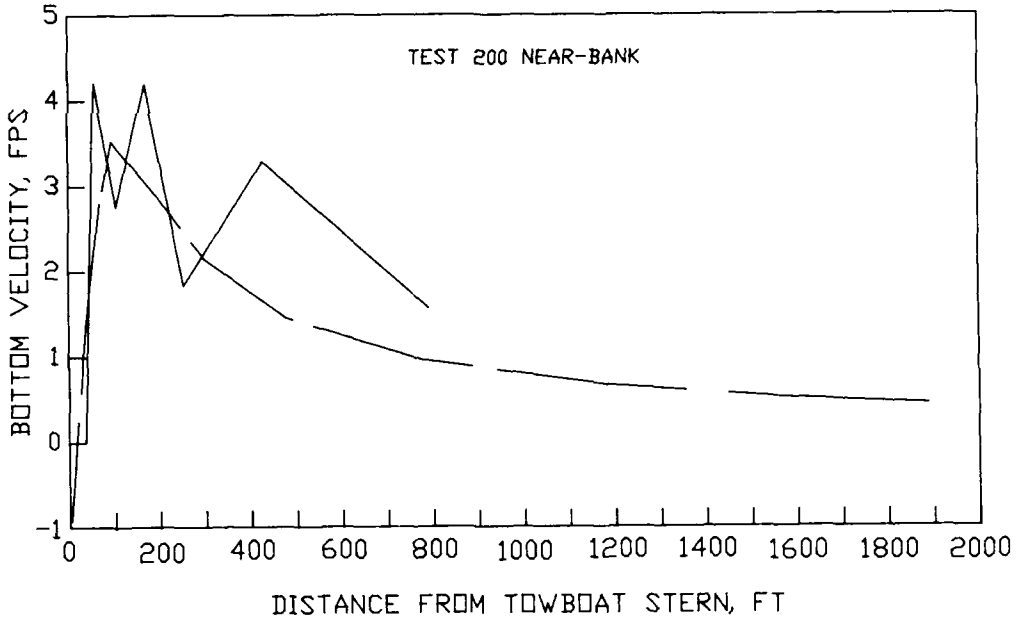

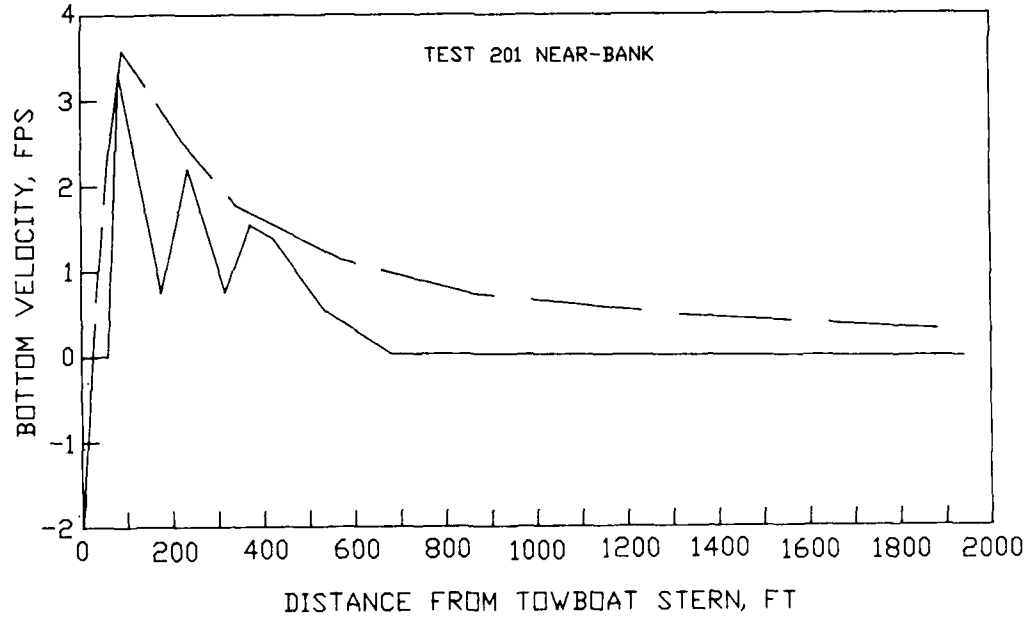

POSITIVE VELOCITY IS OPPOSITE TOW DIRECTION
VELOCITIES ON CENTER LINE OF VESSEL

– – – VERHEY METHOD

——— PHYSICAL MODEL DATA

PHYSICAL MODEL VELOCITIES

VERSUS VERHEY METHOD

TESTS 200 AND 201

PLATE 18

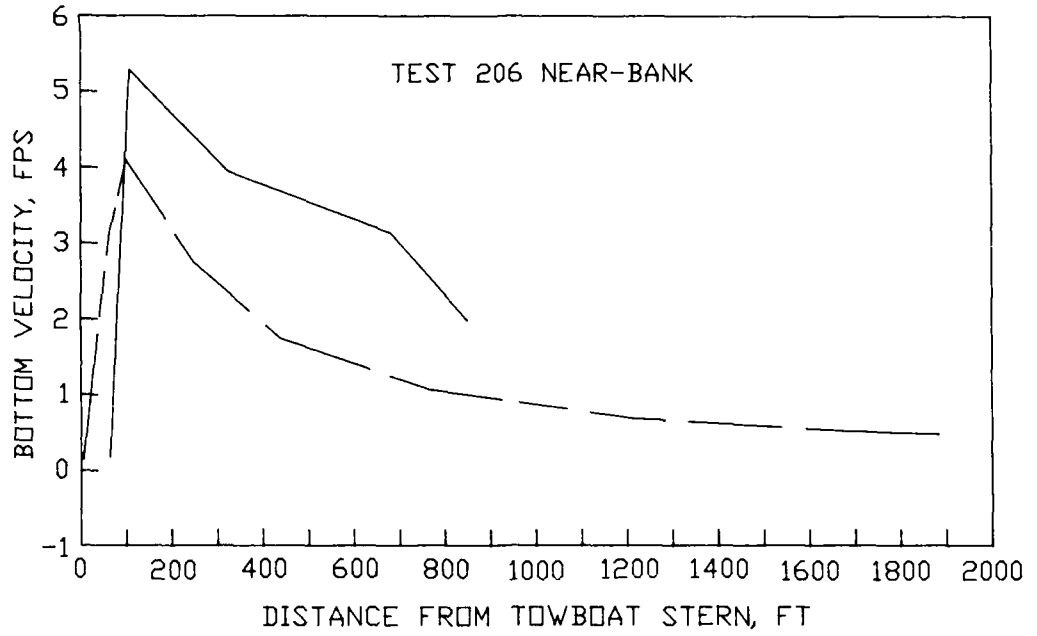

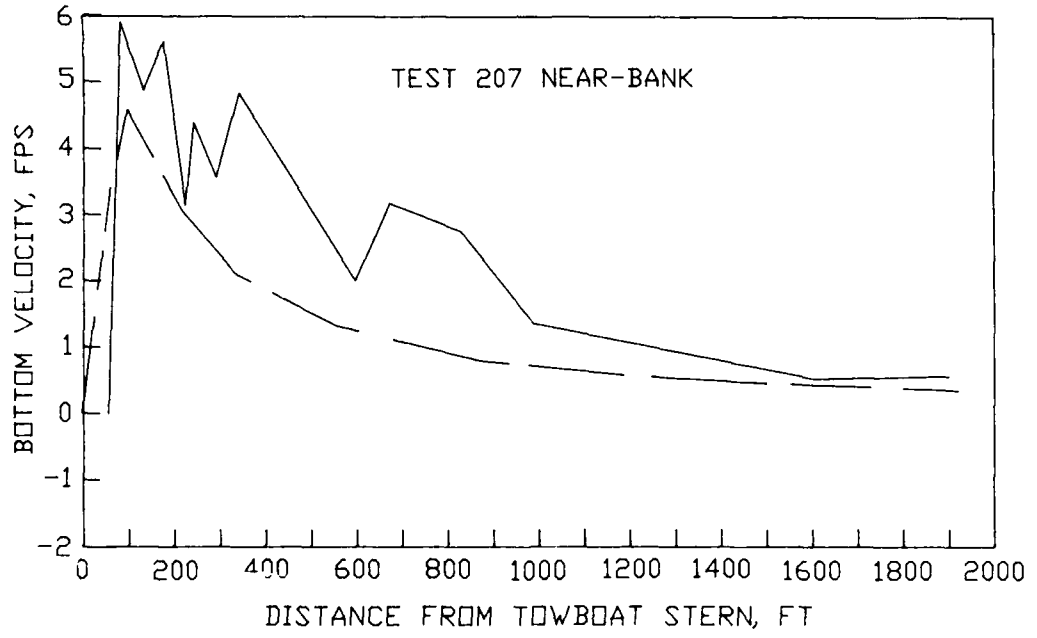

POSITIVE VELOCITY IS OPPOSITE TOW DIRECTION
VELOCITIES ON CENTER LINE OF VESSEL

– – – VERHEY METHOD

——— PHYSICAL MODEL DATA

PHYSICAL MODEL VELOCITIES VERSUS VERHEY METHOD

TESTS 206 AND 207

PLATE 19

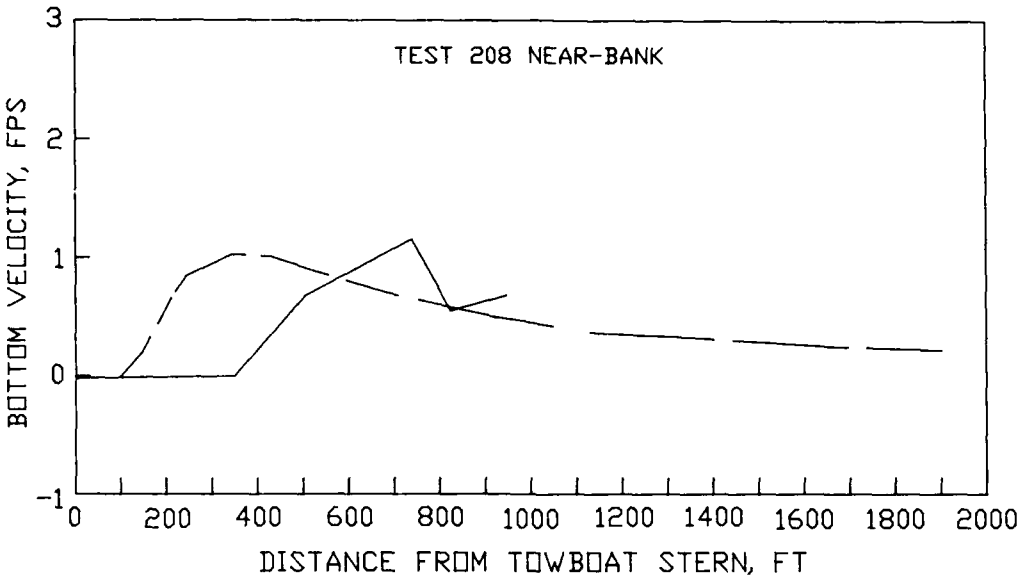

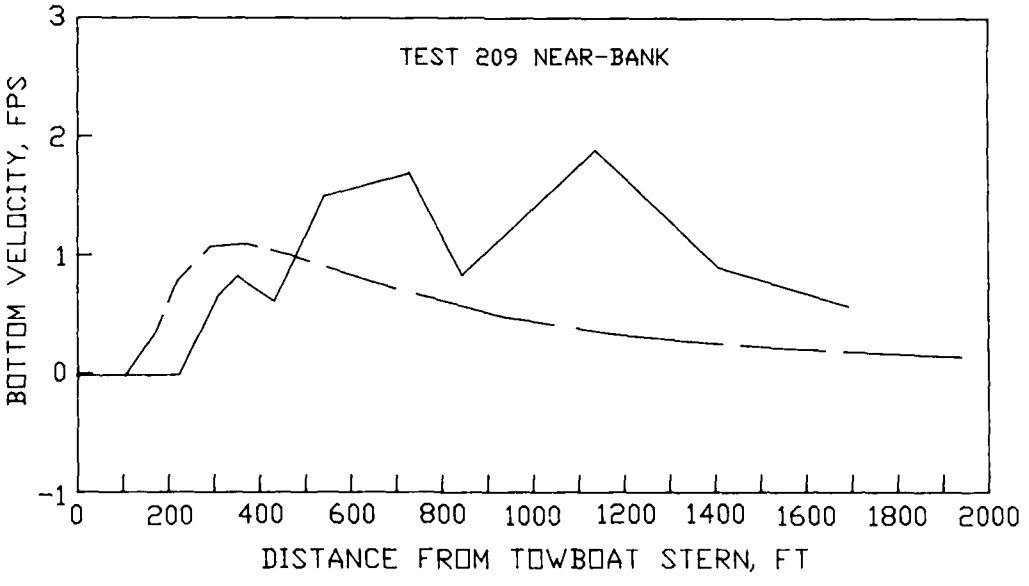

POSITIVE VELOCITY IS OPPOSITE TOW DIRECTION
VELOCITIES ON CENTER LINE OF VESSEL

- - - VERHEY METHOD
——— PHYSICAL MODEL DATA

PHYSICAL MODEL VELOCITIES

VERSUS VERHEY METHOD

TESTS 208 AND 209

PLATE 20

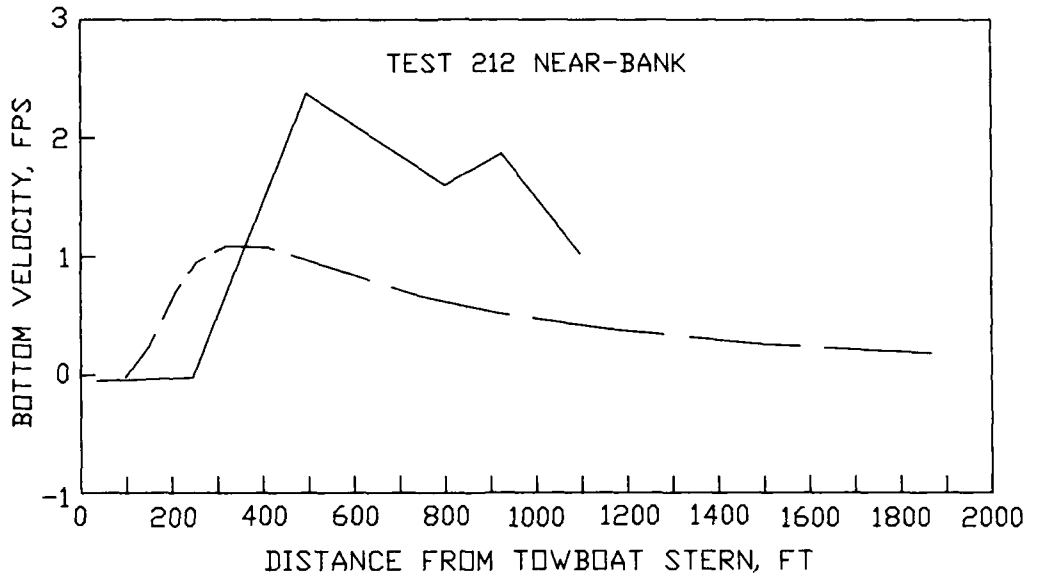

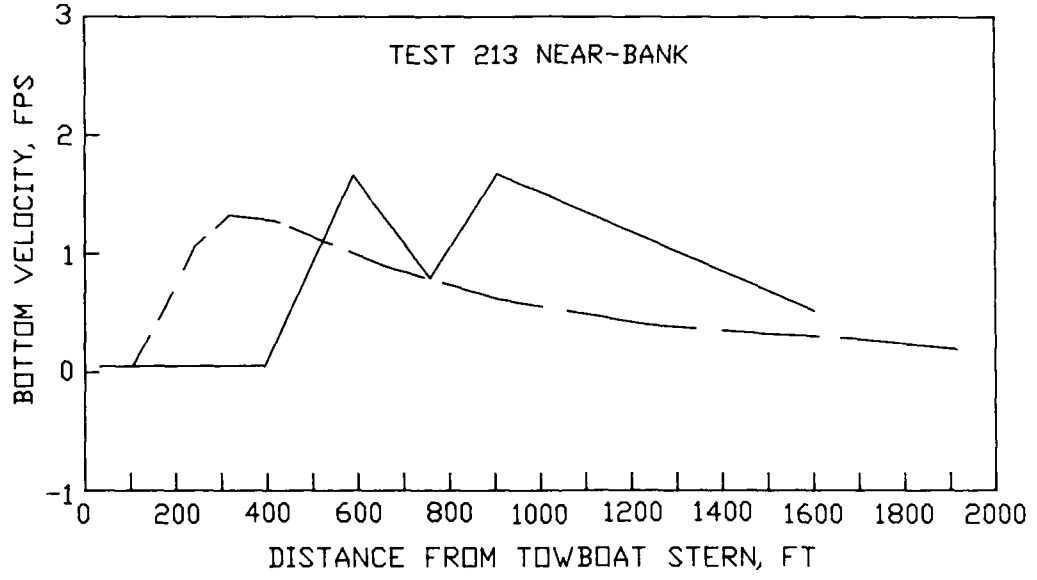

POSITIVE VELOCITY IS OPPOSITE TOW DIRECTION
VELOCITIES ON CENTER LINE OF VESSEL

– – – VERHEY METHOD

——— PHYSICAL MODEL DATA

PHYSICAL MODEL VELOCITIES

VERSUS VERHEY METHOD

TESTS 212 AND 213

PLATE 21

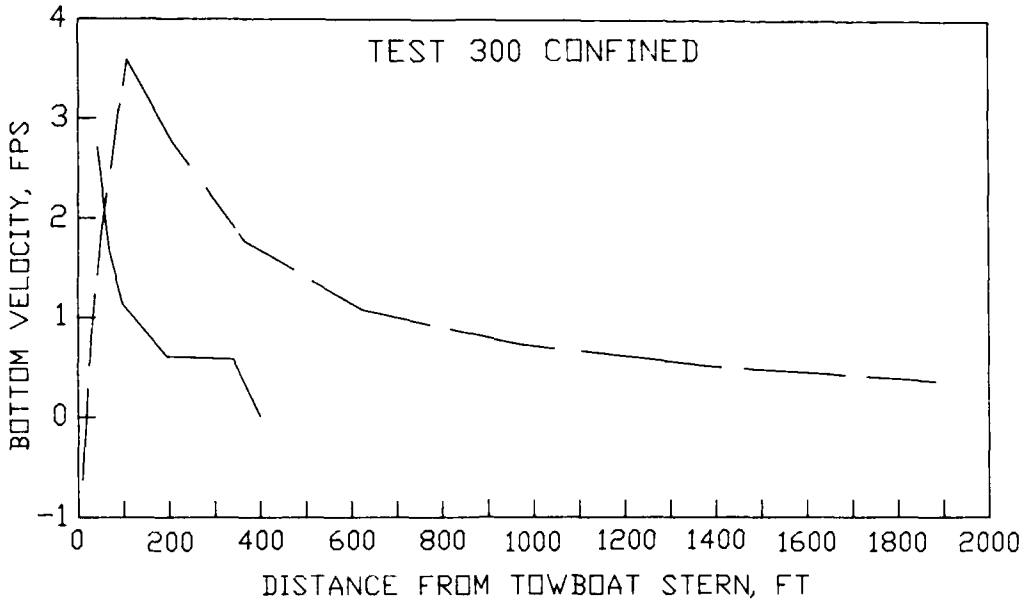

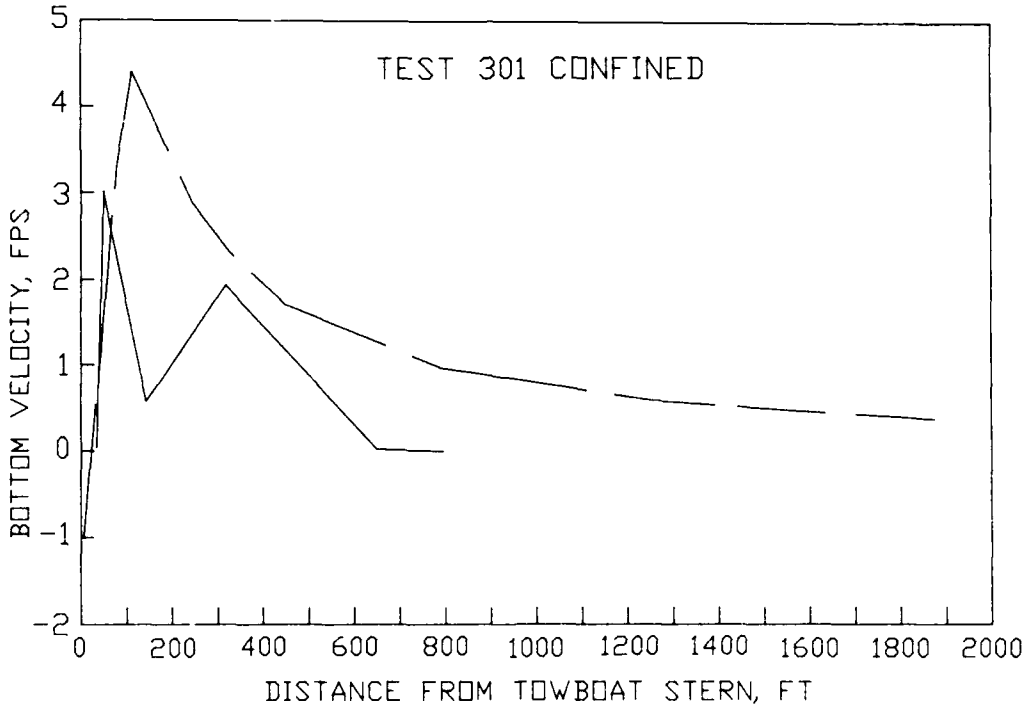

POSITIVE VELOCITY IS OPPOSITE TOW DIRECTION
VELOCITIES ON CENTER LINE OF VESSEL

– – – VERHEY METHOD

——— PHYSICAL MODEL DATA

PHYSICAL MODEL VELOCITIES

VERSUS VERHEY METHOD

TESTS 300 AND 301

PLATE 22

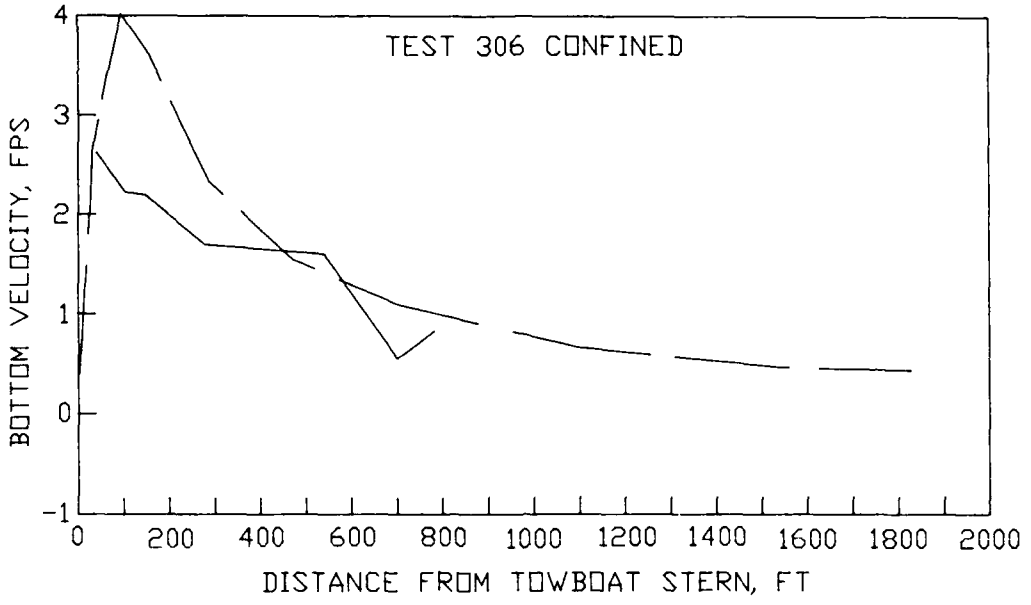

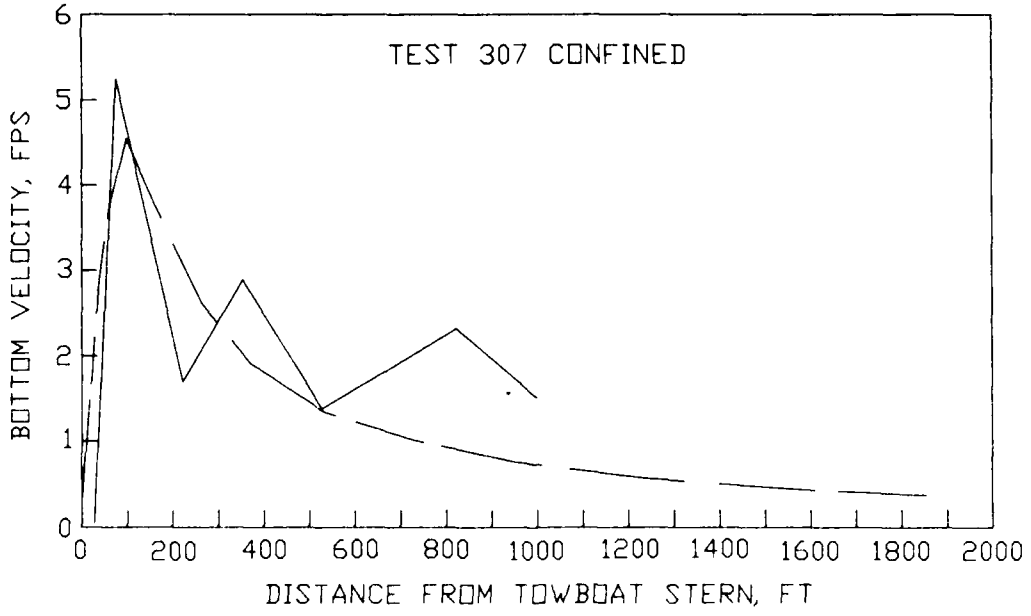

POSITIVE VELOCITY IS OPPOSITE TOW DIRECTION
VELOCITIES ON CENTER LINE OF VESSEL

– – – VERHEY METHOD
——— PHYSICAL MODEL DATA

PHYSICAL MODEL VELOCITIES
VERSUS VERHEY METHOD
TESTS 306 AND 307

PLATE 23

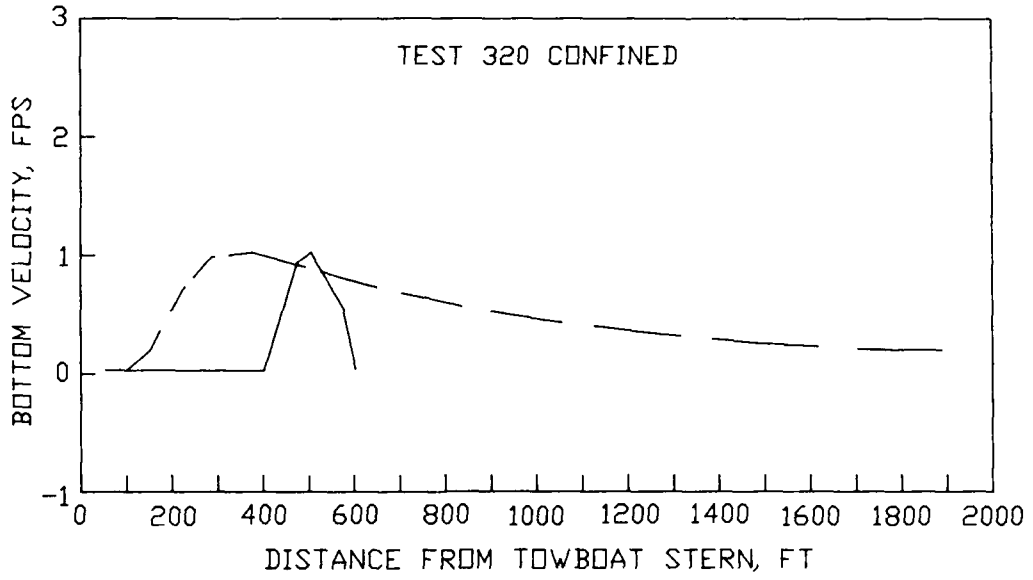

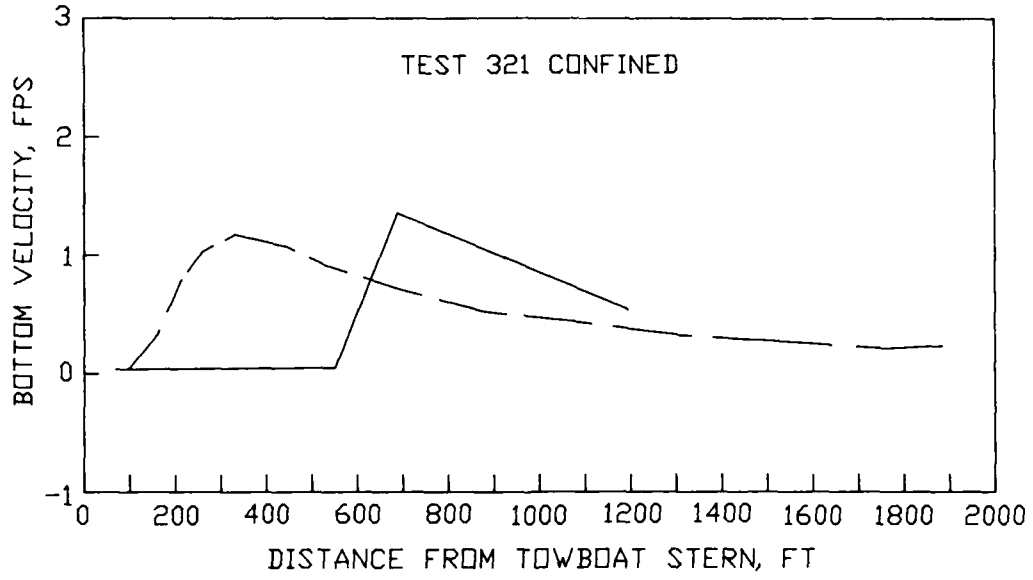

POSITIVE VELOCITY IS OPPOSITE TOW DIRECTION
VELOCITIES ON CENTER LINE OF VESSEL

– – – VERHEY METHOD

——— PHYSICAL MODEL DATA

PHYSICAL MODEL VELOCITIES

VERSUS VERHEY METHOD

TESTS 320 AND 321

PLATE 24

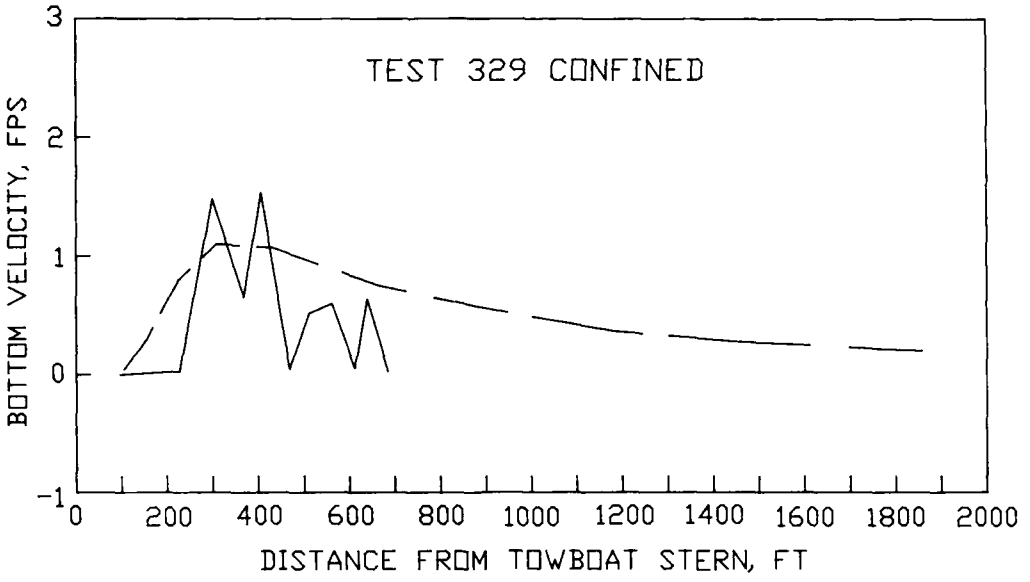

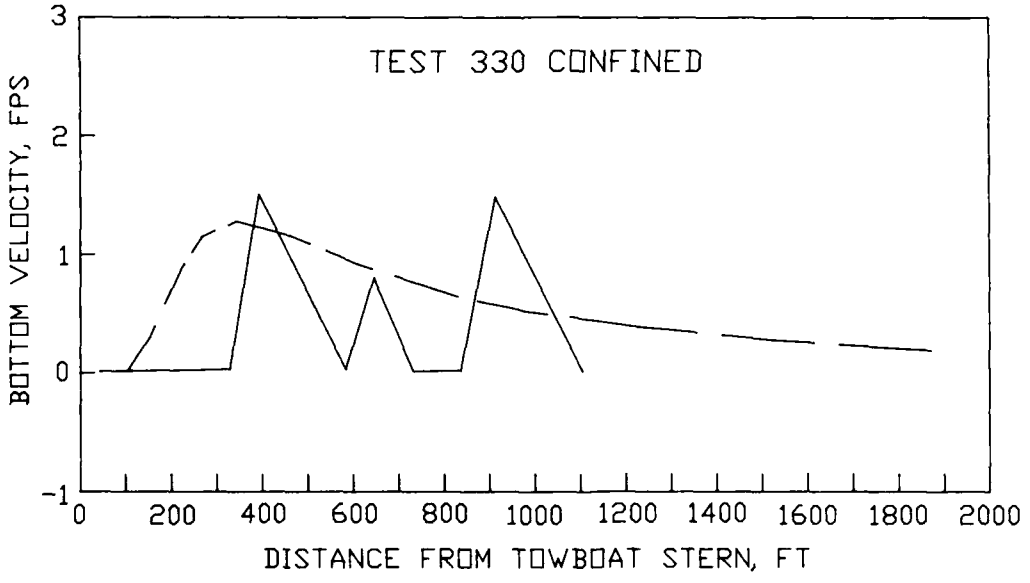

POSITIVE VELOCITY IS OPPOSITE TOW DIRECTION
VELOCITIES ON CENTER LINE OF VESSEL

– – – VERHEY METHOD

——— PHYSICAL MODEL DATA

PHYSICAL MODEL VELOCITIES

VERSUS VERHEY METHOD

TESTS 329 AND 330

PLATE 25

APPENDIX A: TIME-HISTORY VELOCITY PLOTS

Table A1

Meter Reading Versus Prototype Velocity

Meter Reading	Prototype Velocity, fps	
	Outside Meter	Inside Meter
2	0.5	0.5
4	0.73	0.65
6	0.98	0.82
8	1.23	0.98
10	1.47	1.15
12	1.67	1.32
14	1.83	1.47
16	1.97	1.62
18	2.08	1.78
20	2.22	1.98
22	2.35	2.09
24	2.50	2.28
26	2.64	2.48
28	2.77	2.67
30	2.91	2.86
32	3.09	3.03
34	3.26	3.19
36	3.40	3 36
38	3.53	3.53
40	3.70	3.70
45	4.10	4.10
50	4.46	4.46
55	4.80	4.80
60	5.19	5.19
65	5.60	5.60
70	5.98	5.98
75	6.37	6.37

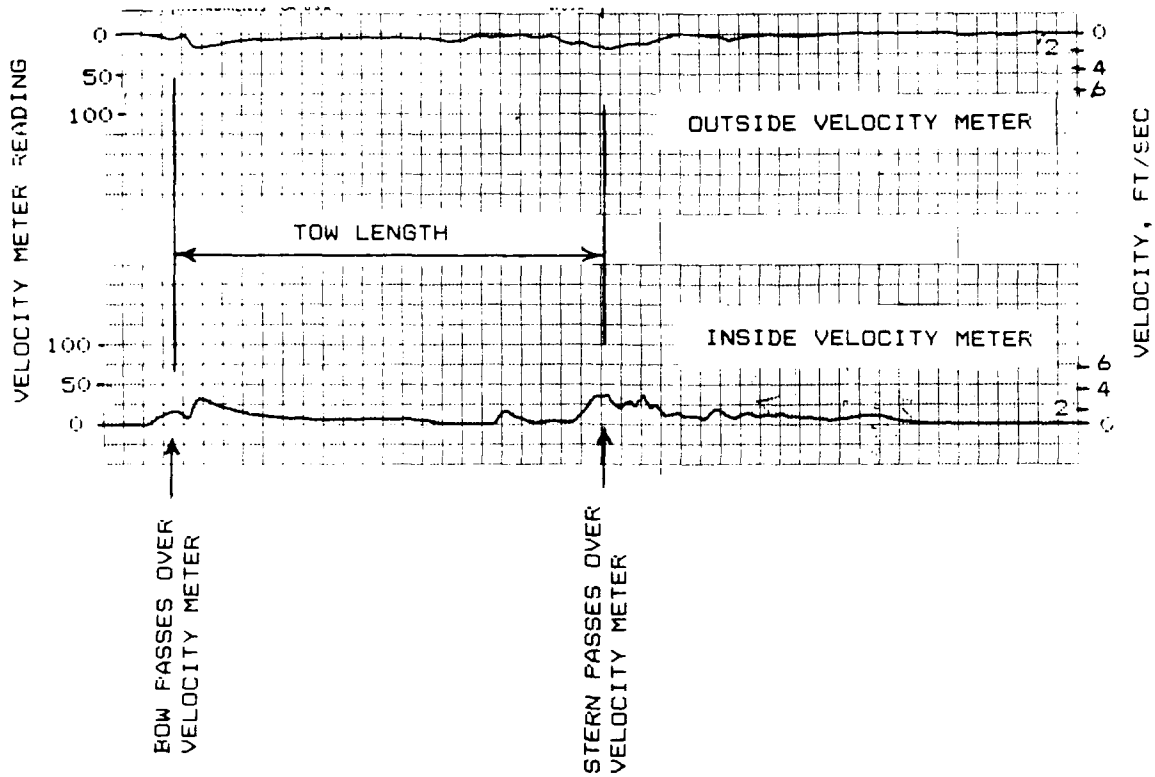

NOTE: HORIZONTAL AXIS IS DISTANCE. TOW LENGTH DEFINES THE SCALE FOR THIS AXIS. TOW LENGTH FOR 2 BARGES PLUS TOWBOAT IS 599 FT. TOW LENGTH FOR 1 BARGE PLUS TOWBOAT IS 404 FT.

SMALLEST DIVISION FOR VELOCITY METER READING IS 5 UNITS. LARGE DIVISION FOR VELOCITY METER READING IS 25 UNITS. RELATIONSHIP BETWEEN VELOCITY METER READING AND PROTOTYPE VELOCITY IS GIVEN IN TABLE A1

MASTER LEGEND FOR BOTTOM VELOCITIES

1:20-SCALE MODEL

PLATE A1

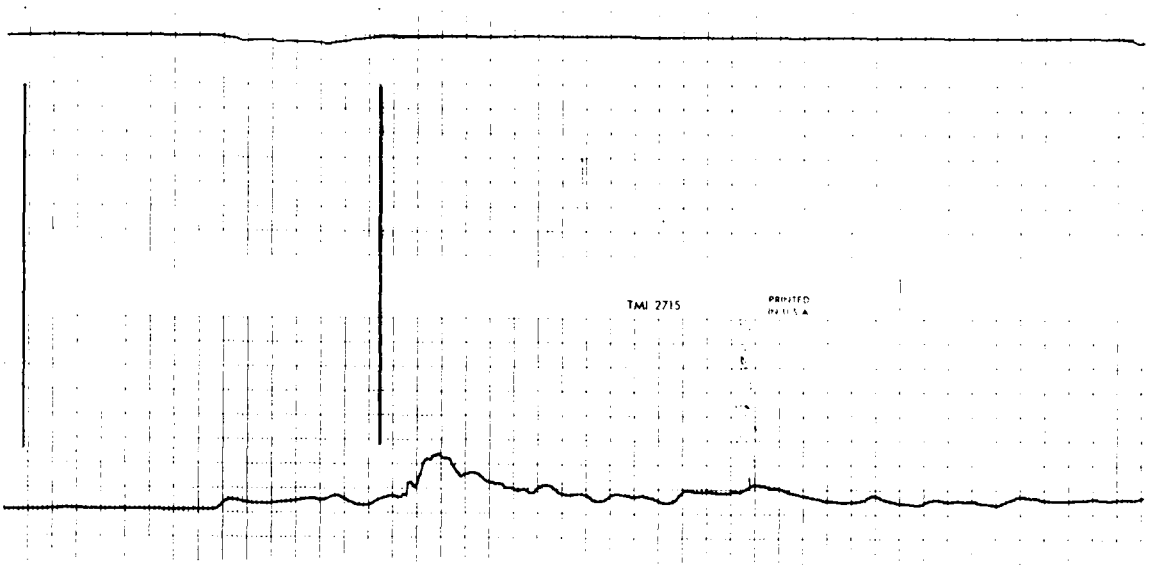

TEST 10

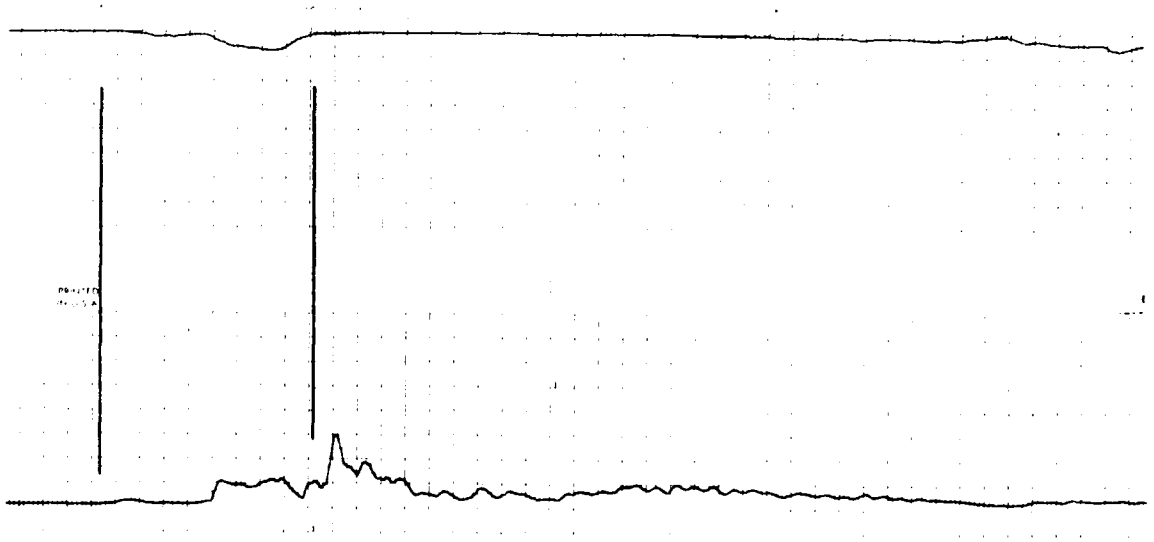

TEST 11

BOTTOM VELOCITIES
1:20-SCALE MODEL
TESTS 10 AND 11

PLATE A2

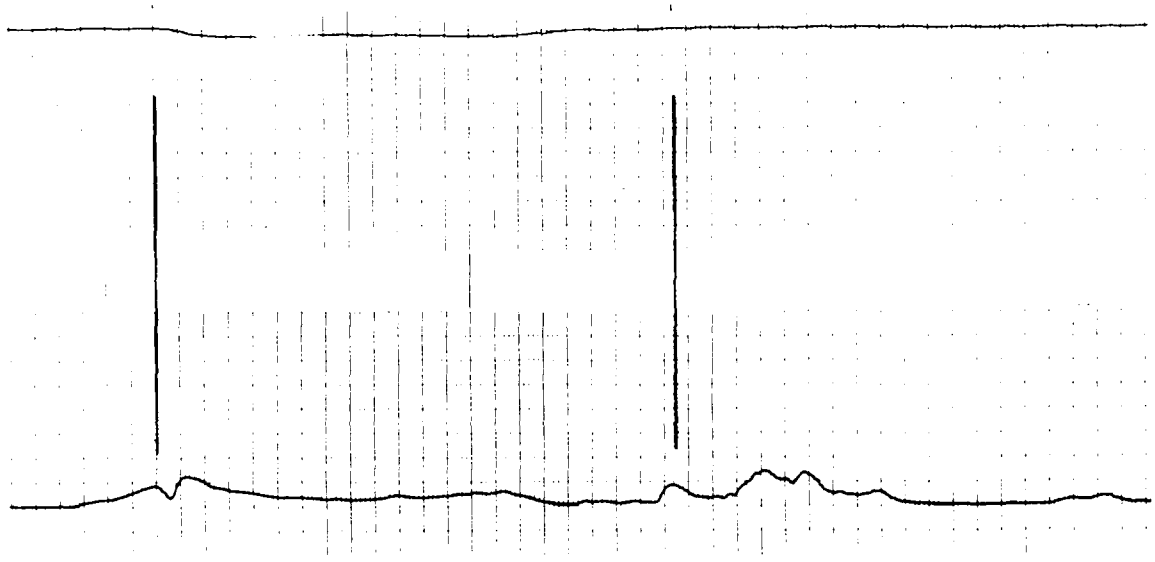

TEST 14

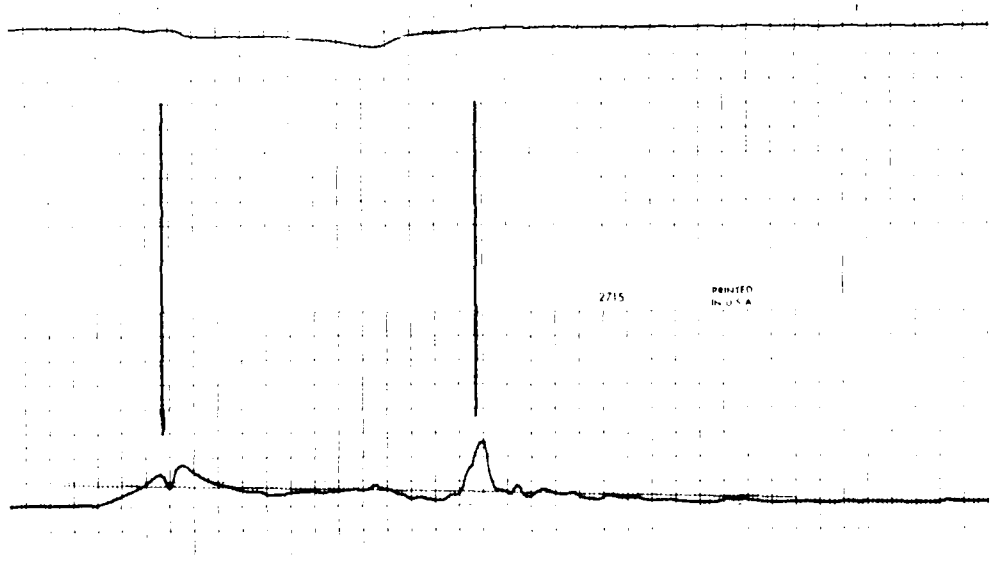

TEST 15

BOTTOM VELOCITIES
1:20-SCALE MODEL
TESTS 14 AND 15

PLATE A3

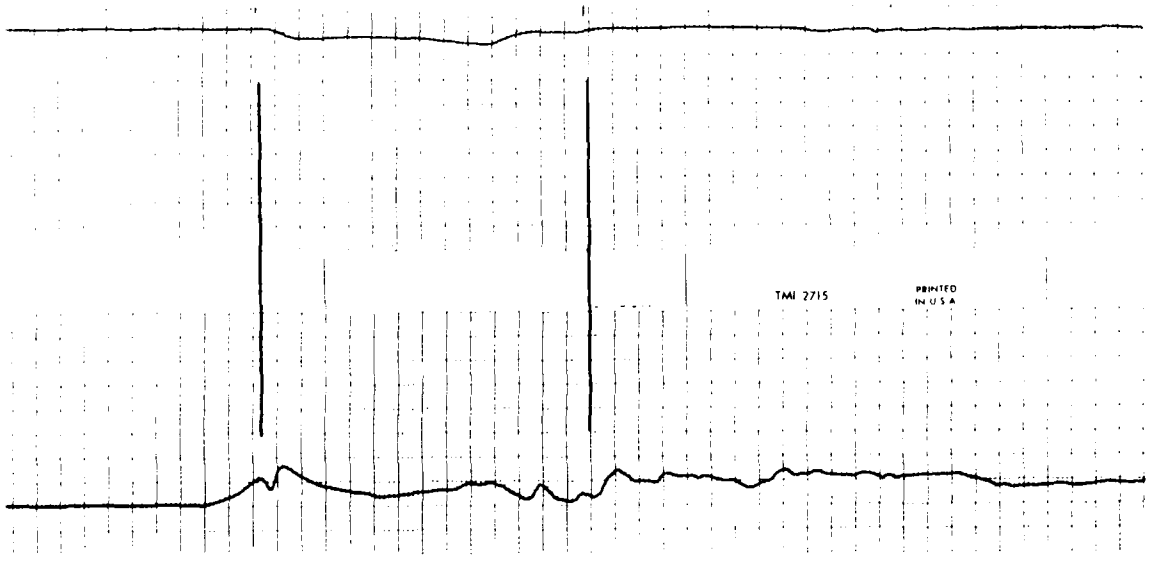

TEST 16

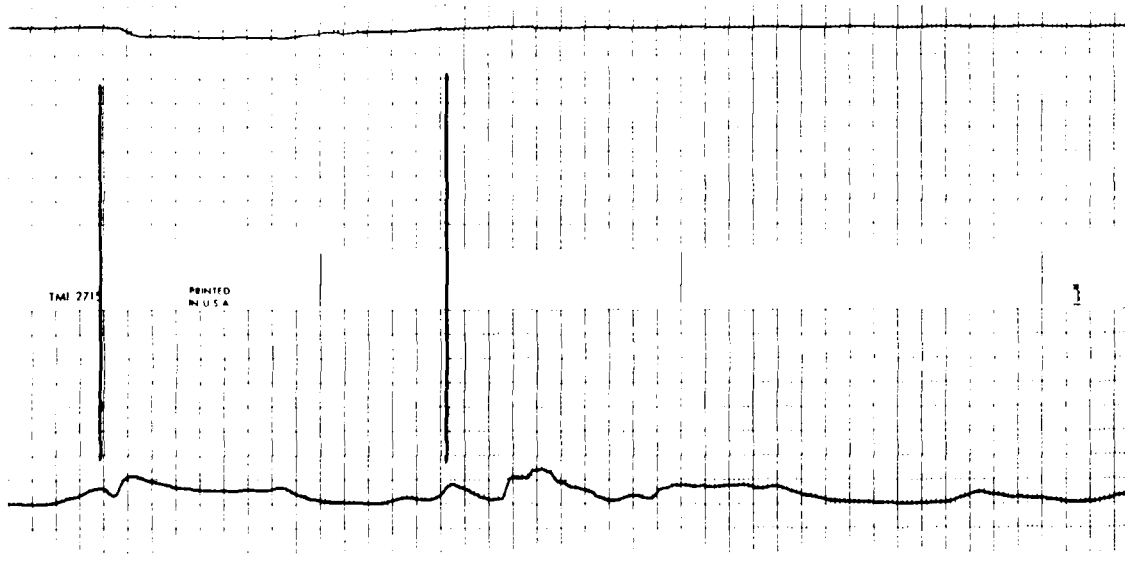

TEST 21

BOTTOM VELOCITIES
1:20-SCALE MODEL
TESTS 16 AND 21

PLATE A4

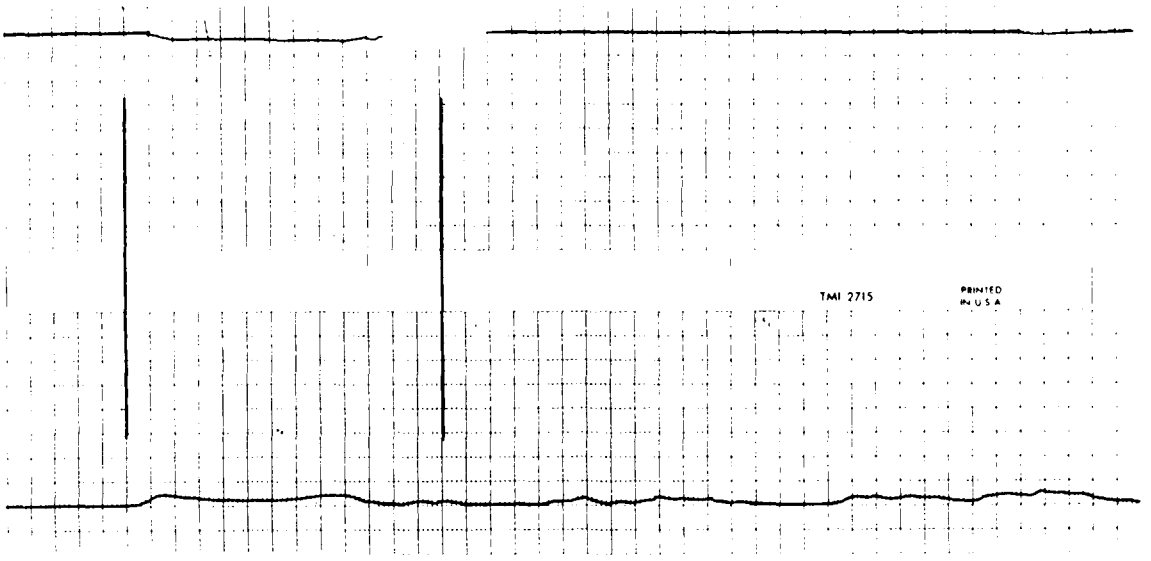

TEST 22

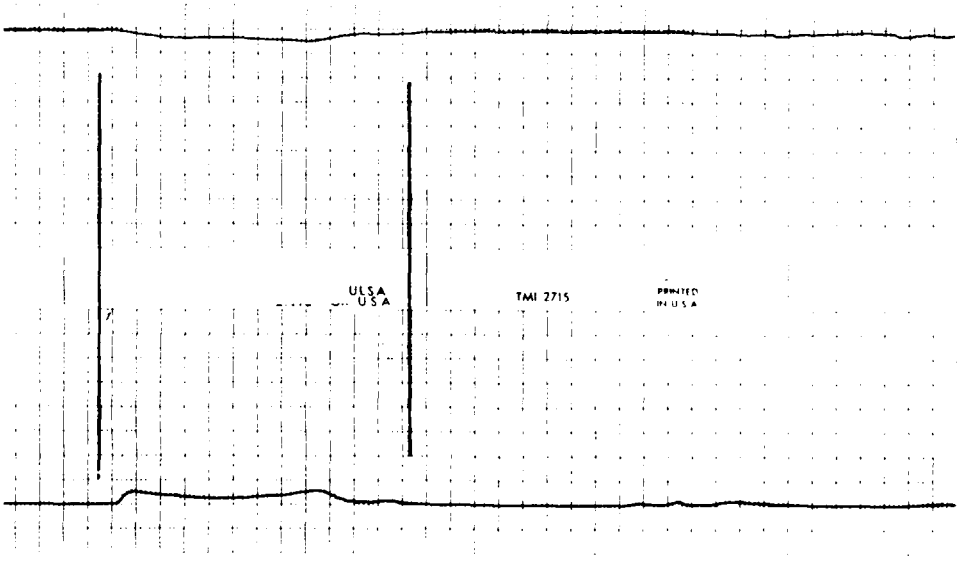

TEST 23

BOTTOM VELOCITIES
1:20-SCALE MODEL
TESTS 22 AND 23

PLATE A5

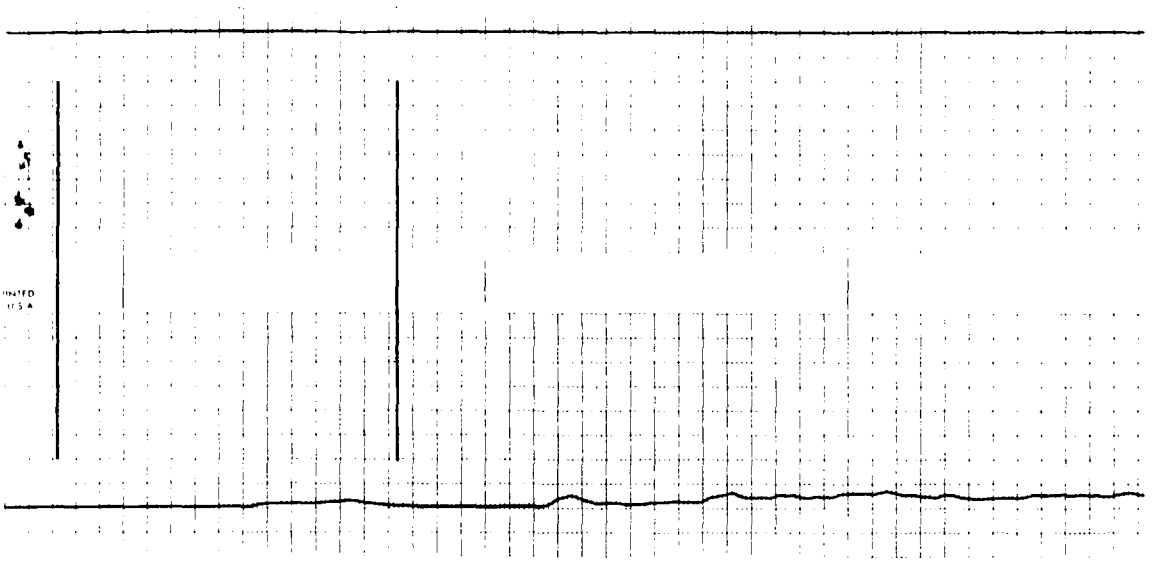

TEST 26

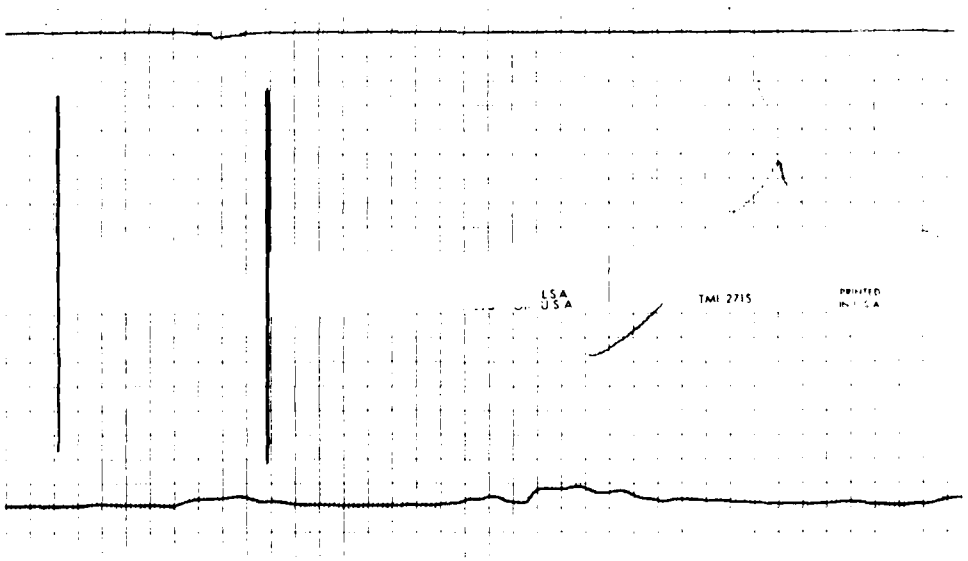

TEST 27

BOTTOM VELOCITIES
1:20-SCALE MODEL
TESTS 26 AND 27

PLATE A6

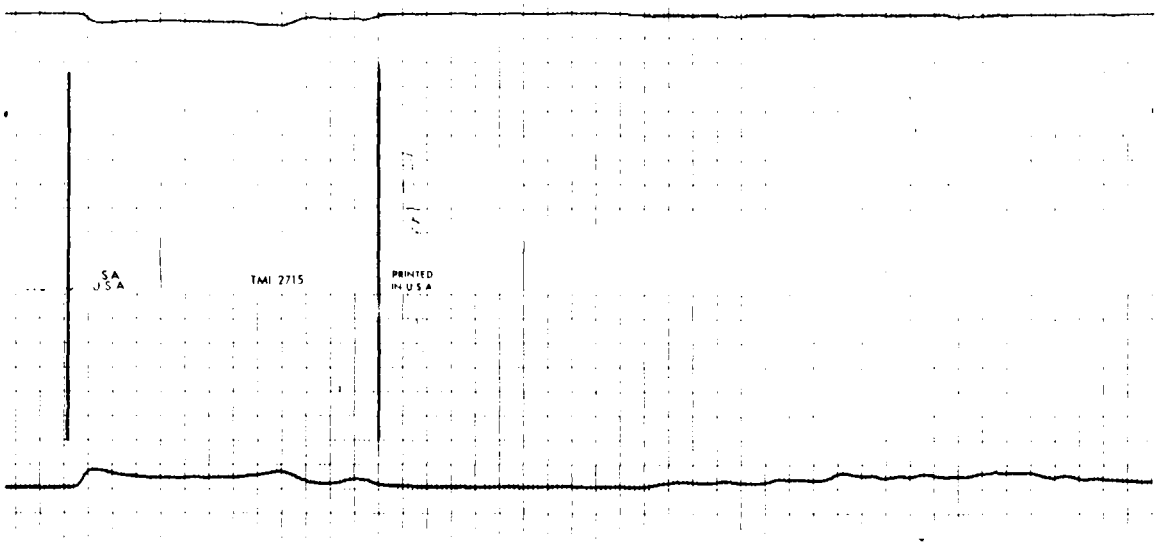

TEST 31

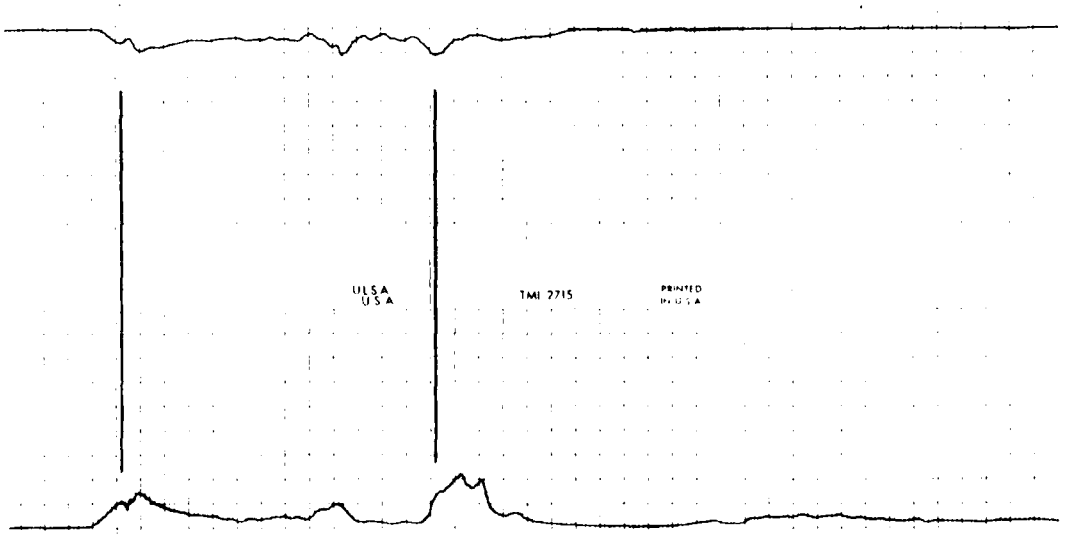

TEST 39

BOTTOM VELOCITIES
1:20-SCALE MODEL
TESTS 31 AND 39

PLATE A7

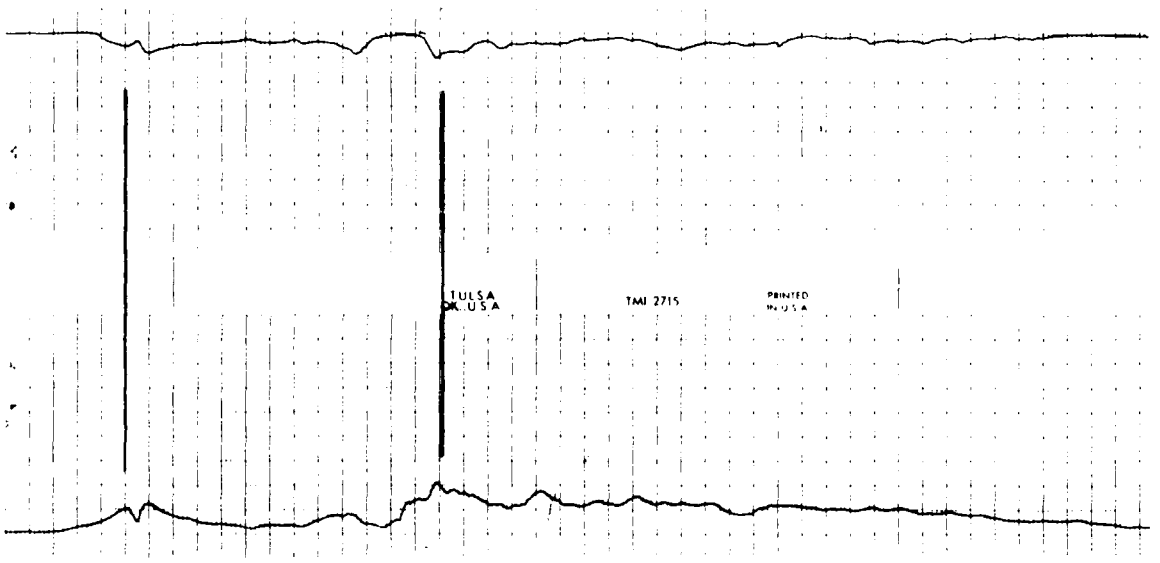

TEST 40

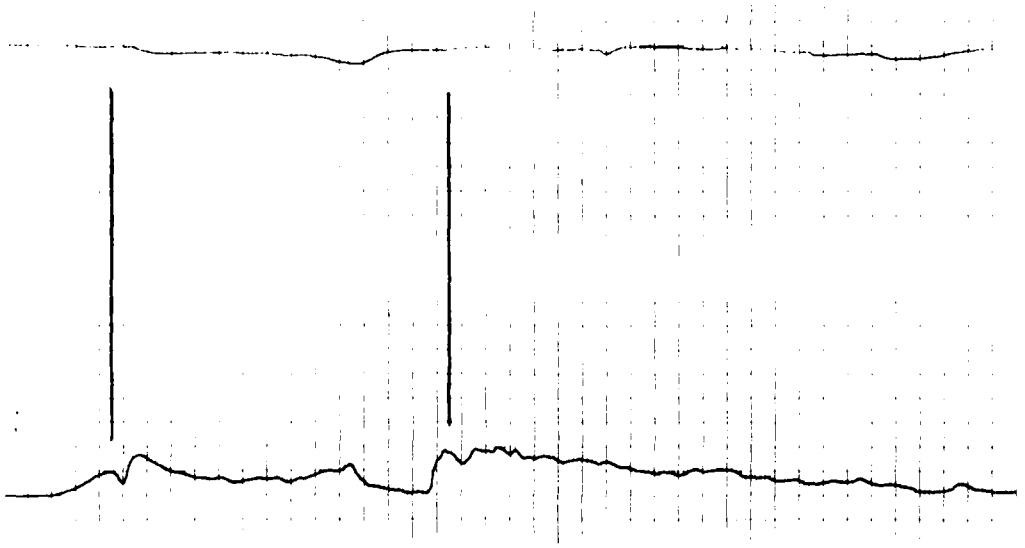

TEST 114

BOTTOM VELOCITIES
1:20-SCALE MODEL
TESTS 40 AND 114

PLATE A8

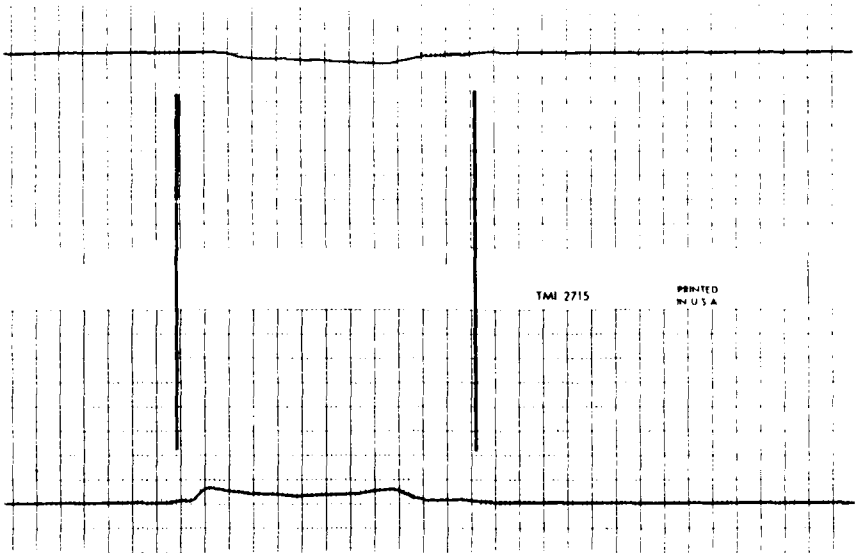

TEST 117

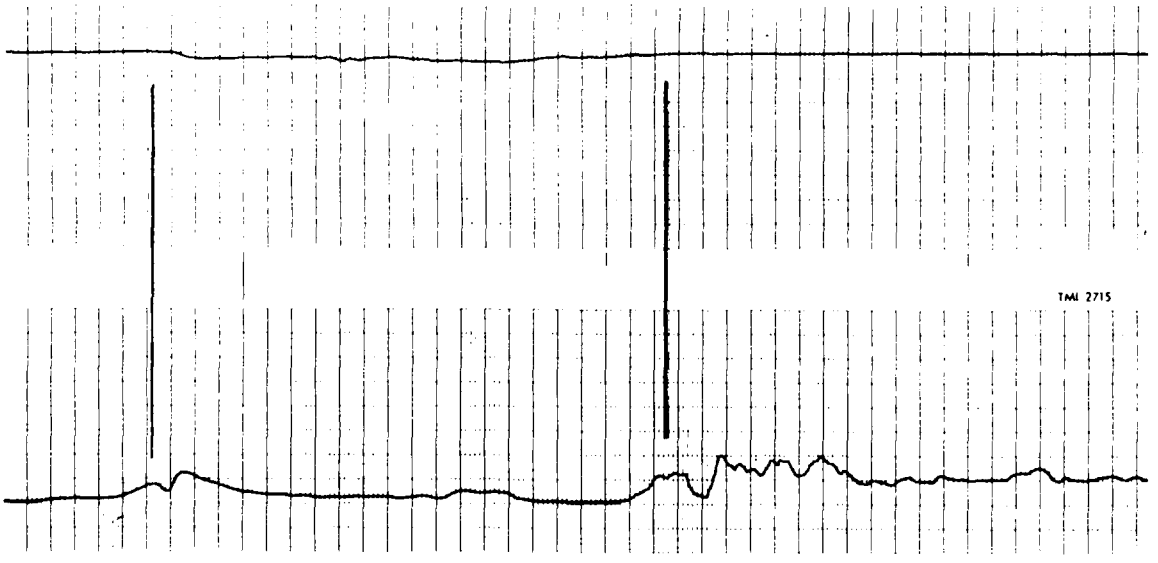

TEST 200

BOTTOM VELOCITIES
1:20-SCALE MODEL
TESTS 117 AND 200

PLATE A9

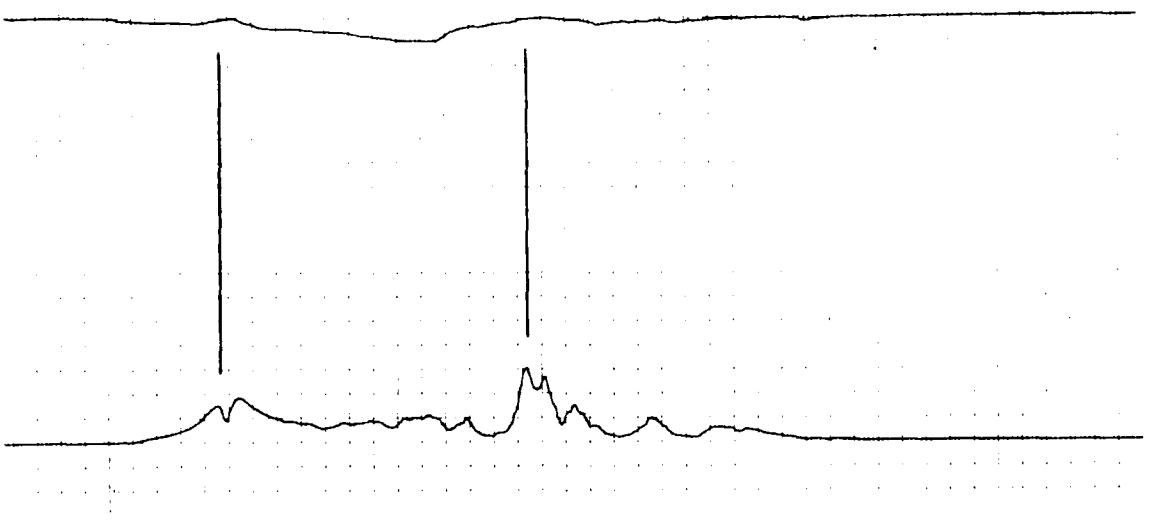

TEST 201

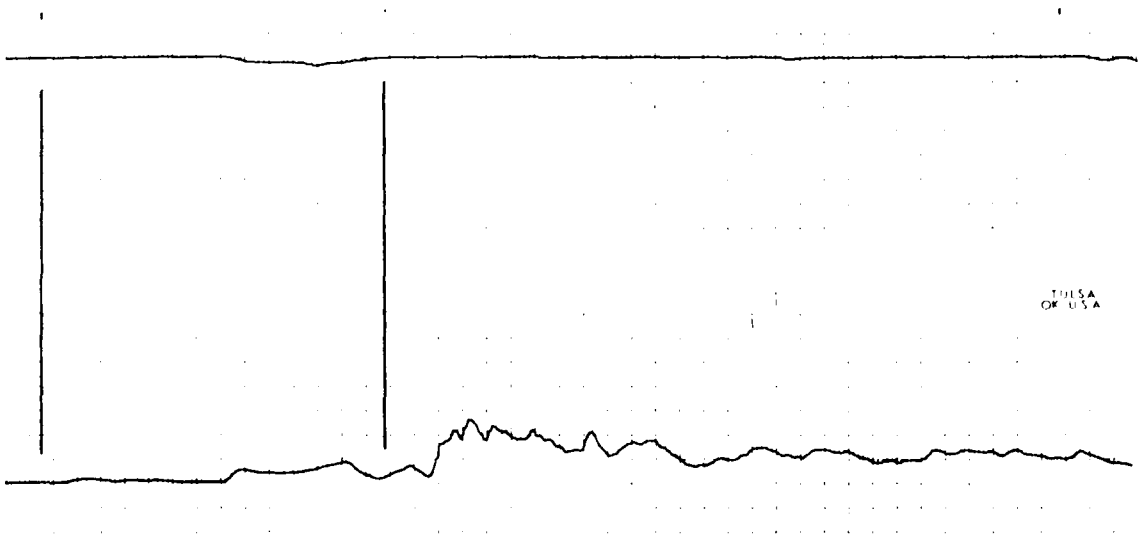

TEST 206

BOTTOM VELOCITIES
1:20-SCALE MODEL
TESTS 201 AND 206

PLATE A10

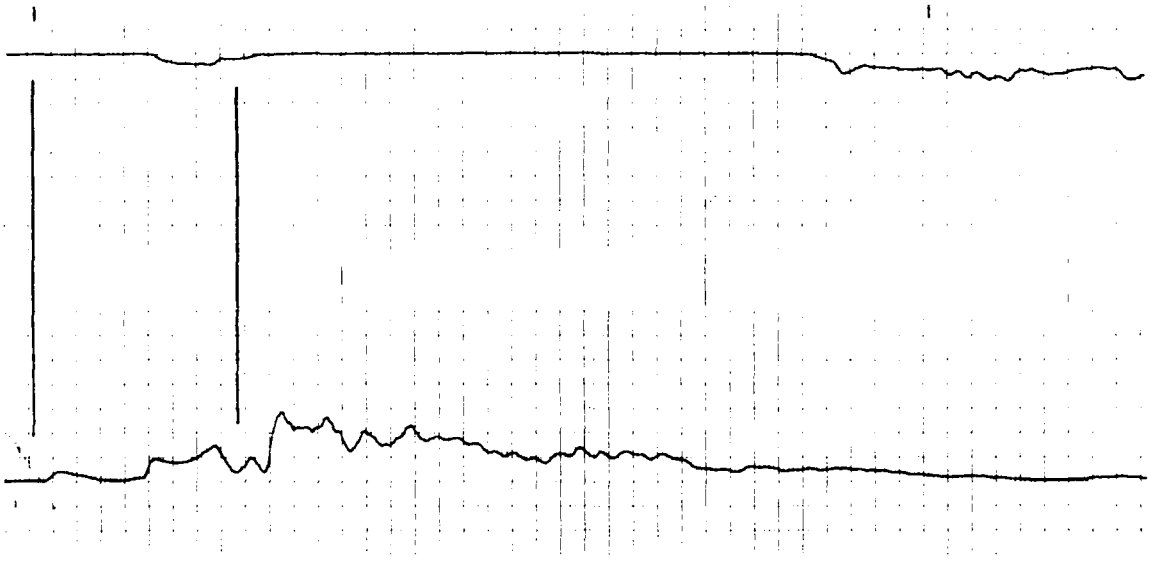

TEST 207

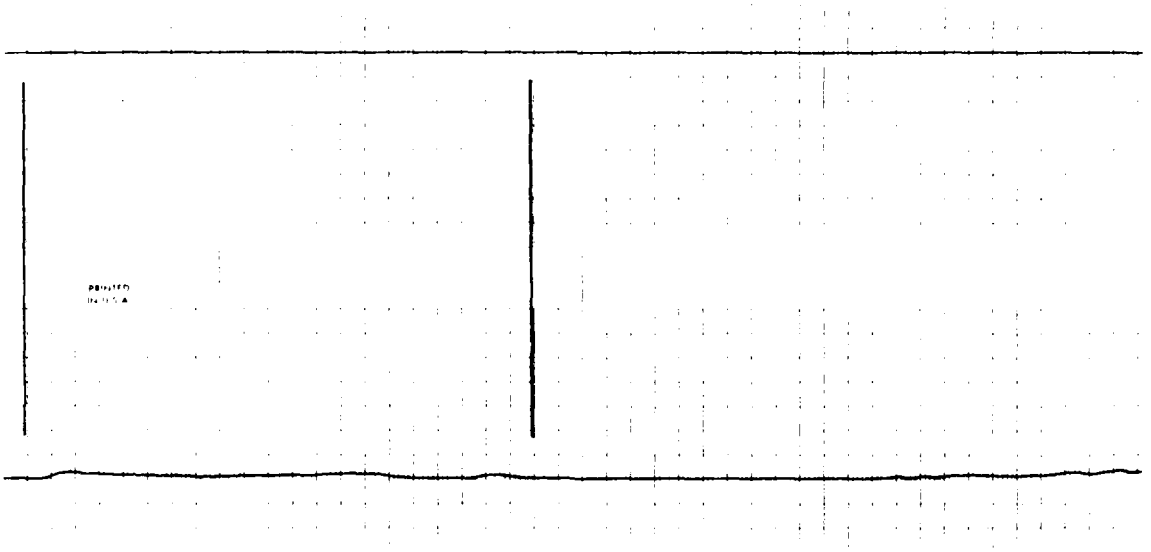

TEST 208

BOTTOM VELOCITIES
1:20-SCALE MODEL
TESTS 207 AND 208

PLATE A11

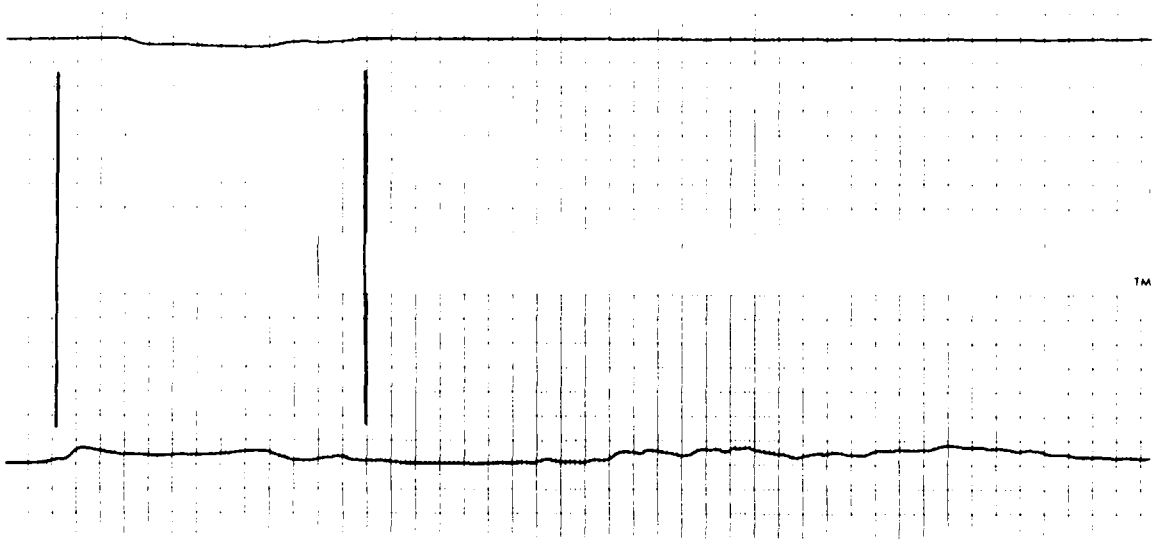

TEST 209

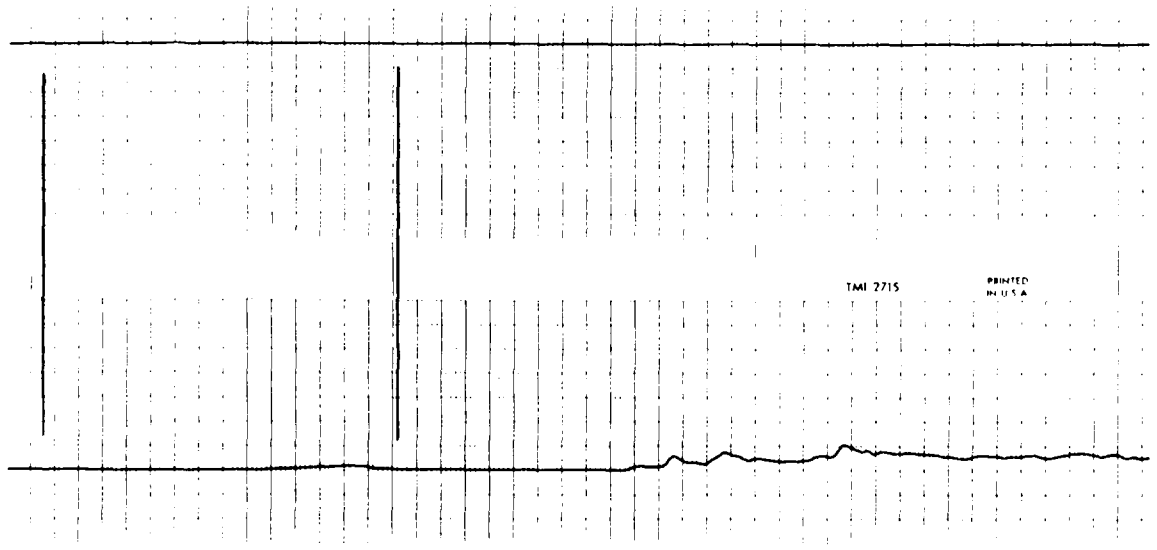

TEST 212

BOTTOM VELOCITIES
1:20-SCALE MODEL
TESTS 209 AND 212

PLATE A12

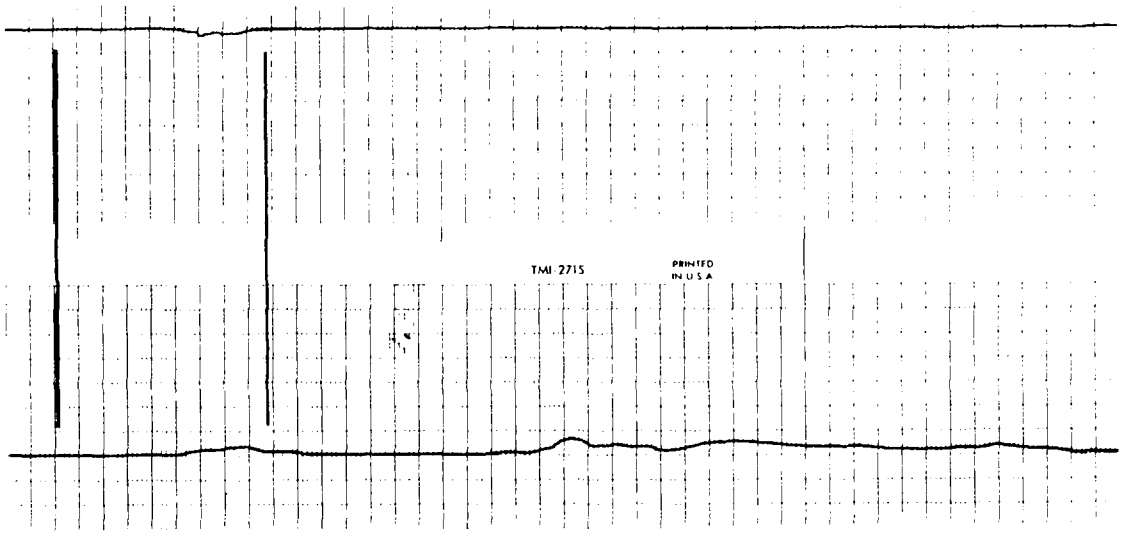

TEST 213

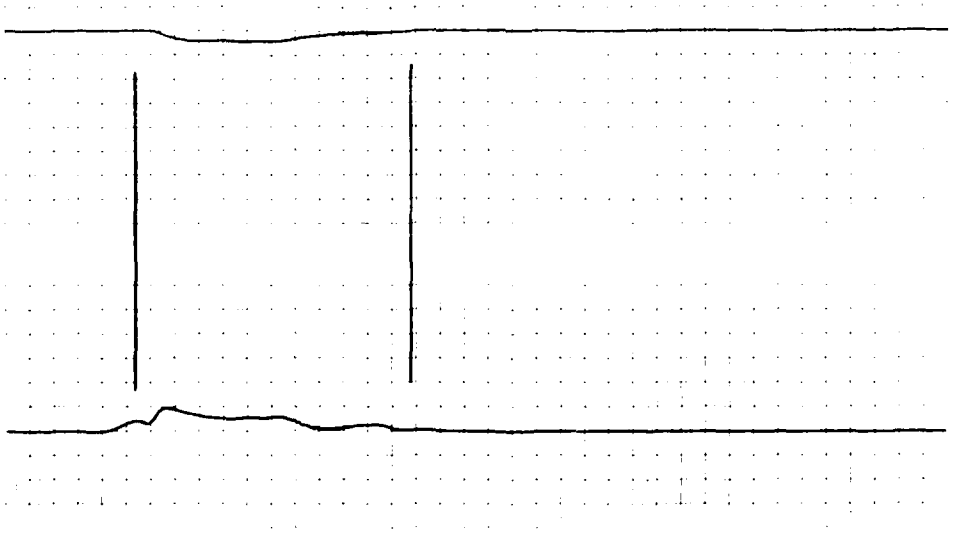

TEST 221

BOTTOM VELOCITIES
1:20-SCALE MODEL
TESTS 213 AND 221

PLATE A13

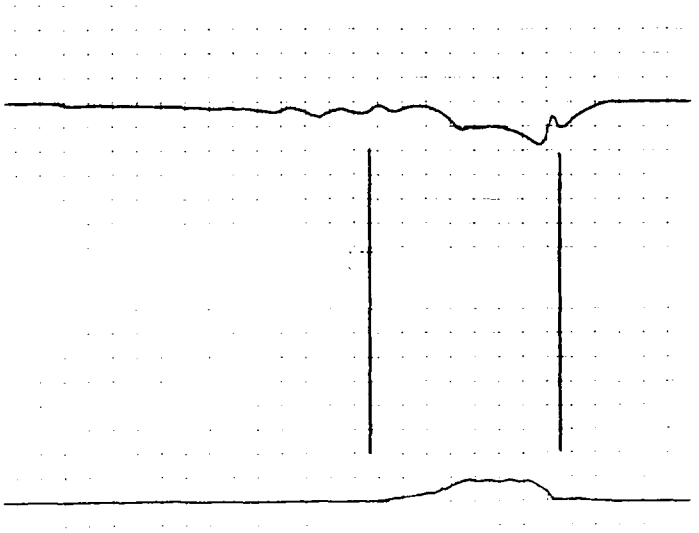

TEST 222

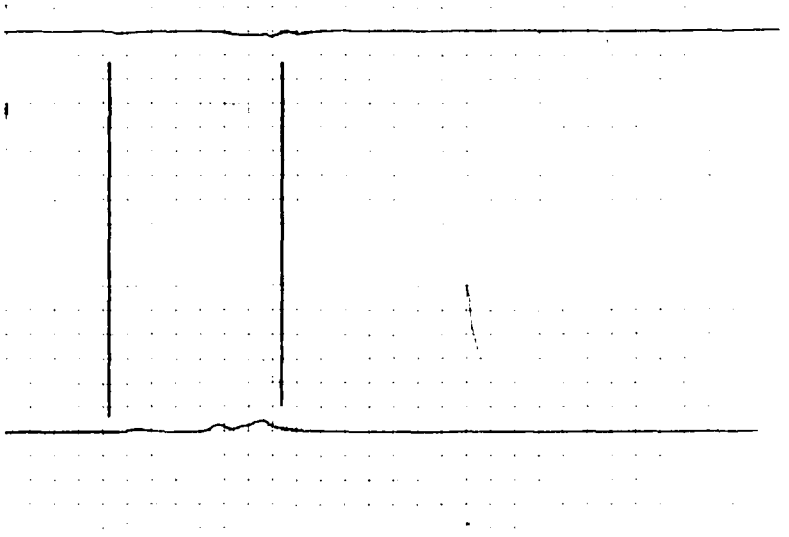

TEST 223

BOTTOM VELOCITIES
1:20-SCALE MODEL
TESTS 222 AND 223

PLATE A14

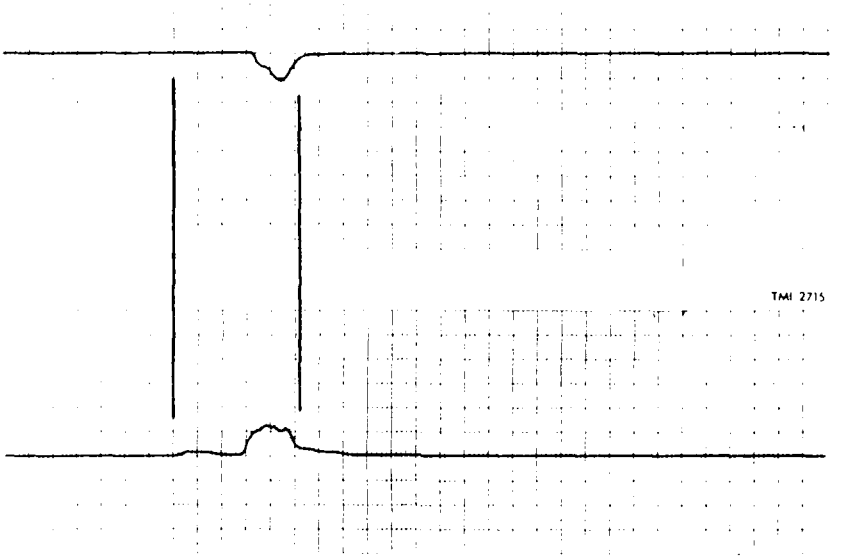

TEST 224

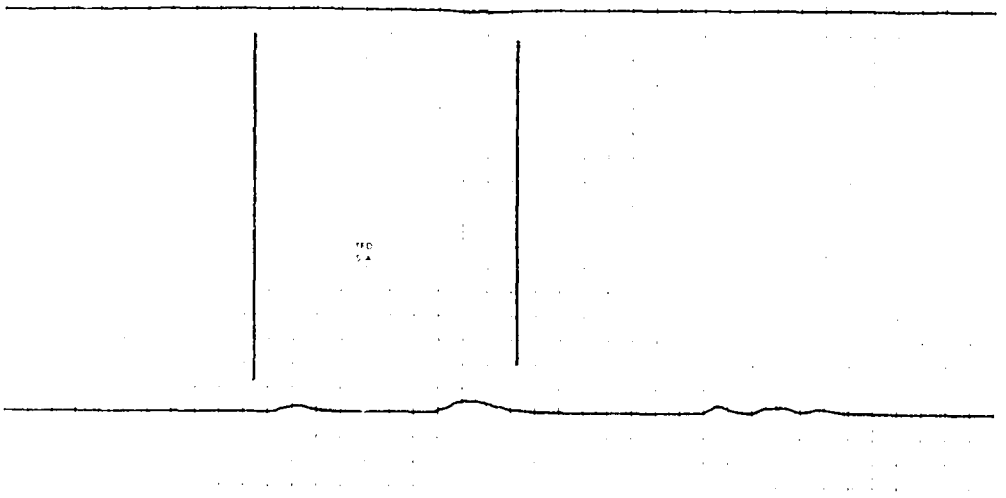

TEST 225

BOTTOM VELOCITIES
1:20-SCALE MODEL
TESTS 224 AND 225

PLATE A15

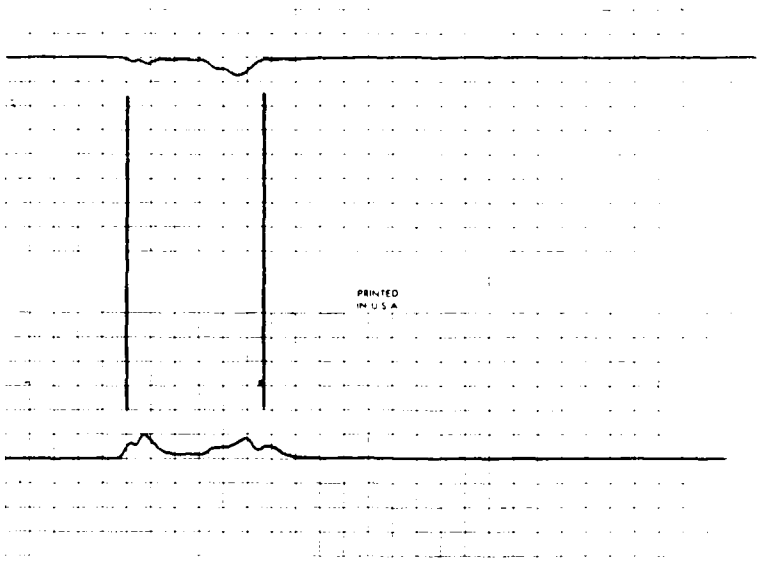

TEST 226

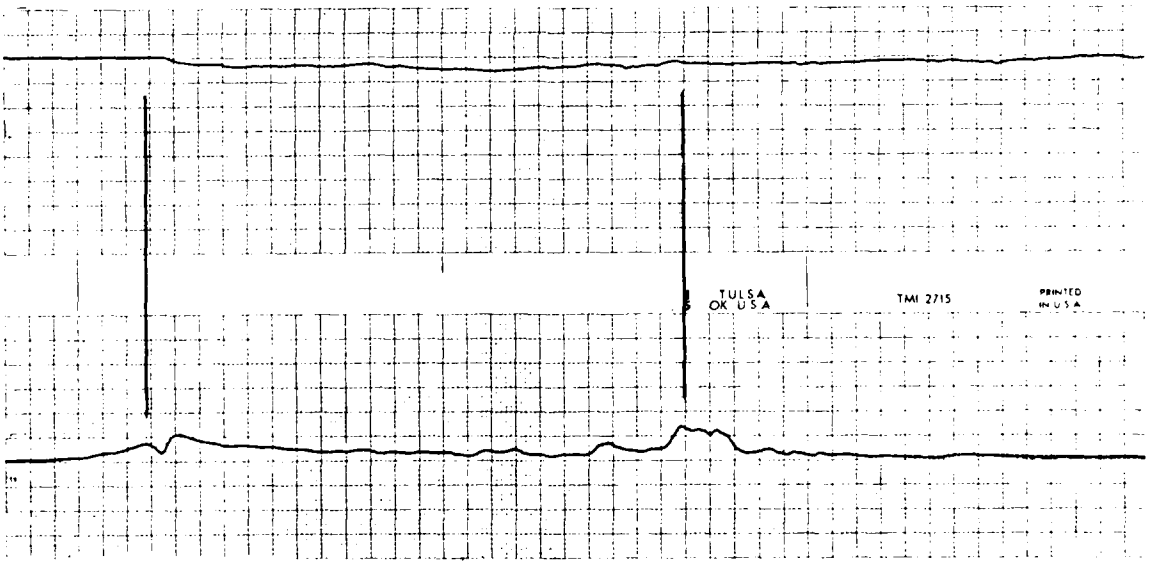

TEST 300

BOTTOM VELOCITIES
1:20-SCALE MODEL
TESTS 226 AND 300

PLATE A16

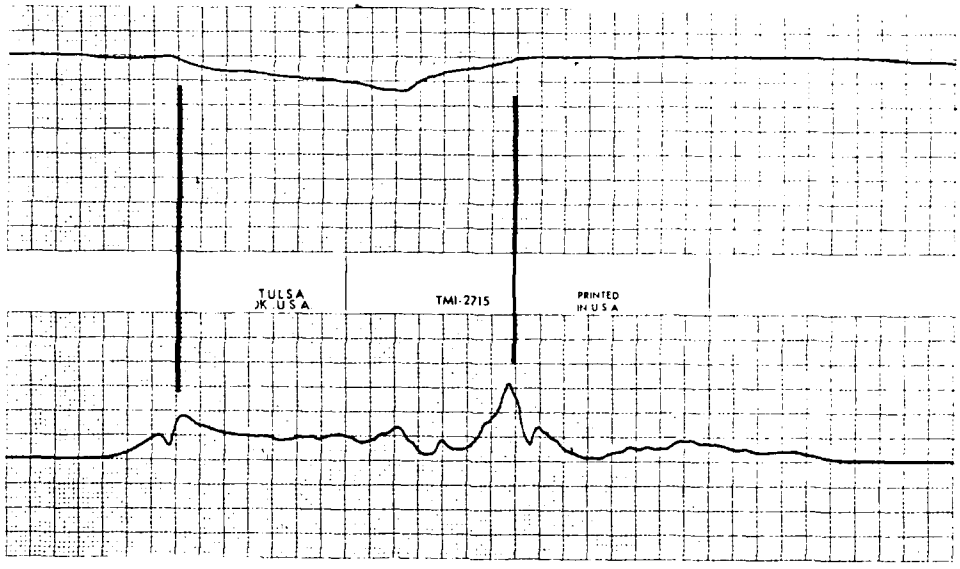

TEST 301

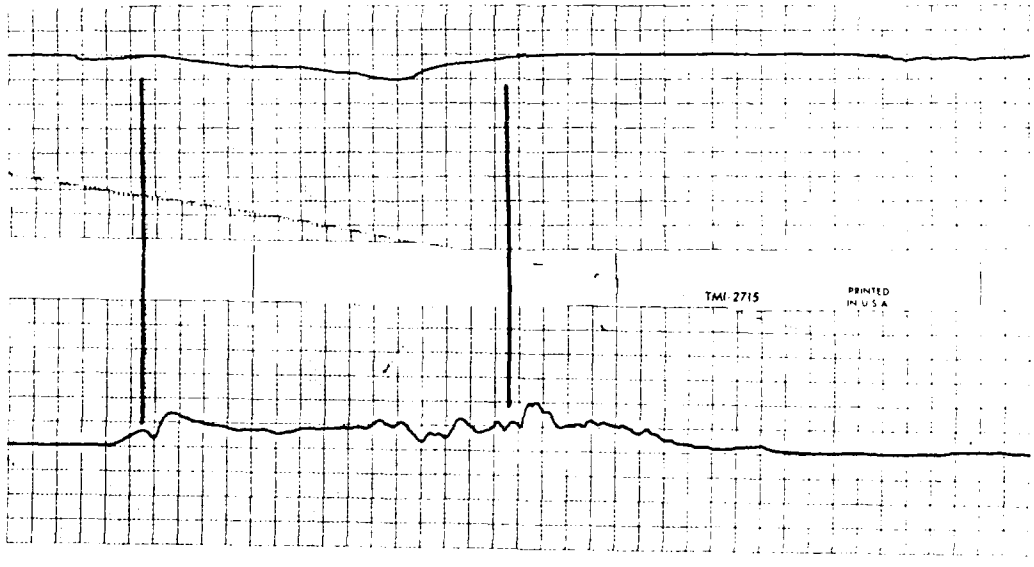

TEST 302

BOTTOM VELOCITIES
1:20-SCALE MODEL
TESTS 301 AND 302

PLATE A17

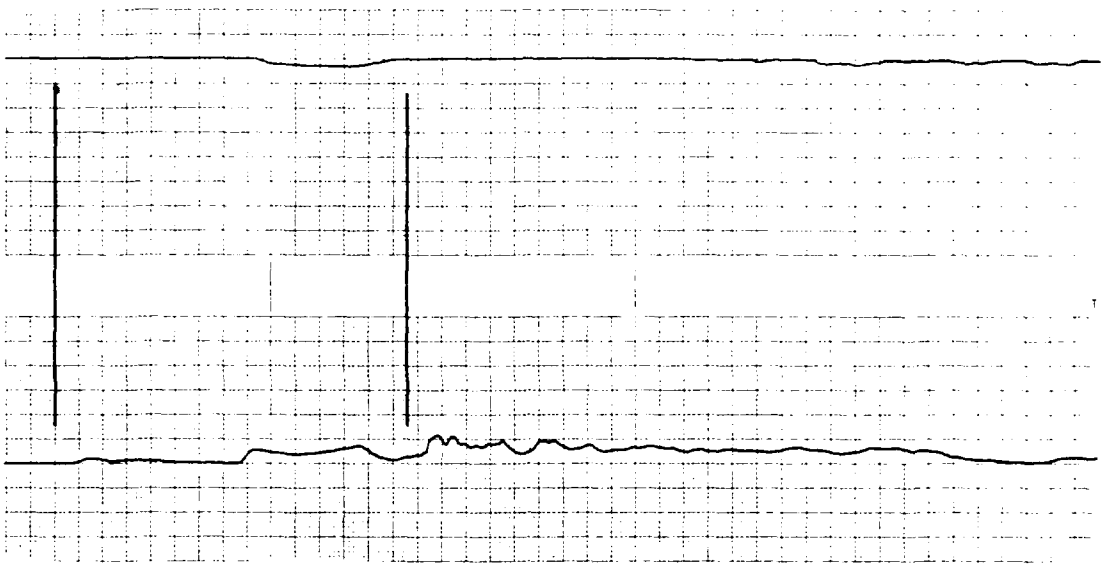

TEST 306

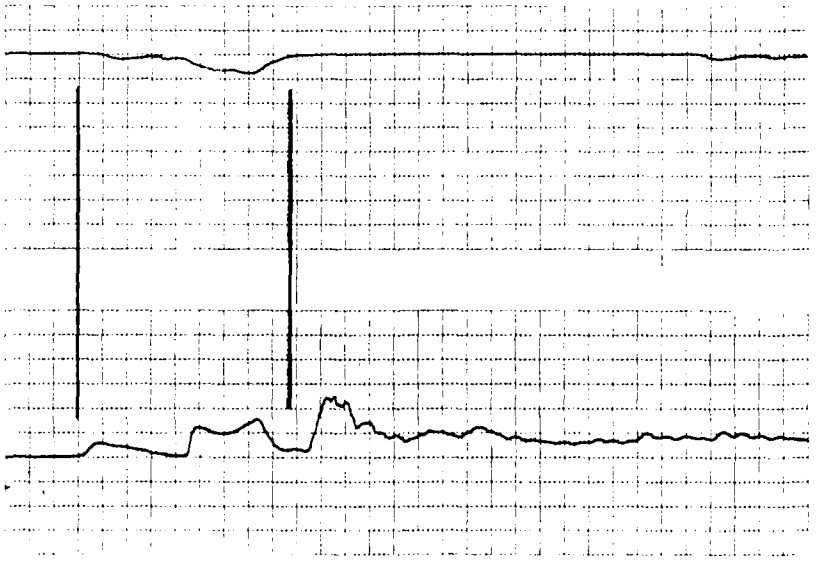

TEST 307

BOTTOM VELOCITIES
1:20-SCALE MODEL
TESTS 306 AND 307

PLATE A18

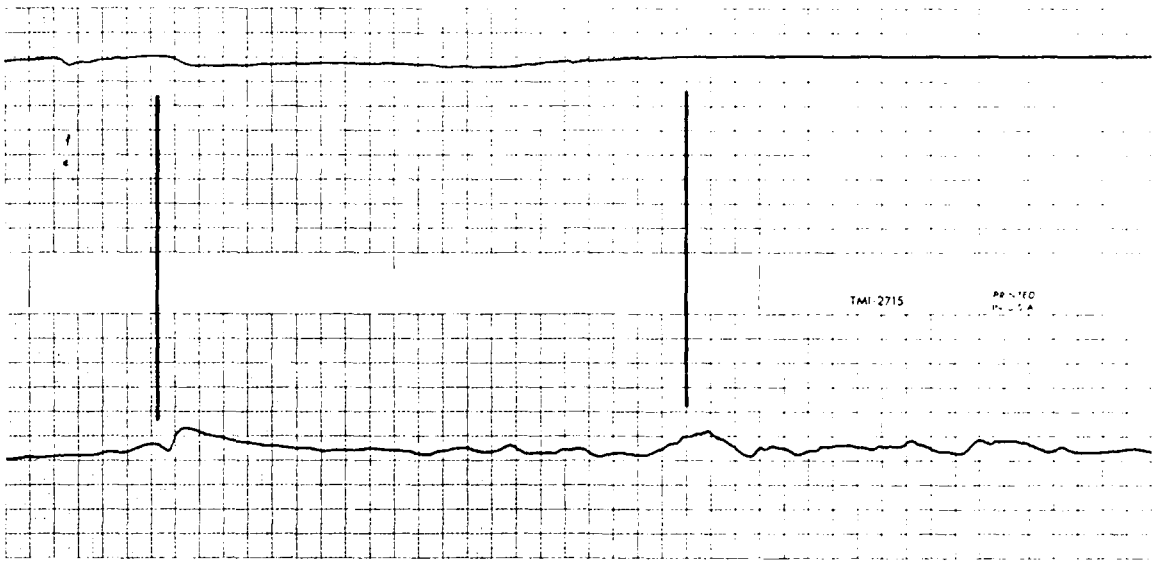

TEST 315

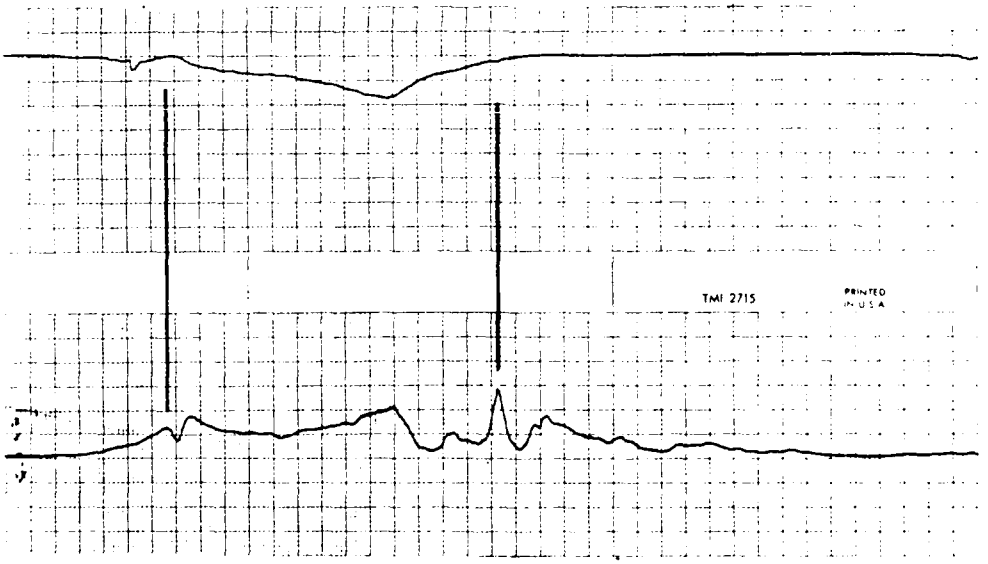

TEST 316

BOTTOM VELOCITIES
1:20-SCALE MODEL
TESTS 315 AND 316

PLATE A19

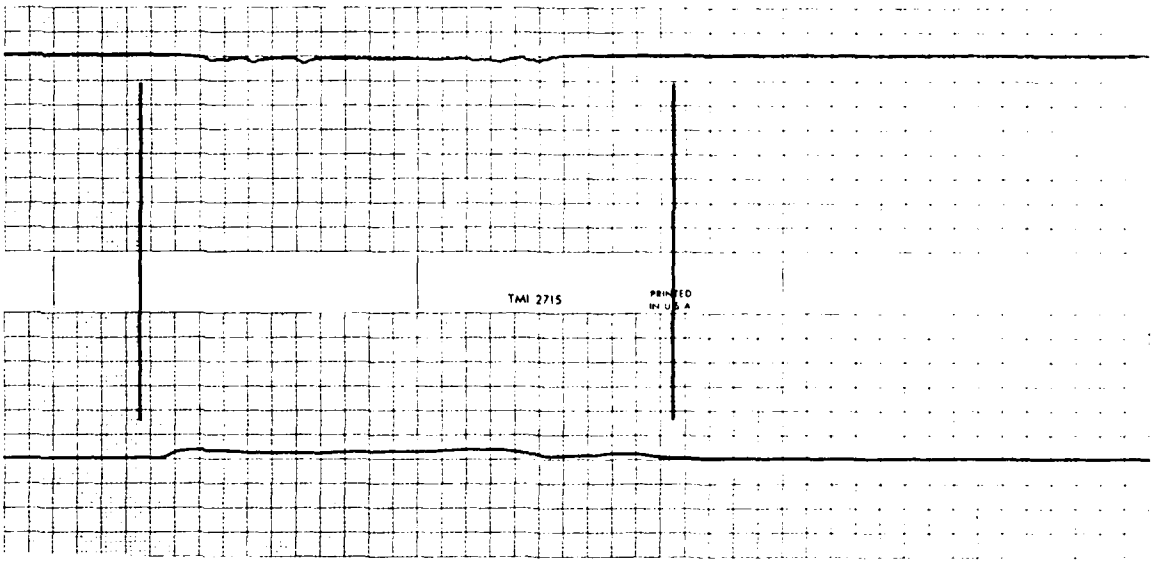

TEST 317

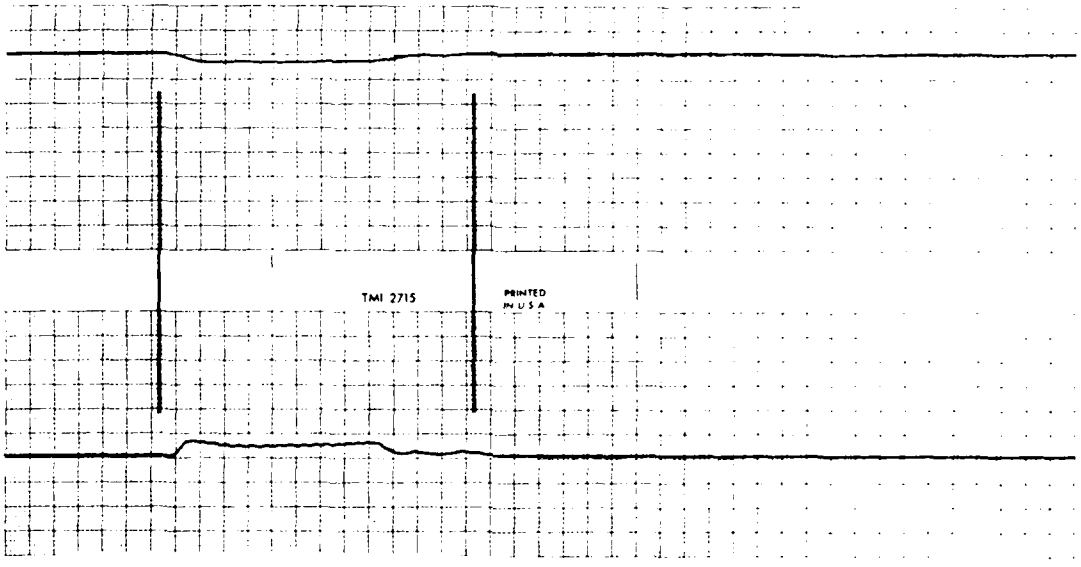

TEST 318

BOTTOM VELOCITIES
1:20-SCALE MODEL
TESTS 317 AND 318

PLATE A20

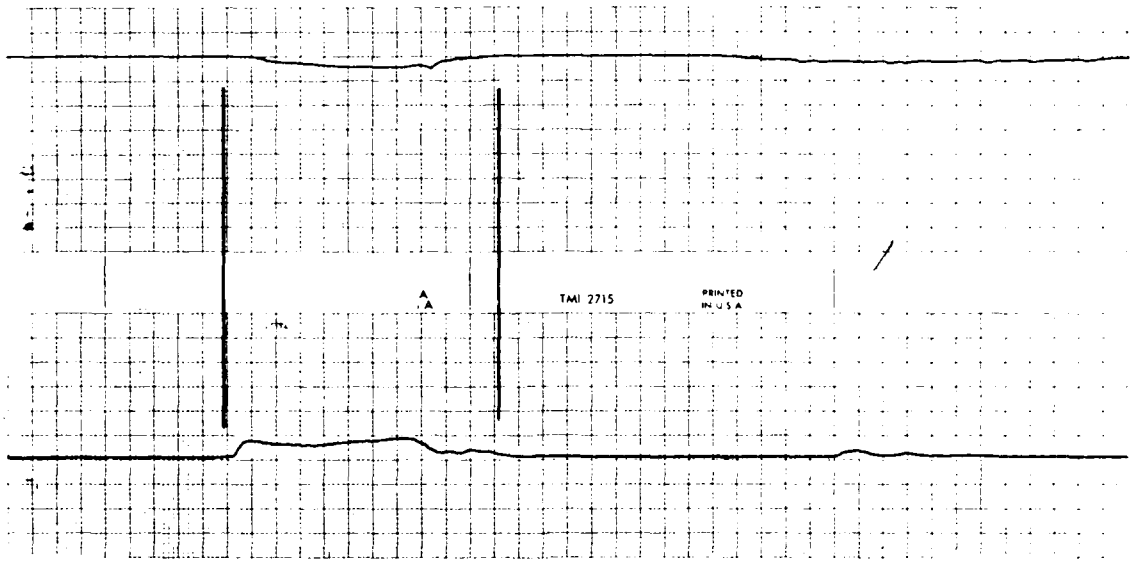

TEST 319

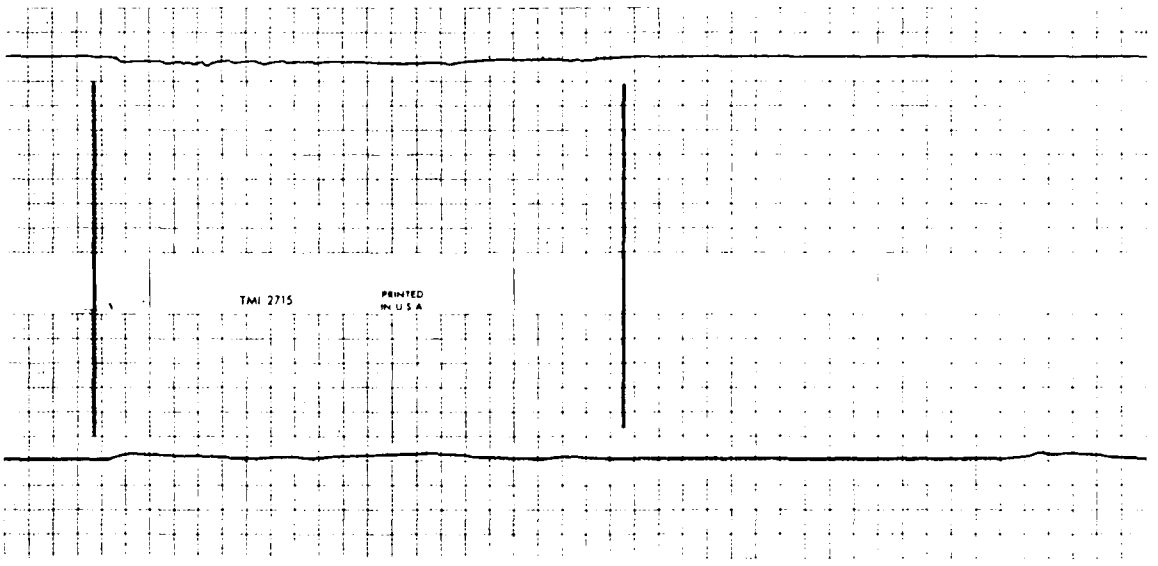

TEST 320

BOTTOM VELOCITIES
1:20-SCALE MODEL
TESTS 319 AND 320

PLATE A21

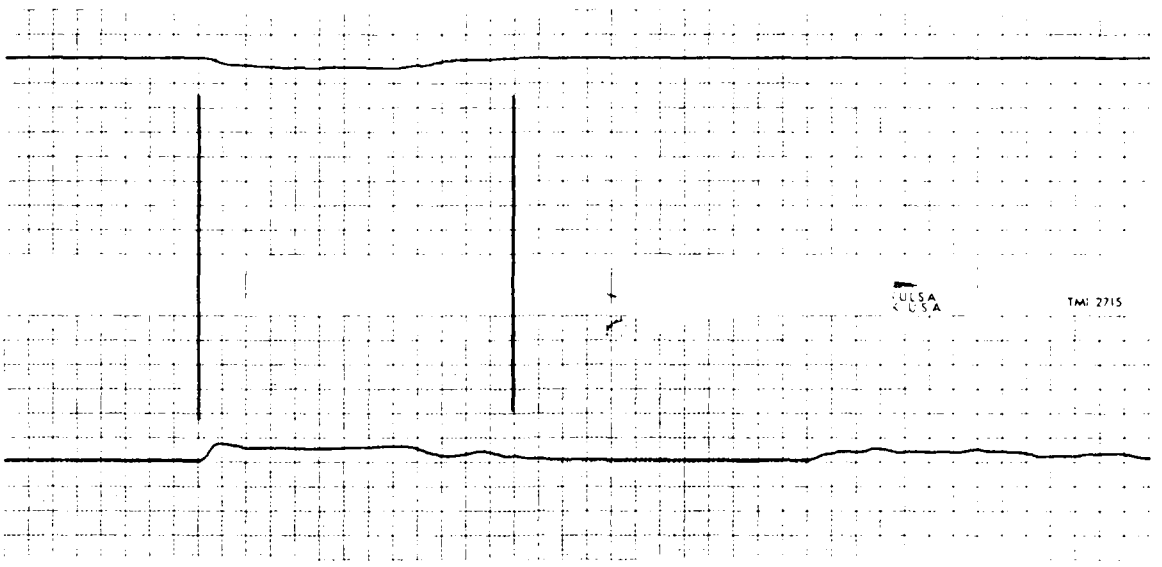

TEST 321

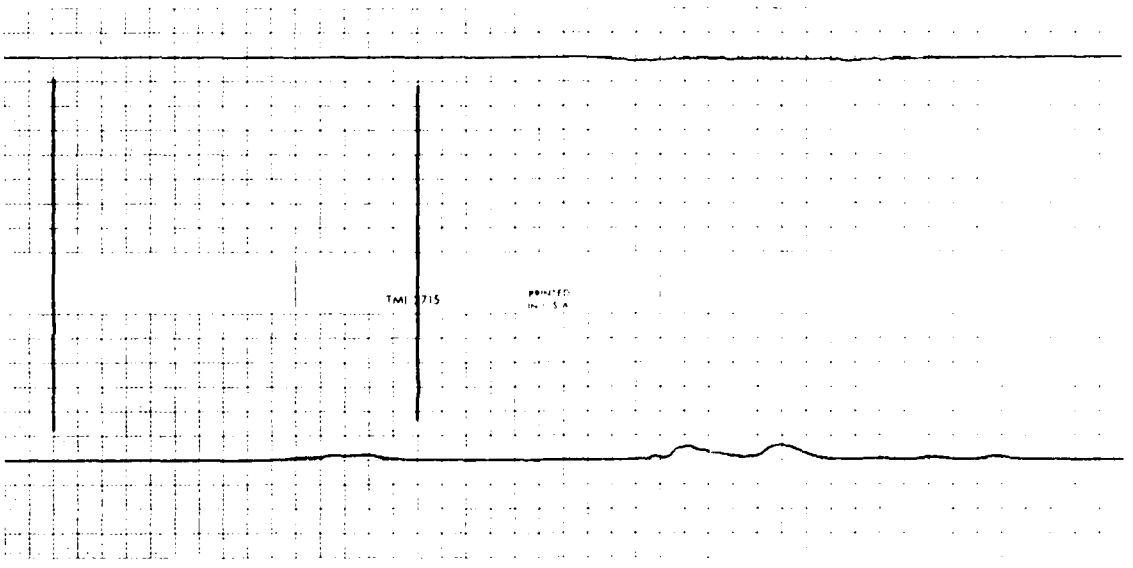

TEST 329

BOTTOM VELOCITIES
1:20-SCALE MODEL
TESTS 321 AND 329

PLATE A22

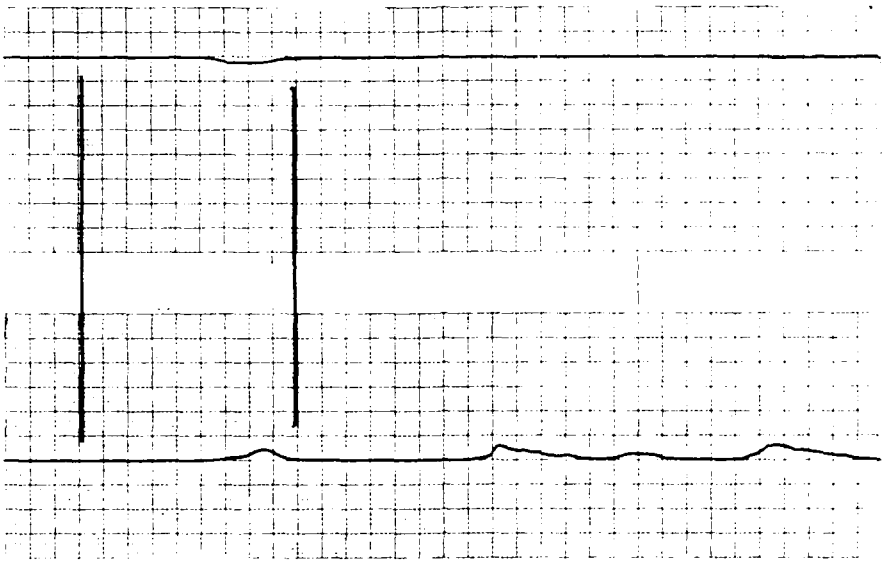

TEST 330

BOTTOM VELOCITIES
1:20-SCALE MODEL
TEST 330

PLATE A23

APPENDIX B: NOTATION

a'	Eccentricity factor for vessel sailing off channel center line
a,A	Coefficients
A	Function of propeller height above bottom and if rudder is present behind propeller
a,B	Coefficients in Hochstein (1967)* return velocity equations
A_{eff}	Effective waterway area for determining return velocity for vessel sailing near bank
A_m	Submerged cross-sectional area of midship section
A_o	Cross-section area of waterway
A_{side}	Waterway area on one side of vessel for which return velocity is being computed
b'	Coefficient
b	Beam of vessel
B_o	Surface width of waterway
B_{eff}	Effective waterway width for determining return velocity for vessel sailing near bank
B_{side}	Surface width of side for which return velocities are being computed
C	Coefficient
C'	Coefficient
C_{fr}	Local skin friction coefficient
d	Draft of vessel
D_o	Orifice diameter or contraction diameter
D_p	Propeller diameter
D_o'	Modified propeller diameter (Oebius 1984)
Dep	Local depth of flow
DW	Characteristic dimension of wake flow
DX	Distance from propeller center to maximum velocity (Oebius 1984)

* References cited in this appendix are included in the References at the end of the main text.

E	Coefficient
$F(\alpha)$,K2	Coefficients in return velocity distribution equation
g	Acceleration due to gravity
h	Average channel depth = A_o/B_o
h_p	Distance from center line of propeller to bottom
J	Modified advance coefficient
J_a	Advance coefficient
k_s	Equivalent sand roughness
K	Constrainment factor for determining V_{cr}
K_t	Thrust coefficient for moving navigation
K_{to}	Thrust coefficient at zero speed of advance
L	Vessel length
n	Propeller speed, revolutions per second
N	Blockage ratio = A_o/A_m
N_p	Number of propellers
N_{side}	Blockage ratio for each side of the vessel
P	Coefficient for determing A_{eff} and B_{eff} ; engine power
r	Radial distance from center of outlet = $\sqrt{Z^2 + y^2}$
R_f	Blade radius (from outside of hub to blade tip)
R_n	Hub radius
s	Cotangent of side slope angle
U_o	Ambient velocity in undisturbed channel
U_2	Velocity increment
V	Vessel speed relative to earth
V_a	Entrance or advance velocity
$V_b(x)$	Bottom velocity in x-direction at coordinate x

V_{bb}	Bottom velocity at bow of vessel acting in the same direction
V_{bd}	Displacement velocity beneath vessel
$V_{b,max}$	Maximum bottom velocity for moving navigation ($v \neq 0$)
$V_{b,max,J=0}$	Maximum bottom velocity for maneuvering navigation ($V = 0$)
V_{cr}	Limiting velocity of self-propelled vessel
V_e	Bottom velocity in the propeller wash region
V_i	Velocity at infinity assumed equal to vessel speed (Oebius 1984)
V_o	Orifice velocity at outlet or jet velocity at propeller
V_{out}	Bottom displacement velocity 27.5 ft outside the edge of the barge
V_r	Return velocity
$V_{r,max}$	Maximum return velocity at the vessel
$V_r(y)$	Variation of return velocity with distance from vessel
V_{rs}	Average return velocity for each side of the vessel
V_{rsm}	Maximum return velocity near tow
V_w	Wake velocity
V_x	Velocity in x-direction at coordinates x,r
V(r)	Maximum propeller jet velocity at radial distance r from propeller axis
$V(x)_{max}$	Velocity in x-direction at coordinates x,r = o
W	Wake fraction
x	Distance from outlet or propeller measured along jet axis
x_o	Limit of flow establishment zone
X	Distance from beginning of boundary layer development to maximum velocity
y	Horizontal distance from the center line of propeller
z	Water-level drawdown
z1	Distance from canal axis to vessel
Z	Vertical coordinate measured from center line of propeller

α Ratio of maximum to average return velocity

α_Q Fuehrer and Romisch (1977) parameter for flow beneath vessel

β Coefficient (Oebius 1984)

ρ Water density

τ Shear stress